

HU-P-D100

**STRONG AND ELECTROMAGNETIC  
TRANSITIONS IN HEAVY FLAVOR MESONS**

**TIMO LÄHDE**

*Faculty of Science  
Helsinki Institute of Physics and Department of Physical Sciences,  
PL 64 University of Helsinki, 00014 Helsinki, Finland  
e-mail: talahde@pcu.helsinki.fi*

*ACADEMIC DISSERTATION*

*To be presented, with the permission of the Faculty of Science  
of the University of Helsinki, for public criticism in Auditorium  
E204 of the Department of Physical Sciences, on December 13th,  
2002, at noon.*

Helsinki 2002

This thesis is dedicated to all those who have shown interest in my work and encouraged me when progress has been slow.

*Ut desint vires,  
tamen est laudanda voluntas.*

ISBN 952-10-0563-7  
ISSN 0356-0961  
Helsinki 2002  
Yliopistopaino

ISBN 952-10-0564-5 (PDF version)  
Helsinki 2002  
Helsingin yliopiston verkkojulkaisut  
<http://ethesis.helsinki.fi/>

# Preface

This thesis is a summary of research done at the Department of Physics of the University of Helsinki, and later at the Department of Physical Sciences and the Helsinki Institute of Physics (HIP), during the years 1998 - 2002. This research has mainly been funded by the University of Helsinki, the Academy of Finland and HIP. Fund grants by the V. K. & Y. Väisälä, M. Ehrnrooth and W. von Frenckell foundations are also gratefully acknowledged.

First and foremost, the author wishes to express his thanks to the esteemed colleague and supervisor of this thesis, Prof. Dan-Olof Riska, who in spite of numerous other pressing duties, including the directorship of HIP, has provided invaluable guidance, without which the completion of this thesis would have been a formidable task. Prof. Dan-Olof Riska and Doc. Mikko Sainio are also gratefully acknowledged by the author for providing a postgraduate researcher position at HIP. Special thanks are due to the chairman of the Department of Physical Sciences, Prof. Juhani Keinonen, for suggesting the referees for this thesis, and to Profs. Anthony Green and Jukka Maalampi for agreeing to referee the manuscript.

The author also wishes to thank all the colleagues at HIP and elsewhere that have in any way contributed to the research presented in this thesis. Special thanks are due to Prof. Anthony Green for his many suggestions and remarks, to Dr. Tomas Lindén for assistance with the typesetting of the manuscript, and to Dr. Christina Helminen, with whom the author has had many useful conversations. Instructive discussions with Profs. Keijo Kajantie, Paul Hoyer, Masud Chaichian, Andy Jackson, Carl Carlson, Doc. Claus Montonen, Doc. Jouni Niskanen, Dr. Gunnar Bali and Dr. M.R. Robilotta are also gratefully acknowledged.

Several other colleagues have also contributed indirectly, most notably Christer Nyfält, Krister Henriksson, Lars-Erik Hannelius, Mikko Jahma, Jonna Koponen and Pekko Piirola. The author has also enjoyed many instructive off-topic conversations with his colleagues at the Department of Theoretical Physics (TFO), the Laser Physics and X-ray Research Units and the group of Doc. Kai Nordlund.

The thorough nitpicking by Christer Nyfl, although a time-consuming source of irritation, is gratefully acknowledged by the author and has led to a substantial improvement in the mathematical quality of the manuscript, and in many cases to a better understanding of the underlying physics. Finally, all colleagues at HIP are acknowledged for the creation of a pleasant working atmosphere.

Helsingfors, October 2002

*Timo Lähde*

# Contents

<b>Preface</b>	<b>I</b>
<b>Abstract</b>	<b>IV</b>
<b>List of Publications</b>	<b>V</b>
<b>Short Introduction to the Papers</b>	<b>VI</b>
<b>1 Introduction</b>	<b>2</b>
1.1 The quark model . . . . .	2
1.2 Quantum Chromodynamics . . . . .	3
1.3 Heavy flavor mesons . . . . .	4
1.4 Transitions in heavy flavor mesons . . . . .	5
1.5 Notation and layout . . . . .	6
<b>2 Models for the Spectra of <math>Q\bar{Q}</math> and <math>Q\bar{q}</math> Mesons</b>	<b>7</b>
2.1 The BSLT quasipotential reduction . . . . .	7
2.2 The BSLT and Lippmann-Schwinger equations . . . . .	10
2.3 The $Q\bar{Q}$ interaction in the BSLT framework . . . . .	11
2.4 Relativistic $Q\bar{Q}$ potentials . . . . .	13
2.5 Spectra of heavy flavor mesons . . . . .	15
<b>3 Electromagnetic Transitions</b>	<b>19</b>
3.1 Charge density and electric dipole operators . . . . .	20
3.2 Current density and magnetic moment operators . . . . .	23
3.3 Widths for radiative decay . . . . .	26

3.4	E1 and M1 transitions in heavy quarkonia . . . . .	28
3.4.1	The M1 transition $J/\psi \rightarrow \eta_c \gamma$ . . . . .	28
3.4.2	The M1 transition $\psi' \rightarrow \eta_c \gamma$ . . . . .	28
3.4.3	Other M1 transitions . . . . .	29
3.4.4	The E1 transitions $\chi_{cJ} \rightarrow J/\psi \gamma$ and $\psi' \rightarrow \chi_{cJ} \gamma$ . . . . .	31
3.4.5	The E1 transitions from the $\chi_{bJ}$ states . . . . .	31
3.4.6	The E1 transitions from the $\Upsilon$ states . . . . .	33
3.4.7	Other E1 transitions . . . . .	33
3.5	M1 transitions in heavy-light mesons . . . . .	35
<b>4</b>	<b>Pionic Transitions</b>	<b>37</b>
4.1	The amplitude for pion emission . . . . .	38
4.2	The pionic widths of the $D$ mesons . . . . .	40
4.3	$\pi^0$ and $\gamma$ transitions from the $D_s^*$ meson . . . . .	41
4.4	Estimation of $f_{\eta_{NN}}$ . . . . .	42
<b>5</b>	<b>Two-pion Transitions</b>	<b>43</b>
5.1	The width for a $\pi\pi$ transition . . . . .	43
5.2	$\pi\pi$ transitions in heavy-light mesons . . . . .	45
5.3	$\pi\pi$ transitions in heavy quarkonia . . . . .	48
5.4	The transitions $\Upsilon' \rightarrow \Upsilon \pi\pi$ and $\psi' \rightarrow J/\psi \pi\pi$ . . . . .	52
<b>6</b>	<b>Conclusions</b>	<b>55</b>
	<b>Svenskspråkigt sammandrag</b>	<b>57</b>
	<b>Suomenkielinen tiivistelmä</b>	<b>59</b>
	<b>References</b>	<b>61</b>

T. Lähde: Strong and Electromagnetic Transitions in Heavy Flavor Mesons, University of Helsinki, 2002, VII, 65 p. + reprints, University of Helsinki Report Series in Physics, HU-P-D100, ISSN 0356-0961, ISBN 952-10-0563-7, ISBN 952-10-0564-5 (PDF version) <http://ethesis.helsinki.fi/>.

Classification (INSPEC): A1240Q, A1325, A1340F, A1340H, A1440L, A1440N

Keywords: charmed mesons, bottom mesons, pionic transitions, electromagnetic transitions, potential models

# Abstract

The electromagnetic and pionic transitions in mesons with heavy flavor charm ( $c$ ) or bottom ( $b$ ) quarks are calculated within the framework of the covariant Blankenbecler-Sugar (BSLT) equation. The magnetic dipole (M1) transitions in the charmonium ( $c\bar{c}$ ) system are shown to be sensitive to the relativistic aspect of the spin-flip magnetic moment operator, and the Lorentz coupling structure of the  $Q\bar{Q}$  interaction. The observed rate for the M1 transition  $J/\psi \rightarrow \eta_c \gamma$  is shown to provide strong evidence for a scalar confining interaction. On the other hand, the electric dipole (E1) transitions are shown to be sensitive to the hyperfine splittings in the  $Q\bar{Q}$  system, and to require a nonperturbative treatment of the hyperfine components in the  $Q\bar{Q}$  interaction.

In addition to the spin-flip M1 transitions, the single pion ( $\pi$ ) and dipion ( $\pi\pi$ ) widths are calculated for the heavy-light ( $Q\bar{q}$ )  $D$  mesons, by employment of the pseudovector pion-quark coupling suggested by chiral perturbation theory. The pionic transitions  $D^* \rightarrow D\pi$  are shown to provide useful and constraining information on the pion-quark axial coupling  $g_A^q$ . It is also shown that axial exchange charge contributions associated with the  $Q\bar{q}$  interaction suppress the axial charge amplitude for pion emission by an order of magnitude. The models for  $\pi$  and M1 transitions also make it possible to estimate the  $\eta$ -nucleon coupling from the transition  $D_s^* \rightarrow D_s \pi^0$ , once the value of the  $\pi^0 - \eta$  mixing angle is known.

Finally, the  $\pi\pi$  dipion transition rates of the  $L = 1$   $D$  mesons are calculated, and are shown to make up a significant fraction of their total widths for strong decay. The  $\pi\pi$  transitions between  $S$ -wave charmonium ( $c\bar{c}$ ) and bottomonium ( $b\bar{b}$ ) states are modeled in terms of a broad  $\sigma$  meson or a glueball, with derivative couplings to pions. The effects of pion rescattering by the spectator quark are also investigated.

# List of Publications

This thesis consists of two parts. The first and main part of the thesis is a summary and discussion of the results obtained in the published, peer-reviewed research papers listed below. Where available, newer and more accurate results are also presented. The second part consists of reprints of selected papers that have been signed by the author. These papers are based on research done at the Department of Physical Sciences of the University of Helsinki and the Helsinki Institute of Physics in 1998 - 2002.

- I** T.A. Lähde, C.J. Nyfält and D.O. Riska,  
*The Confining Interaction and Radiative Decays of Heavy Quarkonia*,  
Published in: Nucl.Phys.**A645:587-603** (1999), eprint hep-ph/9808438
- II** K.O.E. Henriksson, T.A. Lähde, C.J. Nyfält and D.O. Riska,  
*Pion Decay Widths of D Mesons*,  
Published in: Nucl.Phys.**A686:355-378** (2001), eprint hep-ph/0009095
- III** T.A. Lähde and D.O. Riska,  
*Two-Pion Decay Widths of Excited Charm Mesons*,  
Published in: Nucl.Phys.**A693:755-774** (2001), eprint hep-ph/0102039
- IV** T.A. Lähde and D.O. Riska,  
*Pion Rescattering in Two-Pion Decay of Heavy Quarkonia*,  
Published in: Nucl.Phys.**A707:425-451** (2002), eprint hep-ph/0112131
- V** T.A. Lähde and D.O. Riska,  
*The Coupling of  $\eta$  Mesons to Quarks and Baryons from  $D_s^* \rightarrow D_s \pi^0$  Decay*,  
Published in: Nucl.Phys.**A710:99-116** (2002), eprint hep-ph/0204230
- VI** T.A. Lähde,  
*Exchange Current Operators and Electromagnetic Dipole Transitions  
in Heavy Quarkonia*,  
Published in: to be published in Nucl.Phys.**A**, eprint hep-ph/0208110

# Short Introduction to the Papers

- I** This paper presents a calculation of the M1 transition rates in the  $c\bar{c}$  and  $b\bar{b}$  systems within the framework of the nonrelativistic Schrödinger equation. A relativistic version of the single quark spin-flip magnetic moment operator is derived, along with the two-quark exchange current operators for M1 transitions. It is shown that the two-quark operator associated with a scalar confining interaction may provide, together with the relativistic single quark operator, a possible explanation of the empirically measured width of  $\sim 1$  keV for the transition  $J/\psi \rightarrow \eta_c\gamma$ .
- II** The framework of the covariant Blankenbecler-Sugar (BSLT) equation is used together with the pseudovector pion-quark coupling suggested by chiral perturbation theory to predict the widths for pionic transitions in the heavy-light ( $c\bar{q}$ )  $D$  meson systems. It is found that useful and constraining information on the pion-quark axial coupling  $g_A^q$  is provided by the  $D^* \rightarrow D\pi$  transitions. A satisfactory description of the empirically measured pion widths of the  $L = 1$   $D_2^*$  meson is obtained. Also, the axial charge component of the amplitude for pion emission is shown to be suppressed by axial exchange charge contributions associated with the  $Q\bar{q}$  interaction.
- III** The chiral pseudovector Lagrangian, augmented by a Weinberg-Tomozawa term for dipion emission, is used to predict the widths for  $\pi\pi$  transitions from the  $L = 1$   $D$  mesons. It is found that widths of several MeV are expected for these transitions, in analogy with the experimentally well-studied decays of the strange  $K_2^*$  meson. It is thus expected that the  $\pi\pi$  modes should constitute a significant fraction of the total widths of the  $L = 1$   $D$  mesons.
- IV** The dipion transitions between  $S$ -wave states in the charmonium ( $c\bar{c}$ ) and bottomonium ( $b\bar{b}$ ) systems are studied using a phenomenological model with derivative couplings to pions. The dipions are modeled in terms of a broad  $\sigma$  meson or a glueball. Effects of pion rescattering by the spectator quark are investigated and shown to be small for  $2S \rightarrow 1S$  transitions. The present experimental data on these transitions is shown to constrain the  $\sigma$  meson mass to about 500 MeV. Finally, it is demonstrated that the anomalous double-peaked  $\pi\pi$  spectrum of the  $\Upsilon(3S) \rightarrow \Upsilon(1S)\pi\pi$  transition may be modeled in terms of a heavier  $\sim 1500$  MeV scalar meson.

- V** The empirically measured branching ratios for  $D_s^* \rightarrow D_s \pi^0$  and  $D_s^* \rightarrow D_s \gamma$  are shown to provide a means of determining the strength of the  $\eta$  coupling to quarks and baryons. This requires that the value of the  $\pi^0 - \eta$  mixing angle is available, along with realistic models for the M1 and pionic transitions in heavy-light mesons. The value thus obtained for the  $\eta$ -nucleon pseudovector coupling  $f_{\eta NN}$  is shown to be much smaller than that suggested by  $SU(3)$  symmetry, which is consistent with other recent phenomenological analyses. It is also shown that a significant  $\eta$ -charm coupling, if present, serves to increase the estimated value of  $f_{\eta NN}$ .
- VI** The two-quark exchange current operators that arise from the elimination of the negative energy components of the Bethe-Salpeter equation in the BSLT quasipotential reduction, are calculated for electromagnetic E1 and M1 transitions in heavy quarkonium systems. Although the exchange charge operators that contribute to E1 transitions are shown to be mostly negligible, the corresponding exchange current operators for M1 transitions are shown to be crucial, if agreement with the empirical width for  $J/\psi \rightarrow \eta_c \gamma$  is to be achieved. This requires that the effective confining interaction couples as a Lorentz scalar, since an effective vector interaction is shown to yield a spin-flip magnetic moment operator only if the constituent quark masses are unequal. Consequently, in the  $B_c^\pm$  system, the one-gluon exchange interaction also contributes a two-quark spin-flip operator.

# Chapter 1

## Introduction

It has been widely accepted, since the beginning of the 20th century, that the visible matter in the universe is composed of protons and neutrons (or baryons), and electrons (or leptons). However, the discovery of the positron in 1933, predicted by Dirac a few years earlier, suggested that short-lived, transient particles may exist alongside the stable protons and electrons. This was confirmed in 1936, when a heavier, unstable electron-like particle, the muon ( $\mu$ ), was discovered in cosmic ray experiments by Anderson and Neddermeyer. This discovery was followed up in 1947, when the existence of the neutral ( $\pi^0$ ) and charged ( $\pi^\pm$ ) pions, predicted earlier by Yukawa to be the carriers of the strong nuclear force, was confirmed by a similar experiment. These particles were the first ones of a large number of short-lived, unstable baryons, mesons and leptons which were subsequently produced in copious numbers by accelerator experiments. In particular, the pions were shown to be the lightest members of a new family of particles known as mesons, to denote that they are intermediate in mass between the baryons and leptons.

### 1.1 The quark model

Around 1960, the number of short-lived baryons ( $\Delta, \Sigma, \Lambda, \Xi \dots$ ) and mesons ( $\pi, K, \rho, \eta \dots$ ) that had been discovered by accelerator experiments was overwhelming. This suggested that the hypothesis of Mendeleev could be extended to the baryons and mesons; Rather than being elementary, they might possess substructure and could perhaps be classified according to a "periodic table" of subatomic particles. This notion, originally put forward by Gell-Mann [1] and Ne'eman [2] among others, became known as the "Quark Model" and attempts to explain the observed properties (spin, isospin, electric charge, parity) of the mesons and baryons by arranging them into multiplets according to the symmetry group  $SU(3)$ . It was found that three quark flavors, "up" ( $u$ ), "down" ( $d$ ) and "strange" ( $s$ ) with spin 1/2 and fractional electric charges were required to accommodate all of the mesons and baryons known at that time.

The experimental discovery [3] of the  $\Omega$  baryon, which was predicted by the quark model because of a gap in the "periodic table" of the baryons, soon provided dramatic confirmation of the quark hypothesis. Although the quarks were at first only thought of as a useful theoretical tool, their actual existence inside the proton was confirmed [4] by

deep inelastic  $e^-p$  scattering (DIS) experiments at high energies. However, in spite of these remarkable successes, the quark model soon ran into a difficulty of symmetry. The spin-parity quantum numbers of the  $\Delta$  resonance were empirically found to be consistent with a combined spin-flavor and configuration space wavefunction which is symmetric. This is inconsistent with Fermi-Dirac statistics, which requires that the total baryon wavefunction should be antisymmetric.

This critical problem was finally circumvented by the introduction of a new property for the quarks, "color", which allows the wavefunction to be made antisymmetric by means of three color quantum numbers. In order to avoid an undesirable proliferation of unobserved states, a further constraint was placed, namely that the quarks only combine into colorless states (or singlet representations of the color  $SU(3)_C$  group). This restricts the possible ways of combining quarks and antiquarks to hadrons, the simplest being  $q\bar{q}$  (mesons),  $qqq$  (baryons) and  $\bar{q}\bar{q}\bar{q}$  (antibaryons). Together with the proposal [5] that eight spin 1 gauge fields, "gluons", should be associated with the new symmetry group  $SU(3)_C$ , these notions were eventually developed into the theory of strong interactions, called Quantum Chromodynamics (QCD) [6].

It was also realized that a fourth quark is required in the theory of weak interactions to explain e.g. the observed rate for the decay  $K^0 \rightarrow \mu^+\mu^-$ . The fourth quark was eventually discovered in the form of narrow resonances [7] in November 1974 at center-of-mass energies of 3.1 GeV and 3.7 GeV in  $e^+e^-$  annihilation and, independently, in proton-proton collisions. These resonances, named  $J/\psi$  and  $\psi'$ , were interpreted as mesonic bound states of the new "charm" quark and its antiquark,  $c\bar{c}$ . The charm quark turned out to have a mass of  $\sim 1500$  MeV, and is thus much more massive than the  $\sim 5$  MeV  $u, d$  quarks and the  $\sim 100$  MeV  $s$  quark. Later, as higher collision energies became available, an unexpected "bottom" ( $b$ ) quark with a mass of  $\sim 4800$  MeV was similarly discovered in the form of  $b\bar{b}$  or  $\Upsilon$  mesons. This again raised the question of a possible partner for the  $b$  quark, and indeed an extraordinarily heavy "top" ( $t$ ) quark was finally detected [8] in 1995, by the proton-antiproton collider experiments at Fermilab. The  $t$  quark turned out to have a mass of 175 GeV, which makes it the most massive elementary particle known, and it is too short-lived for mesonic  $t\bar{t}$  bound states to form.

## 1.2 Quantum Chromodynamics

In the theory of Quantum Chromodynamics (QCD), the interactions between quarks are mediated by eight massless vector bosons called gluons. However, a number of complications effectively prevent the properties of hadrons to be predicted from QCD; First of all, the theory is nonlinear due to gluon self-interactions, and it describes systems that interact strongly enough so that perturbative methods are inapplicable. Only at the very highest energy scales, where quarks become asymptotically free and the coupling between them small, can the predictions of perturbative QCD be compared with experimental results. At low energies, the quarks interact strongly, are confined into hadronic bound states and acquire effective masses. These constituent quark masses are for the light  $u, d$  quarks of the order  $\sim 400$  MeV.

At present, the only way to analyze QCD at a fundamental level is the method of "lattice QCD" simulations, where the properties of hadrons are probed by means of numerical Monte Carlo algorithms. Although much progress is being made in the development

of more efficient algorithms and the inclusion of dynamical fermions (unquenched lattice QCD) into the simulations, the applicability of such methods is still limited by the huge demands on computing power. In such a situation, it is natural to attempt to understand the properties of hadrons by means of effective theories and phenomenological, QCD-motivated models. The physical motivation of such an approach is that the fundamental degrees of freedom of QCD are quarks and gluons, whereas low-energy experiments observe hadrons, which at least at long range interact by Yukawa-type meson exchange. It is, therefore, a reasonable expectation that the low-energy properties of QCD can be described in terms of an effective theory. In the limit of vanishing quark masses, QCD exhibits an invariance under chiral transformations that involve left- and right-handed quark fields separately. This symmetry is only approximate for quarks with a nonzero mass. The absence of parity doublets in the low-energy region of the hadron spectra suggests that this chiral symmetry is spontaneously broken at low energies [9].

### 1.3 Heavy flavor mesons

Mesons that contain either two heavy quarks ( $c\bar{c}$ ,  $b\bar{b}$ ,  $c\bar{b}$ ) or one heavy quark and one light ( $c\bar{q}$ ,  $c\bar{s}$ ,  $b\bar{q}$ ,  $b\bar{s}$ ) are special, since their masses lie in a region which is intermediate between the high-energy perturbative regime of QCD and the low-energy regime where the dynamics are governed by chiral symmetry breaking. Thus these heavy flavor mesons are likely to share features that are encountered in these two limits of QCD. One task at hand is then to determine phenomenologically, or from lattice QCD [10], the functional form, strength and Lorentz structure of the  $Q\bar{q}$  and  $Q\bar{Q}$  interaction.

Although the nonrelativistic Schrödinger framework [11] can be applied to  $Q\bar{Q}$  systems with some success, a realistic treatment of the  $Q\bar{q}$  system has *a priori* to be relativistic, as the velocity of the confined light constituent quark is close to that of light. The papers presented in this thesis employ the covariant Blankenbecler-Sugar (BSLT) reduction [12] of the Bethe-Salpeter equation, which has the advantage of formal similarity to the Schrödinger framework. An alternate approach is provided by the Gross quasipotential reduction [13], which has been shown [14] to yield comparable results for the spectra of  $Q\bar{Q}$  and  $Q\bar{q}$  mesons.

However, as the mass spectra of the  $Q\bar{Q}$  and  $Q\bar{q}$  mesons are well described [15] by a large number of phenomenological and QCD-motivated models, the spectrum alone cannot discriminate between different assumptions for the  $Q\bar{Q}$  and  $Q\bar{q}$  interaction. Fortunately, as will be shown in this thesis, the observed rates for  $\gamma$  and  $\pi$  transitions in heavy flavor mesons may provide useful and constraining information on the quark-antiquark interaction, the quarkonium wave functions, and in particular, on the Lorentz structure of the effective confining interaction. As the negative energy components of the Bethe-Salpeter equation are eliminated in the BSLT (or Schrödinger) quasipotential reduction, two-quark transition operators that depend explicitly on the Lorentz structure of the  $Q\bar{Q}$  interaction appear as a consequence [16]. In particular, it will be demonstrated in this thesis that a pure scalar confining interaction compares favorably with the current empirical knowledge of M1 transitions in the charmonium system. It is noteworthy, that similar results have been obtained within the instantaneous approximation to the Bethe-Salpeter equation [17], which treats the negative energy components explicitly, i.e. without two-quark currents.

## 1.4 Transitions in heavy flavor mesons

The transitions considered in this thesis include the radiative E1 and M1 transitions in the  $Q\bar{Q}$  systems, the M1 transitions in the heavy-light charm ( $D$ ) and strange charm ( $D_s$ ) mesons, and the  $\pi$  and  $\pi\pi$  transitions in the  $Q\bar{Q}$  and  $Q\bar{q}$  systems. It is shown in papers **I** and **VI** that a possible solution to the long-standing overprediction [18] by a factor  $\sim 3$  of the width for the M1 transition  $J/\psi \rightarrow \eta_c\gamma$  emerges, if the two-quark exchange current operator associated with a scalar confining interaction is included along with a relativistic treatment of the single quark spin-flip operator.

On the other hand, the exchange charge contributions [19] to the E1 transition rates are shown in paper **VI** to be highly suppressed by the large masses of the charm and bottom constituent quarks [20]. Similarly, the nonrelativistic predictions for the spin-flip M1 widths of the  $Q\bar{q}$  mesons are shown in paper **V** to be unrealistic, as the confined light constituent quark requires a relativistic treatment. It is also shown that accidental cancellations in the single quark spin-flip operators render the M1 widths very sensitive to two-quark exchange current contributions. However, as the form of the  $Q\bar{q}$  interaction is uncertain, the results are suggestive rather than definite, quantitative predictions.

In the heavy-light  $D$  mesons, the excited states decay to the ground state predominantly through pion emission. In this thesis, the pionic transitions in the  $D$  mesons are described in terms of the chiral pseudovector Lagrangian which couples the pions to the light constituent quarks. It is shown in paper **II** that the  $D^* \rightarrow D\pi$  transitions can provide useful and constraining information on the pion-quark axial coupling  $g_A^q$ . Also, the axial charge component of the amplitude for pion emission is shown to be highly affected by two-quark axial exchange charge contributions associated with the  $Q\bar{q}$  interaction. The pionic transitions which are driven by the axial charge operator may, therefore, provide information on the Lorentz structure of the  $Q\bar{q}$  interaction. In particular, it is shown that a scalar confining interaction has the effect of reducing the widths for such transitions.

The chiral Lagrangian may, when augmented with a Weinberg-Tomozawa term for dipion emission, describe the  $\pi\pi$  widths of the excited  $L = 1$   $D$  mesons. In this thesis the  $\pi\pi$  widths of the  $D$  mesons are shown to be of significant magnitude compared to the widths for single pion emission. This is known to be the case for the strange  $K_2^*$  meson, where the empirical  $\pi\pi$  width is  $\sim 1/2$  of the  $\pi$  width. This model for pseudoscalar emission has also been applied to the  $D_s^* \rightarrow D_s\pi^0$  transition, which can then be used to extract the coupling of  $\eta$  mesons to quarks and baryons from the empirical branching ratios for those transitions, once an estimate for the  $\pi^0 - \eta$  mixing angle is available. The value for the  $\eta$ -nucleon pseudovector coupling constant  $f_{\eta NN}$  so obtained, is shown to be much smaller than that suggested by naive  $SU(3)$  symmetry, but consistent with other recent phenomenological analyses of e.g. photoproduction of  $\eta$  mesons on the nucleon.

Whereas the dipion transitions in the  $D$  mesons may be modeled in terms of the chiral Lagrangian, the  $\pi\pi$  transitions between  $S$ -wave  $c\bar{c}$  or  $b\bar{b}$  states are likely to involve a broad  $\sigma$  meson or a glueball. It is shown, within a model where the coupling of dipions to heavy quarks is mediated by a broad and heavy scalar meson, that the empirical  $\pi\pi$  energy spectra constrain the  $\sigma$  meson mass to  $\sim 500$  MeV. A possible explanation for the anomalous double-peaked  $\pi\pi$  spectrum of the  $\Upsilon(3S) \rightarrow \Upsilon(1S)\pi\pi$  transition is obtained, if the  $\pi\pi$  emission is described in terms of a heavier ( $\sim 1500$  MeV) scalar meson.

## 1.5 Notation and layout

Throughout this thesis, the natural units with  $\hbar c = 1$  and the  $\delta_{\mu\nu}$  metric have been employed. The Euclidean  $\delta_{\mu\nu}$  or Pauli metric assigns imaginary time components to four-vectors. The momentum four-vector  $k$  is thus of the form  $k = (\mathbf{k}, ik_0)$ , where the three-vector has been denoted by bold-faced type. However, for typesetting reasons, three-vectors in exponents have been denoted with an arrow, according to  $\vec{k}$ . Also, in obvious cases the modulus  $|\mathbf{k}|$  has been denoted simply by  $k$ . In the Pauli metric the square of a four-vector is of the form

$$k^2 = k_\mu k_\mu = \mathbf{k}^2 - k_0^2 = -m^2, \quad (1.1)$$

and the Dirac  $\gamma_\mu$  matrices are all hermitian with square equal to one. The explicit form of these matrices in the Pauli metric is then  $\gamma_\mu = (\boldsymbol{\gamma}, \gamma_4)$  and  $\gamma_5 = \gamma_1 \gamma_2 \gamma_3 \gamma_4$ , where

$$\boldsymbol{\gamma} = \begin{pmatrix} 0 & -i\boldsymbol{\sigma} \\ i\boldsymbol{\sigma} & 0 \end{pmatrix}, \quad \gamma_4 = \begin{pmatrix} \mathbf{1} & 0 \\ 0 & -\mathbf{1} \end{pmatrix}, \quad \gamma_5 = \begin{pmatrix} 0 & -\mathbf{1} \\ -\mathbf{1} & 0 \end{pmatrix}. \quad (1.2)$$

Factors of  $i$  are also introduced into the Dirac current and charge density operators to make them real-valued, and for Lagrangians which include a  $\gamma_5$ , in order to assure hermiticity.

A number of abbreviations that are frequently used in this thesis are OGE (one-gluon exchange), BSLT (Blankenbecler-Sugar-Logunov-Tavkhelidze), NRIA (non-relativistic impulse approximation) and RIA (relativistic impulse approximation). Excited states in the heavy quarkonium systems have been denoted either by the  $\psi(nJ)$  or the primed notation, where the  $n$ th excited state is denoted by  $n$  primes, e.g.  $\psi(3S) \equiv \psi'''$ . Note that in the primed notation, the primes refer to radial excitations only.

This thesis contains a summary which comprises six chapters, and reprints of selected research papers that have been signed by the author. Chapter 2 of the summary presents the Blankenbecler-Sugar quasipotential reduction, the  $Q\bar{Q}$  and  $Q\bar{q}$  Hamiltonian models and the numerical results for the spectra of the heavy flavor mesons. Chapter 3 discusses the calculations of the electromagnetic E1 and M1 widths of papers **I**, **V** and **VI**, while chapter 4 presents the calculation of the pionic transitions in the  $D$  mesons of paper **II** and the estimation of the  $\eta$ -nucleon pseudovector coupling  $f_{\eta NN}$  from paper **V**. Chapter 5 deals with the  $\pi\pi$  transitions in the  $D$  mesons (paper **III**) and the model for the  $\pi\pi$  transitions in the  $Q\bar{Q}$  mesons from paper **IV**. Chapter 6 contains a concluding discussion.

## Chapter 2

# Models for the Spectra of $Q\bar{Q}$ and $Q\bar{q}$ Mesons

Although several phenomenological models that employ a nonrelativistic treatment of the heavy quarkonia [11] have succeeded in describing many features of the  $c\bar{c}$  and  $b\bar{b}$  systems, a realistic treatment of the heavy-light mesons has *a priori* to be relativistic as the velocity of the confined light constituent quark is close to that of light. Also in the case of charmonium and bottomonium, the compact size of the  $Q\bar{Q}$  system causes the charm and bottom quarks to move with relativistic velocities, in spite of their large masses. The reason for this is the effective confining interaction, which has a string tension of  $\sim 1$  GeV/fm and confines the constituent quarks to a region of radius  $< 0.5$  fm. In this situation, a quasipotential reduction of the relativistic Bethe-Salpeter equation suggests itself as a natural framework for a covariant description of the heavy quarkonium systems.

### 2.1 The BSLT quasipotential reduction

The field-theoretical scattering matrix  $S$  may be written in the form

$$S_{fi} = \delta_{fi} - i(2\pi)^4 \delta(P_f - P_i) \mathcal{M}_{fi}, \quad (2.1)$$

where the second term on the r.h.s. has been defined, for notational convenience, with a minus sign. The scattering amplitude  $M$  is then defined as

$$\mathcal{M}_{fi} = \bar{u}(\mathbf{p}'_Q) \bar{u}(\mathbf{p}'_q) M u(\mathbf{p}_Q) u(\mathbf{p}_q), \quad (2.2)$$

where  $p_i$  and  $p'_i$  denote the initial and final four-momenta of the quarks. Note that the antiquark will be described throughout by positive energy spinors. The Bethe-Salpeter equation for the scattering amplitude  $M$  can then be written (schematically) in the form

$$M = K + K G M, \quad (2.3)$$

or explicitly, for an arbitrary frame, as

$$M(p', p, P) = K(p', p, P) + i \int \frac{d^4 k}{(2\pi)^4} K(p', k, P) G(k, P) M(k, p, P), \quad (2.4)$$

where  $P$  is the total four-momentum of the  $Q\bar{q}$  system, and  $p, k$  and  $p'$  denote the initial, intermediate, and final relative four-momenta of the constituent quarks. In eq. (2.4),  $K$  denotes the interaction kernel of the Bethe-Salpeter equation, which in the nonrelativistic limit corresponds to the potential defined for the Schrödinger equation. This can be seen by comparison of eq. (2.3) and eq. (2.1) in the Born approximation. Also,  $G$  denotes the Green's function of the Bethe-Salpeter equation, which is here taken to be the free fermion propagator. When bound states are considered, the inhomogeneous term in eq. (2.4) is dropped. The second term of the Bethe-Salpeter scattering equation is illustrated, along with the choice of momentum variables for the Blankenbecler-Sugar quasipotential reduction, by Fig. 2.1.

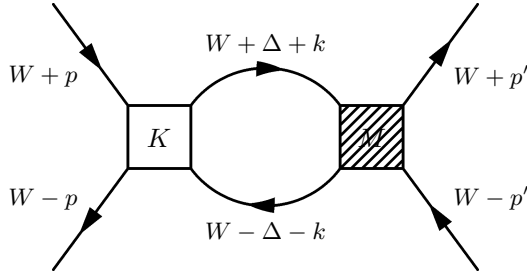


Figure 2.1: Illustration of the choice of frame and variables for the derivation of the Blankenbecler-Sugar (BSLT) reduction of the Bethe-Salpeter scattering equation for unequal quark masses. The upper and lower quark lines are taken to have masses  $m_Q$  and  $m_{\bar{q}}$ , respectively. The four-momenta are defined as  $W = (0, iP_0/2)$ ,  $\Delta = (0, i[m_Q^2 - m_{\bar{q}}^2]/4W_0)$ ,  $p = (\mathbf{p}, ip_0)$  and  $k = (\mathbf{k}, ik_0)$ .

It is instructive, in order to perform the BSLT quasipotential reduction, to introduce the variables presented in Fig. 2.1 and write the Bethe-Salpeter equation, schematically, as two coupled integral equations,

$$M = U + U g M \quad (2.5)$$

$$U = K + K (G - g) U. \quad (2.6)$$

Here the quasipotential  $U$  is defined by eq. (2.6) in terms of the Bethe-Salpeter propagator  $G$  and a three-dimensional propagator  $g$ . The propagator  $g$  is then constructed so that it has an identical elastic unitarity cut (right hand cut) as  $G$  in the physical region. The approximation  $U \simeq K$  will be employed here, in order to arrive at a major simplification of the Bethe-Salpeter problem. The propagators  $G$  and  $g$  will have identical discontinuities across the right hand cut if  $\text{Disc } G = 2i \text{Im } g$ . By means of the Cutkosky rules,  $\text{Im } g$  may then be obtained as

$$\text{Im } g = -\frac{2\pi^2}{(2\pi)^4} [\gamma^Q (W + k + \Delta) + im_Q] [\gamma^{\bar{q}} (W - k - \Delta) + im_{\bar{q}}] \delta^{(+)} [(W + k + \Delta)^2 + m_Q^2] \delta^{(+)} [(W - k - \Delta)^2 + m_{\bar{q}}^2], \quad (2.7)$$

where it has been indicated that only the positive energy roots of the arguments in the delta functions are to be included. The complete propagator  $g$  is then reconstructed by

means of the dispersion integral

$$g = \frac{1}{\pi} \int_0^\infty \frac{d\mathbf{q}^2}{\mathbf{q}^2 - \mathbf{p}^2 - i\epsilon} \text{Im } g(W', k, \Delta'), \quad (2.8)$$

where  $W'$  is defined as  $q_0/2$  with  $q_0$  on shell. Evaluation of the above integral yields the following form for the BSLT propagator  $g$ :

$$g = -\frac{1}{2} \frac{\delta(k_0)}{(2\pi)^3} \frac{[\gamma_0^Q E_Q(\mathbf{k}) - \gamma^Q \cdot \mathbf{k} - im_Q] [\gamma_0^{\bar{q}} E_{\bar{q}}(\mathbf{k}) + \gamma^{\bar{q}} \cdot \mathbf{k} - im_{\bar{q}}]}{(E_Q(\mathbf{k}) + E_{\bar{q}}(\mathbf{k})) (\mathbf{k}^2 - \mathbf{p}^2 - i\epsilon)}, \quad (2.9)$$

where the delta function ensures the condition  $k_0 = 0$  in the resulting three-dimensional integral equation. Note that the (in principle arbitrary) variable  $\Delta$  was chosen so that this condition is realized also in the case of unequal constituent quark masses. By introduction of the positive energy projection operators  $\Lambda_+^i$ , the above propagator can be written in the form

$$g = -\frac{\delta(k_0)}{(2\pi)^3} \frac{2m_Q m_{\bar{q}}}{E_Q(\mathbf{k}) + E_{\bar{q}}(\mathbf{k})} \frac{\Lambda_+^Q(\mathbf{k}) \Lambda_+^{\bar{q}}(-\mathbf{k})}{\mathbf{k}^2 - \mathbf{p}^2 - i\epsilon}. \quad (2.10)$$

This form is convenient when matrix elements are taken between positive-energy spinors according to

$$\mathcal{M}, \mathcal{V}(\mathbf{p}', \mathbf{p}) = \bar{u}_Q(\mathbf{p}') \bar{u}_{\bar{q}}(-\mathbf{p}') M, U(\mathbf{p}', \mathbf{p}) u_Q(\mathbf{p}) u_{\bar{q}}(-\mathbf{p}), \quad (2.11)$$

which, together with eq. (2.5), yields the three-dimensional BSLT scattering equation

$$\mathcal{M}(\mathbf{p}', \mathbf{p}) = \mathcal{V}(\mathbf{p}', \mathbf{p}) - \int \frac{d^3k}{(2\pi)^3} \mathcal{V}(\mathbf{p}', \mathbf{k}) \left( \frac{2m_Q m_{\bar{q}}}{E_Q(\mathbf{k}) + E_{\bar{q}}(\mathbf{k})} \right) \frac{1}{\mathbf{k}^2 - \mathbf{p}^2 - i\epsilon} \mathcal{M}(\mathbf{k}, \mathbf{p}), \quad (2.12)$$

where  $\mathcal{V}$  denotes the nonlocal interaction operator as obtained from the Feynman rules for  $S_{fi}$  using eq. (2.1) in the Born approximation. The above extension of the original BSLT equation to the case of unequal masses is similar to that of ref. [21], which has been employed in ref. [22] for the case of  $\Lambda N$  scattering.

The elimination of the negative energy components of the Bethe-Salpeter equation in the derivation of eq. (2.12) has been shown [16] to give rise to two-quark exchange current operators that depend explicitly on the Lorentz structure of the quark-antiquark interaction. These may then contribute significantly to the strong and electromagnetic transition rates in the  $Q\bar{q}$  and  $Q\bar{Q}$  systems. In particular, the exchange current operator associated with the scalar confining interaction has been shown to be of decisive importance for the M1 transitions of heavy quarkonia [23]. It should be noted that the appearance of such two-quark operators depends on the type of quasipotential reduction.

Although eq. (2.12) is a widely used quasipotential reduction of the type discussed in this thesis, there is in principle an infinite number of different ways to reduce the Bethe-Salpeter equation to a 3-dimensional form. Another commonly used reduction is the Thompson equation [24], which differs from the BSLT equation by the choice of the dispersion integral (2.8). These have been shown to produce results that are very close to the full Bethe-Salpeter equation in ref. [25]. There exists also a large variety of quasipotential reductions that differ in the choice of the propagator (2.10), which attempt to include the effects of intermediate negative energy states by various combinations of the negative energy projection operators [26].

It is also noteworthy that the Bethe-Salpeter equation in the ladder approximation has been shown [27], not to reduce to the desired one-body (Dirac) equation when one of the quarks becomes much heavier than the other. However, a large number of quasipotential reductions (e.g. Gross) are known to be closely related to the Dirac equation. This suggests that such reductions are more appropriate for two-quark systems with a large difference between the constituent masses, while the BSLT equation is ideal for quarkonia such as  $c\bar{c}$  and  $b\bar{b}$ . As the light constituent quarks in  $Q\bar{q}$  mesons have masses that are lighter than those of the heavy quarks by factors of 3 – 10, then the Gross and BSLT reductions are expected to give results of similar quality, which indeed appears to be the case [14].

## 2.2 The BSLT and Lippmann-Schwinger equations

As eq. (2.12) is similar to the nonrelativistic Lippmann-Schwinger equation, except for the factor in parentheses, then it can be transformed into such an equation by means of the "minimal relativity" ansatz [28]

$$T(\mathbf{p}', \mathbf{p}) = \left( \frac{m_Q + m_{\bar{q}}}{E_Q(\mathbf{p}') + E_{\bar{q}}(\mathbf{p}')} \right)^{\frac{1}{2}} \mathcal{M}(\mathbf{p}', \mathbf{p}) \left( \frac{m_Q + m_{\bar{q}}}{E_Q(\mathbf{p}) + E_{\bar{q}}(\mathbf{p})} \right)^{\frac{1}{2}}, \quad (2.13)$$

$$V(\mathbf{p}', \mathbf{p}) = \left( \frac{m_Q + m_{\bar{q}}}{E_Q(\mathbf{p}') + E_{\bar{q}}(\mathbf{p}')} \right)^{\frac{1}{2}} \mathcal{V}(\mathbf{p}', \mathbf{p}) \left( \frac{m_Q + m_{\bar{q}}}{E_Q(\mathbf{p}) + E_{\bar{q}}(\mathbf{p})} \right)^{\frac{1}{2}}. \quad (2.14)$$

This yields the equation

$$T(\mathbf{p}', \mathbf{p}) = V(\mathbf{p}', \mathbf{p}) - \int \frac{d^3k}{(2\pi)^3} V(\mathbf{p}', \mathbf{k}) \frac{2\mu}{\mathbf{k}^2 - \mathbf{p}^2 - i\epsilon} T(\mathbf{k}, \mathbf{p}), \quad (2.15)$$

which is formally identical to the Lippmann-Schwinger equation. Here  $\mu$  stands for the usual reduced mass of the two-quark system. The advantage of eq. (2.15) is that it can be transformed to a Schrödinger-type differential equation where the potential is given by eq. (2.14). This transformation gives the differential equation

$$\left( H_0 - \frac{\mathbf{p}^2}{2\mu} \right) \psi_{\text{nlm}}(\mathbf{r}) = -V \psi_{\text{nlm}}(\mathbf{r}), \quad (2.16)$$

where  $H_0$  is the kinetic energy operator of the nonrelativistic Schrödinger equation. The factor  $\mathbf{p}^2$  can be expressed in terms of the total energy of the  $Q\bar{q}$  state and the constituent quark masses  $m_Q$  and  $m_{\bar{q}}$ .

The eigenvalue  $\varepsilon$  of the BSLT equation is obtained as

$$\varepsilon = \frac{\mathbf{p}^2}{2\mu} = \frac{[E^2 - (m_Q + m_{\bar{q}})^2][E^2 - (m_Q - m_{\bar{q}})^2]}{8\mu E^2}, \quad (2.17)$$

where  $E$  is the mass of the  $Q\bar{q}$  state. The BSLT equation can thus be expressed as an eigenvalue equation of the form

$$(H_0 + H_{\text{int}}) \psi_{\text{nlm}}(\mathbf{r}) = \varepsilon \psi_{\text{nlm}}(\mathbf{r}), \quad (2.18)$$

where the interaction Hamiltonian  $H_{\text{int}}$  is given in terms of the potential defined in eq. (2.14). The introduction of the quadratic mass operator (2.17) leads to an effective weakening of the repulsive kinetic energy operator, which means that higher excited states will have lower masses in the BSLT equation than they would in the Schrödinger framework. The BSLT eigenvalue  $\varepsilon$ , expressed in terms of the Schrödinger excitation energy  $E_{\text{ex}} = E - (m_1 + m_2)$ , is of the form

$$\varepsilon = \frac{E_{\text{ex}}}{8\mu} \left[ \frac{(E_{\text{ex}} + 2(m_Q + m_{\bar{q}}))(E_{\text{ex}}^2 + 2E_{\text{ex}}(m_Q + m_{\bar{q}}) + 4m_Q m_{\bar{q}})}{E_{\text{ex}}^2 + 2E_{\text{ex}}(m_Q + m_{\bar{q}}) + (m_Q + m_{\bar{q}})^2} \right], \quad (2.19)$$

where the expression in parentheses tends toward  $8\mu$  when  $m_Q, m_{\bar{q}} \rightarrow \infty$ . This demonstrates that in the limit of heavy quark masses, or when the quark masses become large compared to the excitation energy  $E_{\text{ex}}$ , the BSLT equation reduces to the nonrelativistic Schrödinger equation.

Although the role of the BSLT potential  $V$  as given by eq. (2.14) is equivalent to that of the nonrelativistic, static potential in the Schrödinger framework, the multiplication of the full non-local interaction (in momentum space) by the minimal relativity square root factors is shown in the next section to have important consequences, not only for the numerical treatment of eq. (2.18) but also for the modeling of the strong and electromagnetic transitions between  $Q\bar{q}$  and  $Q\bar{Q}$  states. In particular, the well-known problem of too singular and thus illegal hyperfine operators in the Schrödinger equation is shown to disappear in the BSLT framework.

### 2.3 The $Q\bar{Q}$ interaction in the BSLT framework

The interaction between heavy quarks and heavy or light antiquarks is dominated by the (presumably linearly) rising confining interaction. The observed spectra of  $Q\bar{Q}$  mesons also require the presence of a short-range hyperfine interaction that gives rise to e.g. the  $J/\psi - \eta_c$  splitting. The one-gluon exchange (OGE) interaction [29] of perturbative QCD is a natural candidate for the  $Q\bar{Q}$  systems, whereas the origin of the hyperfine interaction in the  $Q\bar{q}$  systems is less obvious. A recently suggested possibility is the pointlike instanton induced interaction proposed by ref. [30]. The interaction Hamiltonians used in this thesis in conjunction with the covariant BSLT equation are, therefore, of the form

$$H_{\text{int}} = V_{\text{conf}} + V_{\text{OGE}} + V_{\text{inst}}, \quad (2.20)$$

with confining, OGE, and instanton induced components, respectively. The effective confining interaction is taken to have scalar Lorentz structure, while the OGE interaction

has vector coupling structure. In the nonrelativistic approximation, the effective linear confining interaction has the form (in the  $LS$ -coupling scheme):

$$V_{\text{conf}} = cr \left[ 1 - \frac{3}{2} \frac{\mathbf{P}^2}{m_Q^2 m_{\bar{q}}^2} \left( \frac{m_Q^2 + m_{\bar{q}}^2 + m_Q m_{\bar{q}}}{3} \right) \right] + \frac{c}{4m_Q m_{\bar{q}} r} - \frac{c}{r} \frac{m_Q^2 + m_{\bar{q}}^2}{4m_Q^2 m_{\bar{q}}^2} \mathbf{S} \cdot \mathbf{L} + \frac{c}{r} \frac{m_Q^2 - m_{\bar{q}}^2}{8m_Q^2 m_{\bar{q}}^2} (\boldsymbol{\sigma}_Q - \boldsymbol{\sigma}_{\bar{q}}) \cdot \mathbf{L}, \quad (2.21)$$

where the string tension  $c$  [15] is of the order  $\sim 1$  GeV/fm. The above form contains also the momentum dependent terms from eq. (2.14) up to second order in  $v^2/c^2$ . In the Schrödinger framework (i.e. without the minimal relativity factors), the numerical factor  $3/2$  in front of the  $\mathbf{P}^2$  term would be 1. Likewise, the Darwin-Foldy term in eq. (2.21) would vanish. In addition to the familiar Thomas-precession term, an antisymmetric spin-orbit interaction also appears for unequal quark masses, which mixes the states with  $L = 1$  and  $J = 1$ .

The interaction components associated with the perturbative OGE interaction are, to order  $v^2/c^2$  in the nonrelativistic approximation, of the form

$$V_{\text{OGE}} = -\frac{4}{3} \alpha_s \left[ \frac{1}{r} - \frac{3\pi}{2} \left( \frac{m_Q^2 + m_{\bar{q}}^2 + m_Q m_{\bar{q}}}{3 m_Q^2 m_{\bar{q}}^2} \right) \delta(\mathbf{r}) + \frac{1}{2} \frac{\mathbf{P}^2}{m_Q m_{\bar{q}} r} \right] + \frac{2}{3} \frac{\alpha_s}{r^3} \left( \frac{m_Q^2 + m_{\bar{q}}^2}{2m_Q^2 m_{\bar{q}}^2} + \frac{2}{m_Q m_{\bar{q}}} \right) \mathbf{S} \cdot \mathbf{L} + \frac{\alpha_s}{6r^3} \frac{m_Q^2 - m_{\bar{q}}^2}{m_Q^2 m_{\bar{q}}^2} (\boldsymbol{\sigma}_Q - \boldsymbol{\sigma}_{\bar{q}}) \cdot \mathbf{L} + \frac{8\pi}{9} \frac{\alpha_s}{m_Q m_{\bar{q}}} \delta(\mathbf{r}) \boldsymbol{\sigma}_Q \cdot \boldsymbol{\sigma}_{\bar{q}} + \frac{\alpha_s}{3m_Q m_{\bar{q}} r^3} S_{12}, \quad (2.22)$$

where  $\alpha_s$  denotes the strong coupling of perturbative QCD, and  $S_{12}$  is the tensor operator  $S_{12} = 3(\boldsymbol{\sigma}_Q \cdot \hat{\mathbf{r}})(\boldsymbol{\sigma}_{\bar{q}} \cdot \hat{\mathbf{r}}) - \boldsymbol{\sigma}_Q \cdot \boldsymbol{\sigma}_{\bar{q}}$ . In the Schrödinger framework, the coefficients for the contact and  $\mathbf{P}^2$  terms would be  $-\pi$  and 1, respectively.

The instanton induced interaction, considered by ref. [30] for systems with heavy quarks, consists of a spin-independent term as well as a  $\boldsymbol{\sigma}_Q \cdot \boldsymbol{\sigma}_{\bar{q}}$  term which contributes to the pseudoscalar-vector splittings in heavy quarkonia. The effective instanton interaction derived in ref. [30] is of the form

$$V_{\text{inst}} = -\frac{\Delta M_Q \Delta M_{\bar{q}}}{4n} \delta(\mathbf{r}) + \frac{\Delta M_Q^{\text{spin}} \Delta M_{\bar{q}}}{4n} \delta(\mathbf{r}) \boldsymbol{\sigma}_Q \cdot \boldsymbol{\sigma}_{\bar{q}}, \quad (2.23)$$

where the factors  $\Delta M_Q$  and  $\Delta M_{\bar{q}}$  denote the mass shifts of the heavy and light constituent quarks due to the instanton induced interaction. These shifts are, for light constituent quarks, of the order of the constituent quark mass ( $\sim 400$  MeV), and smaller ( $\sim 100$  MeV) for the charm quark. The parameter  $M_Q^{\text{spin}}$  controls the strength of the spin-spin interaction, which has the same sign as that from the perturbative OGE interaction. The parameter  $n$  represents the instanton density, which is typically assigned values around  $\sim 1 \text{ fm}^{-4}$ . The spin-independent term has scalar coupling for the light constituent quark line and a mixed scalar- $\gamma_0$  vertex for the heavy quark.

## 2.4 Relativistic $Q\bar{Q}$ potentials

For systems that contain light quarks, the above static interaction Hamiltonians have but qualitative value because of the slow convergence of the asymptotic expansion in  $v/c$ . Even for systems composed of heavy quarks only, the compact size of the wave functions lead to very large matrix elements in first order perturbation theory for the  $\mathbf{P}^2$  terms in eqs. (2.21) and (2.22). Therefore, it was chosen in ref. [20] to employ a local interaction model for the heavy quarkonium systems which takes into account the minimal relativity factors (2.14), as well as the relativistic effects due to the quark spinors and the running coupling of QCD. The central, spin-independent part of the OGE interaction is thus modified to

$$V_{\text{OGE}}^0(r) = -\frac{4}{3} \frac{2}{\pi} \int_0^\infty dk j_0(kr) W_{Q\bar{q}} \frac{m_Q m_{\bar{q}}}{e_Q e_{\bar{q}}} \alpha_s(\mathbf{k}^2), \quad (2.24)$$

where the following notation has been introduced for convenience:

$$e_Q = \sqrt{m_Q^2 + \frac{\mathbf{k}^2}{4}}, \quad e_{\bar{q}} = \sqrt{m_{\bar{q}}^2 + \frac{\mathbf{k}^2}{4}}, \quad W_{Q\bar{q}} = \left( \frac{m_Q + m_{\bar{q}}}{e_Q + e_{\bar{q}}} \right). \quad (2.25)$$

For the running QCD coupling  $\alpha_s(\mathbf{k}^2)$ , the parameterization of ref. [31]:

$$\alpha_s(\mathbf{k}^2) = \frac{12\pi}{27} \ln^{-1} \left[ \frac{\mathbf{k}^2 + 4m_g^2}{\Lambda_{\text{QCD}}^2} \right]. \quad (2.26)$$

has been employed. Here the QCD scale parameter  $\Lambda_{\text{QCD}}$  and the dynamical gluon mass  $m_g$ , which determines the low-momentum cutoff of the inverse logarithmic behavior of  $\alpha_s$  have been determined by a fit to the experimental spectra of the  $Q\bar{Q}$  and  $Q\bar{q}$  systems.

In general, the relativistic effects in eq. (2.24) lead to a strong suppression of the short-range coulombic potential. On the other hand, the running coupling  $\alpha_s$ , when employed according to eq. (2.26), increases the strength of the OGE interaction for large distances. The end result is, that the OGE interaction, when calculated using eqs. (2.24) and (2.26) bears little or no resemblance to a coulombic potential, even for the heavy  $c\bar{c}$  system. This can potentially have serious phenomenological consequences since models that employ a short-range coulombic interaction have, in general, provided good descriptions of the  $c\bar{c}$  and  $b\bar{b}$  spectra. However, the spin-independent part of the instanton induced interaction (2.23) has been shown in paper **VI** to provide the necessary short-range attraction, even if the OGE interaction becomes weak. In principle, the effective confining interaction is also subject to similar relativistic effects, but in view of its long-range nature, their effect will be very small.

The hyperfine components of the  $Q\bar{Q}$  interaction, as given by eqs. (2.21) and (2.22) are usually treated as first order perturbations since their behavior for small  $r$  is too singular to allow for direct numerical treatment. Modification of those hyperfine components according to eq. (2.14) leads to expressions, which are weaker and more well-behaved, and may consequently be fully taken into account. The employment of individual wave functions for each member in a given hyperfine multiplet was shown, in paper **VI**, to be important for a realistic description of several electromagnetic E1 and M1 transitions in the heavy quarkonium systems.

The expressions for the local hyperfine components of the  $Q\bar{q}$  interaction that take into account the minimal relativity factors and the running QCD coupling are, in configuration space, of the form

$$V_{\text{OGE}}^{\text{LS}} = \frac{4}{3\pi r} \mathbf{S} \cdot \mathbf{L} \int_0^\infty dk k j_1(kr) \frac{W_{Q\bar{q}}}{e_Q e_{\bar{q}}} \left[ 2 + \frac{m_Q}{e_{\bar{q}} + m_q} + \frac{m_{\bar{q}}}{e_{\bar{Q}} + m_Q} \right] \alpha_s(\mathbf{k}^2), \quad (2.27)$$

$$V_{\text{conf}}^{\text{LS}} = -\frac{2}{\pi} \frac{c}{r} \mathbf{S} \cdot \mathbf{L} \int_0^\infty dk \frac{j_1(kr)}{k} \frac{W_{Q\bar{q}}}{e_Q e_{\bar{q}}} \left[ \frac{e_{\bar{q}}}{e_Q + m_Q} + \frac{e_Q}{e_{\bar{q}} + m_{\bar{q}}} \right], \quad (2.28)$$

$$V_{\text{OGE}}^{\text{SS}} = \frac{4}{9\pi} \boldsymbol{\sigma}_Q \cdot \boldsymbol{\sigma}_{\bar{q}} \int_0^\infty dk k^2 j_0(kr) \frac{W_{Q\bar{q}}}{e_Q e_{\bar{q}}} \alpha_s(\mathbf{k}^2), \quad (2.29)$$

$$V_{\text{OGE}}^{\text{T}} = \frac{2}{9\pi} S_{12} \int_0^\infty dk k^2 j_2(kr) \frac{W_{Q\bar{q}}}{e_Q e_{\bar{q}}} \alpha_s(\mathbf{k}^2), \quad (2.30)$$

for the spin-orbit, spin-spin and tensor components of the OGE interaction, and the spin-orbit (Thomas precession) term from the effective scalar confining interaction. Note that the expression (2.28) for the spin-orbit term associated with the linear scalar confining interaction is obtained by means of the representation  $-8\pi c/\mathbf{k}^4$  in momentum space. This can be understood as the Fourier transform of a modified linear potential  $cr e^{-\lambda r}$  in the limit  $\lambda \rightarrow 0$ . The integral (2.28) is convergent even if that limit is taken analytically. The above expressions are also free of singularities that require a perturbative treatment. If the QCD coupling  $\alpha_s$  is taken to be constant, then the hyperfine components, as given by eqs. (2.27)-(2.30), reduce to the static expressions of eqs. (2.21) and (2.22) for large distances.

As the instanton induced interaction for  $Q\bar{q}$  systems, as given by ref. [30], consists of delta functions, it has to be treated as a first order perturbation. Such a treatment is very unfortunate here since the repulsive kinetic energy as given by the BSLT quadratic mass operator (2.17) is very sensitive to the ground state energy relative to the sum of the quark masses. A perturbative treatment of a strong attractive interaction component would thus effectively lead to unrealistically small level spacings between the higher excited states. In view of this, the delta function of eq. (2.23) has been treated according to

$$V_{\text{inst}} = -\frac{\Delta M_Q \Delta M_{\bar{q}}}{4n} \int_0^\infty dk k^2 j_0(kr) W_{Q\bar{q}} \frac{m_Q m_{\bar{q}}}{e_Q e_{\bar{q}}}, \quad (2.31)$$

which effectively leads to a smeared-out form of the instanton induced interaction. While the presence of  $W_{Q\bar{q}}$  is naturally suggested by the BSLT minimal relativity factors, the  $m_Q/e_Q$  factors are entirely phenomenological, and have been inserted to allow for better convergence of the above integral. In the limit of very large constituent masses (the static limit), the above equation reduces to the form (2.23). The spin-spin component of the instanton induced interaction was found in ref. [30] to be significant for the heavy-light  $Q\bar{q}$  systems, but very weak for the heavy-heavy  $Q\bar{Q}$  mesons. Because of this, the spectra shown in Table 2.1 and Fig. 2.2 do not include that interaction. The calculated  $Q\bar{q}$  spectra employed in paper **II**, shown for the  $D$  meson in Fig. 2.3, do not include the instanton induced interaction, since sufficient attraction was provided there by the OGE interaction, although at the price of an unrealistically large value for the QCD scale parameter  $\Lambda_{\text{QCD}}$ .

## 2.5 Spectra of heavy flavor mesons

The  $c\bar{c}$ ,  $b\bar{b}$  and  $B_c^\pm$  spectra that are shown in Table 2.1 and Fig. 2.2 have been obtained by solution of the BSLT equation for a linear scalar confining interaction, and OGE + instanton components modeled according to the expressions given in this section. The hyperfine components have been taken fully into account, so that all the states given in Table 2.1 are represented by different radial wave functions. This model has been employed for the calculations of the electromagnetic transitions in paper **VI** as well as the dipion transitions in paper **IV**.

Table 2.1: Calculated and experimental  $c\bar{c}$ ,  $b\bar{b}$  and  $B_c^\pm$  states rounded to the nearest MeV, as obtained in papers **IV** and **VI**. The states are classified according to excitation number  $n$ , total spin  $S$ , total orbital angular momentum  $L$  and total angular momentum  $J$ . The experimental values are from ref. [32], except for the recently observed [33]  $\eta_c(2S)$ .

$n^{2S+1}L_J$	$b\bar{b}$	Exp( $b\bar{b}$ )	$c\bar{c}$	Exp( $c\bar{c}$ )	$c\bar{b}$
$1^1S_0$	9401	–	2997	$2980 \pm 1.8$	6308
$2^1S_0$	10005	–	3640	$3654 \pm 6$ [33]	6888
$3^1S_0$	10361	–	4015	–	7229
$4^1S_0$	10634	–	4300	–	7488
$1^3S_1$	9458	9460	3099	3097	6361
$2^3S_1$	10030	10023	3678	3686	6910
$3^3S_1$	10377	10355	4040	$4040 \pm 10$	7244
$4^3S_1$	10648	10580	4319	$4159 \pm 20$ ?	7500
$1^1P_1$	9888	–	3513	–	6754
$2^1P_1$	10266	–	3912	–	7126
$3^1P_1$	10552	–	4211	–	7401
$1^3P_0$	9855	9860	3464	3415	6723
$2^3P_0$	10244	10232	3884	–	7107
$3^3P_0$	10535	–	4192	–	7387
$1^3P_1$	9883	9893	3513	3511	6751
$2^3P_1$	10263	10255	3913	–	7125
$3^3P_1$	10550	–	4213	–	7400
$1^3P_2$	9903	9913	3540	3556	6770
$2^3P_2$	10277	10269	3930	–	7136
$3^3P_2$	10561	–	4226	–	7410
$1^3D_3$	10158	–	3790	–	7009
$1^3D_2$	10149	–	3784	–	7006
$1^3D_1$	10139	–	3768	$3770 \pm 2.5$	6998

Although preliminary, the measured mass of the  $B_c^\pm$  was reported in ref. [34] as  $6.40 \pm 0.39$  GeV, which is about  $\sim 100$  MeV higher than the predicted 6308 MeV, and most other models [35] give even lower masses for the  $B_c^\pm$  ground state. However, the predicted  $B_c^\pm$  spectrum agrees very well with the QCD-inspired model of ref. [36].

The quality of the calculated  $Q\bar{Q}$  spectra in Table 2.1 is generally quite satisfactory, as both the  $\psi' - J/\psi$  and  $J/\psi - \eta_c$  splittings are given realistically. In particular, the  $\eta_c(2S)$  state has recently been reported by the BELLE collaboration [33] with a mass of about 3650 MeV. This suggests that the spin-spin splitting is much smaller for the  $2S$  states than for the  $J/\psi$  and the  $\eta_c$ , a feature which is well described by the present model. The main difficulty is the prediction of the hyperfine splittings in the  $L = 1$  multiplet of charmonium. Table 2.1 and Fig. 2.2 indicate that the splittings are underpredicted for  $c\bar{c}$  but in reasonable agreement with experiment for  $b\bar{b}$ . This problem can be traced, in part, to the weakness of the OGE tensor interaction as given by eq. (2.30).

	Paper VI	Other models
$M_b$	4885 MeV	4870 MeV [14]
$M_c$	1500 MeV	1530 MeV [14]
$\Lambda_{\text{QCD}}$	260 MeV	200-300 MeV [31]
$m_g$	290 MeV	$m_g > \Lambda_{\text{QCD}}$ [31]
$c$	890 MeV/fm	912 MeV/fm [14]
$\frac{(\Delta M_c)^2}{4n}$	0.084 fm <sup>2</sup>	$\sim 0.05$ fm <sup>2</sup> [30]
$\frac{(\Delta M_b)^2}{4n}$	0.004 fm <sup>2</sup>	?

Table 2.2: Quark masses and coupling constants used for the calculated spectra in Fig. 2.2. The values should be considered as best fits within the BSLT model to the empirical  $c\bar{c}$  and  $b\bar{b}$  spectra.

The heavy quark masses are close to those obtained by Roberts *et al.* in ref. [14] within the framework of the Gross equation. The values of  $\Lambda_{\text{QCD}}$  and  $m_g$  are in line with those suggested in ref. [31], while the string tension  $c$  is somewhat smaller than that suggested by the lattice QCD calculations of ref. [37]. The strength of the instanton induced interaction in the  $c\bar{c}$  system is comparable to the estimate given in ref. [30]. In spite of the generally satisfactory results, perfect agreement with experiment had to be sacrificed in the  $b\bar{b}$  system in order to obtain an optimal description of the  $c\bar{c}$  spectrum with the same set of parameters. As this nevertheless is a small effect, the results indicate that a flavor-independent confining interaction is a reasonable first approximation, in contrast to the instanton induced interaction, the strength of which depends explicitly on the quark flavors involved.

The spectra of the heavy-light  $Q\bar{q}$  mesons that were obtained in ref. [38] within the framework of the BSLT equation have been used here for calculation of the M1 and pion widths of the  $Q\bar{q}$  states. The  $D$  meson spectrum so obtained is shown in Fig. 2.3. Although quite satisfactory agreement with the empirical  $Q\bar{q}$  spectra was achieved, this was only at the price of a very strong OGE interaction and the introduction of a negative constant into the scalar confining interaction, which was treated as a free parameter. The hyperfine components of the OGE and scalar confining interactions were treated as perturbations, while the instanton induced interaction was dropped since the OGE interaction was found to give sufficient attraction to account for the empirical spectra. However, later (unpublished) calculations of the  $Q\bar{q}$  spectra have indicated that a non-perturbative treatment of the OGE spin-spin interaction strongly favors the inclusion of the instanton induced spin-spin interaction proposed by ref. [30], in which case the spin-independent term of that interaction may also lead to a more realistic strength and low-momentum behavior of  $\alpha_s$ .

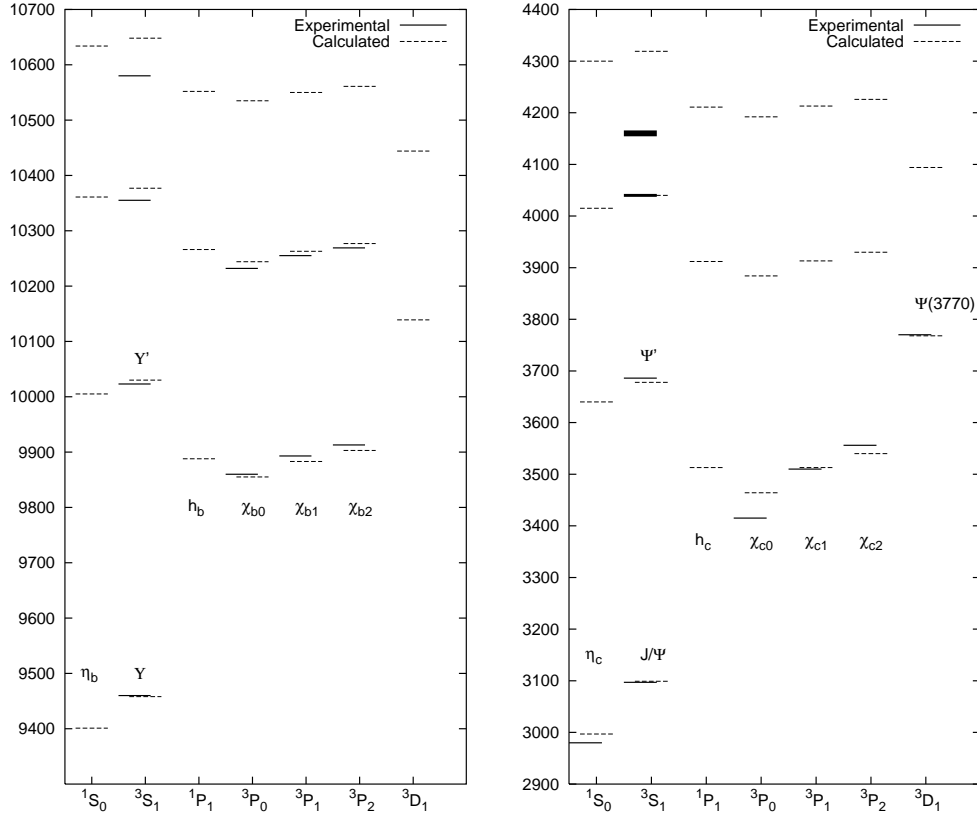


Figure 2.2: Calculated and experimental  $b\bar{b}$  and  $c\bar{c}$  spectra. All states are given in MeV, and correspond to the data in Table 2.1. The thickness of the lines denoting the experimentally determined states indicates the uncertainty in the mass of the state. Note that the identification of the  $4^3S_1$  state in charmonium is uncertain, and may actually be a  $2^3D_1$  state, or a mixture of the two. The threshold for  $D\bar{D}$  decay is at  $\sim 3750$  MeV, and for  $B\bar{B}$  decay at  $\sim 10500$  MeV.

The small number of empirically known  $Q\bar{q}$  states makes a determination of the quality of a given model difficult. However, the most significant unsolved problem in the case of the  $Q\bar{q}$  spectra is the ordering of the  $L = 1$  multiplet, of which only two resonances have been detected so far. These probably correspond to spin-triplet states with  $J = 2$  and  $J = 1$  ( $j_q = 3/2$  in the heavy quark limit), and are denoted  $D_2^*$  and  $D_1$ , respectively (note the notational confusion). The empirical fact that the  $D_2^*$  is higher in mass by  $\sim 40$  MeV then suggests that the ordering of the  $L = 1$  states in the  $D$  mesons is similar to that observed for the  $c\bar{c}$  and  $b\bar{b}$  systems. It is reassuring that this result is consistent with lattice QCD calculations of the spin-orbit splittings in heavy-light mesons [39] although the problem of poor convergence of such calculations is still not solved to satisfaction. In view of these results, it appears that the possibility [40] of spin-orbit inversion in heavy-light mesons is not realized. It should be noted, however, that the spin-orbit splittings as calculated from static expressions like eqs. (2.21) and (2.22) are unrealistic because of the low masses of the light constituent quarks. An unphysical dominance of the Thomas precession associated with the scalar confining interaction may then suggest that the spin-orbit splittings of the  $L = 1$   $Q\bar{q}$  states should be inverted.

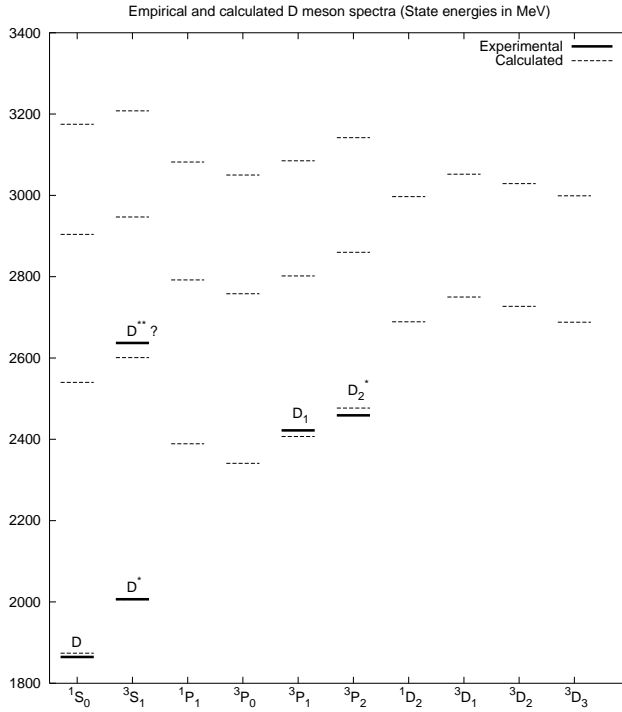


Figure 2.3: Experimental and calculated  $D$  meson spectra from ref. [38]. It should be noted that the excited  $2S$  state  $D^{**}$  at  $\sim 2630$  MeV, which was reported by ref. [41] was not detected by a subsequent search [42] and may therefore not exist at that energy.

It is instructive to compare the parameters of ref. [38] with the values suggested by the more realistic calculation (paper **VI**) of the  $Q\bar{Q}$  spectra in Table 2.2. The heavy quark masses  $m_c = 1580$  MeV and  $m_b = 4885$  MeV of ref. [38], though slightly higher, agree quite well with those of Table 2.2. On the other hand, the masses of the light quarks were obtained as  $m_{u,d} = 450$  MeV and  $m_s = 560$  MeV, respectively. Although the light quark mass is higher than the usual phenomenological value of  $\sim 350$  MeV, it is close to the value 420 MeV which has been employed [30] for the instanton induced interaction. It has also been suggested [43] that a natural value of the constituent quark mass is one third of the  $\Delta$  mass, rather than the nucleon mass.

The parameters  $\Lambda_{\text{QCD}}$  and  $m_g$  were obtained as 280 MeV and 240 MeV in ref. [38] and lead to a much stronger coupling  $\alpha_s$  than is necessary in paper **VI**. Most other analyses [31] suggest a much weaker form. The phenomenological consequences of a very strong OGE interaction for light constituent quarks are potentially serious [9], since incorrect ordering of the positive and negative parity nucleon and  $\Lambda$  states may result. Moreover, the relativistic damping of the short-range part of the attractive coulombic OGE potential in ref. [38] is such that the OGE interaction alone cannot describe e.g. the  $1S - 1P$  level splittings in the  $Q\bar{q}$  spectra. It was therefore necessary to push the other parameters of that model to their limits.

In this situation, the instanton induced interaction of ref. [30] suggests itself naturally as it provides both a strong attraction in the  $S$ -wave and contributes to the  $D^* - D$  splitting. Also, the OGE potential of eq. (2.24) for a system composed of two light ( $\sim 400$  MeV) quarks, becomes depleted for distances equal to the meson radius. The central OGE component may therefore only play a minor role in the dynamics of light constituent quarks, while for the  $Q\bar{q}$  mesons, the short-range attraction may turn out to be best described by a combination of OGE and instanton induced components.

## Chapter 3

# Electromagnetic Transitions

The radiative transitions in heavy quarkonium ( $c\bar{c}$ ,  $b\bar{b}$ ,  $c\bar{b}$ ) systems have drawn much theoretical interest [44, 45], as they can provide direct information on both the heavy quarkonium wave functions and the  $Q\bar{Q}$  interaction. As reasonably reliable empirical data now exists for a number of transitions in both the  $c\bar{c}$  and  $b\bar{b}$  systems [46], a fair assessment of the quality of theoretical models is already possible. The measured  $\gamma$  transitions in the charmonium ( $c\bar{c}$ ) system include the E1 transitions  $\chi_{cJ} \rightarrow J/\psi \gamma$  and  $\psi' \rightarrow \chi_{cJ} \gamma$ , as well as the spin-flip M1 transitions  $J/\psi \rightarrow \eta_c \gamma$  and  $\psi' \rightarrow \eta_c \gamma$ . The situation concerning the analogous transitions in the bottomonium ( $b\bar{b}$ ) system is, however, less satisfactory as the total widths of the  $\chi_{bJ}$  states are not known, and none of the spin-flip M1 transitions observed.

Previous calculations of the E1 widths of heavy quarkonia have demonstrated that the E1 approximation leads to overpredictions of most transition rates, and that this overprediction can be significantly reduced, if not entirely eliminated, by the consideration of relativistic effects. On the other hand, theoretical predictions for the M1 transitions have remained unsatisfactory for a long time [18] as the width for  $J/\psi \rightarrow \eta_c \gamma$  has typically been overpredicted by a factor  $\sim 3$ . However, calculations of M1 widths using the non-relativistic Schrödinger equation in ref. [47] and paper **I** have demonstrated that the M1 transitions in charmonium are sensitive both to the relativistic aspects of the spin-flip operator as well as the Lorentz structure of the  $Q\bar{Q}$  interaction. The results obtained in papers **I** and **VI** suggest that a scalar confining interaction may explain the observed width of  $\sim 1$  keV for  $J/\psi \rightarrow \eta_c \gamma$ , provided that an unapproximated single quark spin-flip operator is used. This conclusion is supported by the calculation of ref. [17], which is based on the instantaneous approximation to the Bethe-Salpeter equation, even though a quantitative understanding of the radiative transitions in charmonium was not achieved.

The situation concerning the M1 transitions in the heavy-light  $Q\bar{q}$  mesons is more uncertain because of the scarcity of reliable empirical data. Only recently has a first measurement of the width of the  $D^*$  state been published, which allows a determination of the partial width for the M1 transition  $D^{\pm*} \rightarrow D^{\pm} \gamma$  from its known branching fraction. Even though the total width of the  $D^{0*}$  is not known, the partial width for  $D^{0*} \rightarrow D^0 \gamma$  can be inferred from the measured width of the  $D^{\pm*}$  and model calculations of the pionic widths of the  $D^*$  mesons, as the relative branching fractions for  $\pi$  and  $\gamma$  emission are known.

As the velocity of the light constituent quark in the  $Q\bar{q}$  systems is close to that of light, the relativistic corrections to both single quark and two-quark operators will *a priori* be large. It is shown in paper **V** that the large relativistic corrections to the single quark spin-flip operators, that yield unfavorable results for the M1 widths of  $Q\bar{q}$  mesons, are in general counteracted by the two-quark operators associated with an interaction Hamiltonian that consists of OGE + scalar confinement components, thus allowing for better agreement with experiment. It is also suggested that the instanton induced interaction for  $Q\bar{q}$  systems of ref. [30] may have a favorable effect on the predictions for the M1 widths of the  $D^*$  mesons.

### 3.1 Charge density and electric dipole operators

The electromagnetic transition amplitude for a two-quark system, in the impulse approximation, is of the form

$$T_{fi} = - \int d^3r_1 d^3r_2 \varphi_f^*(\mathbf{r}_1, \mathbf{r}_2) \hat{\boldsymbol{\epsilon}} \cdot [e^{i\bar{q}\cdot\bar{\mathbf{r}}_1} \mathbf{j}_1(\mathbf{q}) + e^{i\bar{q}\cdot\bar{\mathbf{r}}_2} \mathbf{j}_2(\mathbf{q})] \varphi_i(\mathbf{r}_1, \mathbf{r}_2), \quad (3.1)$$

where  $\mathbf{q}$  and  $\hat{\boldsymbol{\epsilon}}$  denote the momentum and polarization of the emitted photon, respectively, while  $\varphi_i$  and  $\varphi_f$  denote the orbital wave functions of the initial and final heavy quarkonium states. In the above equation,  $\mathbf{j}_1$  and  $\mathbf{j}_2$  denote the single quark current operators of quarks 1 and 2, respectively. By Fourier transformation, the current operators may be rewritten as

$$\mathbf{j}(\mathbf{q}) = \int d^3r' e^{i\bar{q}\cdot\bar{\mathbf{r}}'} \mathbf{j}(\mathbf{r}') \quad (3.2)$$

$$= - \int d^3r' \mathbf{r}' (\mathbf{j} \cdot \nabla) e^{i\bar{q}\cdot\bar{\mathbf{r}}'} - \int d^3r' e^{i\bar{q}\cdot\bar{\mathbf{r}}'} \mathbf{r}' (\nabla \cdot \mathbf{j}), \quad (3.3)$$

from which the E1 approximation is obtained if the exponentials in eq. (3.3) are dropped (i.e.  $\mathbf{q} \rightarrow 0$ ). Application of the continuity equation then gives  $\nabla \cdot \mathbf{j} = i\omega\rho$ . For nonzero  $\mathbf{q}$ , the second term in eq. (3.3) has to be retained without approximation. Note that  $\mathbf{j}(\mathbf{q})$  is taken to contain the quantity in square brackets in eq. (3.1). Application of eq. (3.3) together with eq. (3.1) then leads to the following form for the amplitude of a  $\gamma$  transition,

$$T_{fi} = i|\mathbf{q}| \int d^3r_1 d^3r_2 \varphi_f^*(\mathbf{r}_1, \mathbf{r}_2) \hat{\boldsymbol{\epsilon}} \cdot \mathbf{d}(\mathbf{r}_1, \mathbf{r}_2) \varphi_i(\mathbf{r}_1, \mathbf{r}_2). \quad (3.4)$$

The dipole operator  $\mathbf{d}(\mathbf{r}_1, \mathbf{r}_2)$ ,

$$\mathbf{d}(\mathbf{r}_1, \mathbf{r}_2) = \int d^3r' e^{i\bar{q}\cdot\bar{\mathbf{r}}'} \mathbf{r}' \rho(\mathbf{r}', \mathbf{r}_1, \mathbf{r}_2), \quad (3.5)$$

reduces to the E1 approximation in the limit  $\mathbf{q} \rightarrow 0$ . In general, the charge density operator  $\rho(\mathbf{r}')$  contains, in addition to the single quark contribution  $\rho_{\text{sq}}$ , an exchange part  $\rho_{\text{ex}}$ , which arises from the two-quark currents that are illustrated by the diagrams in Fig. 3.1. A necessary constraint is that two-quark contributions to the charge density must have vanishing volume integrals. The dipole operator that corresponds to the single quark charge operator  $\rho_{\text{sq}}(\mathbf{r}', \mathbf{r}) = \rho_1(\mathbf{r}', \mathbf{r}_1) + \rho_2(\mathbf{r}', \mathbf{r}_2)$  may be expressed as

$$\mathbf{d}_{\text{sq}}(\mathbf{r}_1, \mathbf{r}_2) = \int \frac{d^3q}{(2\pi)^3} d^3r' e^{i\bar{q}_f \cdot \bar{\mathbf{r}}'} \left[ \rho_1(\mathbf{q}) \mathbf{r}' e^{i\bar{q} \cdot (\bar{\mathbf{r}}_1 - \bar{\mathbf{r}}')} + \rho_2(\mathbf{q}) \mathbf{r}' e^{i\bar{q} \cdot (\bar{\mathbf{r}}_2 - \bar{\mathbf{r}}')} \right], \quad (3.6)$$

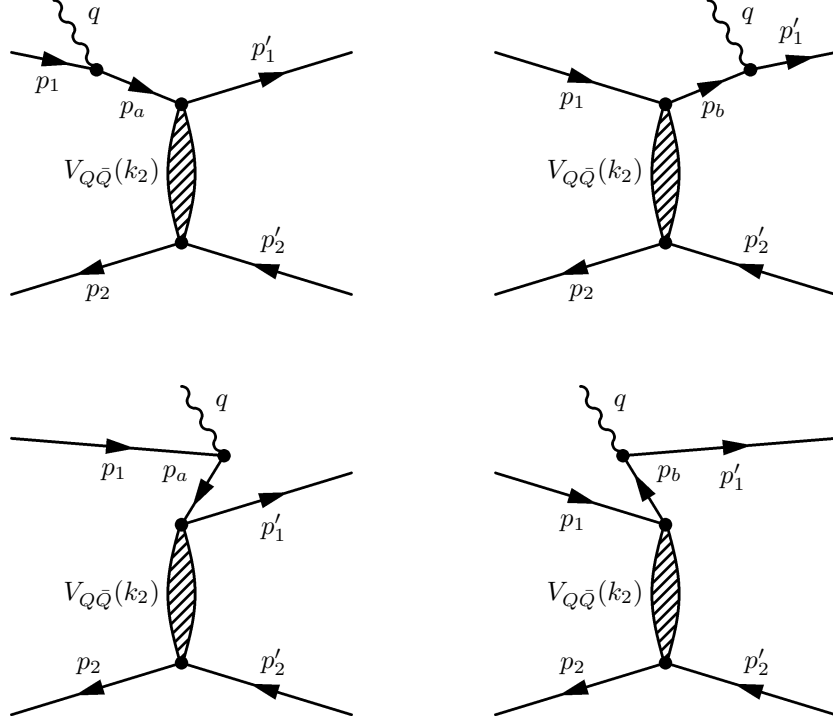


Figure 3.1: Two-quark contributions to the  $Q\bar{Q}$  current and charge density operators. In the decomposition of the  $Q\bar{Q}\gamma$  vertex, the irreducible two-quark contributions give rise to exchange current operators, the most important of which are illustrated by the upper Born diagrams. In order to obtain the correct two-quark contribution, the positive energy part of the intermediate propagator is subtracted in the lower Born diagrams, since that part is already accounted for by the impulse approximation. Note that similar diagrams describe photon emission by the heavy antiquark. In the case of the  $Q\bar{Q}$  interaction, the scalar photon confining and vector OGE components have been taken into account. The contributions from the instanton induced interaction have not been considered but are in any case small for the  $Q\bar{Q}$  systems.

which upon evaluation yields

$$\mathbf{d}_{\text{sq}}(\mathbf{r}_1, \mathbf{r}_2) = \lim_{q \rightarrow q_f} \left[ \mathbf{r}_1 e^{i\vec{q} \cdot \vec{r}_1} \rho_1(\mathbf{q}) + e^{i\vec{q} \cdot \vec{r}_1} i\nabla_{\vec{q}} \rho_1(\mathbf{q}) \right] + (1 \rightarrow 2), \quad (3.7)$$

where  $q_f$  refers to the physical photon momentum of each transition. The above form reduces to the E1 expression by the substitution  $q_f \rightarrow 0$ . The nonrelativistic single quark dipole operator is therefore of the form

$$\mathbf{d}_{\text{sq}}(\mathbf{r}_1, \mathbf{r}_2) = Q_1 \mathbf{r}_1 e^{i\vec{q}_f \cdot \vec{r}_1} + Q_2 \mathbf{r}_2 e^{i\vec{q}_f \cdot \vec{r}_2}, \quad (3.8)$$

where  $Q_1$  is the charge of the heavy quark, while  $Q_2$  denotes that of the heavy antiquark. Insertion of eq. (3.8) into eq. (3.4) yields the single quark dipole operator

$$\mathbf{d}_{\text{sq}}(\mathbf{r}) = \left[ \frac{Q_1 m_2 - Q_2 m_1}{m_1 + m_2} \right] \mathbf{r} e^{i\vec{q}_f \cdot \vec{r}/2}. \quad (3.9)$$

The charge density operator in eq. (3.7) is, to second order in  $v/c$ , of the form [19]

$$\rho_{\text{sq}} \simeq Q_1 \left[ 1 - \frac{\mathbf{q}^2}{8m^2} + \frac{i\boldsymbol{\sigma}_1 \cdot \mathbf{p}'_1 \times \mathbf{p}_1}{4m^2} \right] + (1 \rightarrow 2), \quad (3.10)$$

where the second term on the r.h.s. is the relativistic Darwin-Foldy term. The effect of this term is very small because of the large masses of the heavy constituent quarks. The justification of this expansion lies in the small coefficient of that term; It has been shown e.g. in papers **I** and **VI** that such an expansion cannot be used for the magnetic moment operator.

If the two-quark exchange charge operators from the Born diagrams in Fig. 3.1 are decomposed as  $\rho_{\text{ex}}(\mathbf{r}', \mathbf{r}_1, \mathbf{r}_2) = \rho_{\text{ex1}}(\mathbf{r}', \mathbf{r}_1) + \rho_{\text{ex2}}(\mathbf{r}', \mathbf{r}_2)$ , then the contribution from quark 1 may be expressed as

$$\rho_{\text{ex1}}(\mathbf{r}', \mathbf{r}_1) = \int \frac{d^3\mathbf{q}}{(2\pi)^3} e^{i\vec{q} \cdot (\vec{r}_1 - \vec{r}')} \int \frac{d^3\mathbf{k}_2}{(2\pi)^3} e^{-i\vec{k}_2 \cdot \vec{r}} \rho_{\text{ex1}}(\mathbf{q}, \mathbf{k}_2). \quad (3.11)$$

Here  $\mathbf{k}_2$  is the momentum transferred to the heavy antiquark and  $\mathbf{r}$  is defined as  $\mathbf{r}_1 - \mathbf{r}_2$ . The exchange charge contribution to the two-quark dipole operator

$$\mathbf{d}_{\text{ex}}(\mathbf{r}_1, \mathbf{r}_2) = \int d^3r' e^{i\vec{q}_f \cdot \vec{r}'} \mathbf{r}' \rho_{\text{ex}}(\mathbf{r}', \mathbf{r}_1, \mathbf{r}_2) \quad (3.12)$$

from quark 1 may then be expressed as

$$\begin{aligned} \mathbf{d}_{\text{ex1}}(\mathbf{r}_1) &= \mathbf{r}_1 e^{i\vec{q}_f \cdot \vec{r}_1} \int \frac{d^3\mathbf{k}_2}{(2\pi)^3} e^{-i\vec{k}_2 \cdot \vec{r}} \rho_{\text{ex1}}(\mathbf{q}_f, \mathbf{k}_2) \\ &\quad - \lim_{q \rightarrow q_f} \left[ e^{i\vec{q} \cdot \vec{r}_1} i\nabla_{\vec{q}} \int \frac{d^3\mathbf{k}_2}{(2\pi)^3} e^{-i\vec{k}_2 \cdot \vec{r}} \rho_{\text{ex1}}(\mathbf{q}, \mathbf{k}_2) \right], \end{aligned} \quad (3.13)$$

which again reduces to the E1 approximation by the substitution  $q_f \rightarrow 0$ .

The exchange charge density operators that are associated with the  $Q\bar{Q}$  interaction have been extracted in ref. [19], for different Lorentz invariants for equal-mass systems. When generalized to unequal quark masses, the required operators are obtained as

$$\rho_{\text{ex}}^{\text{c}} = \frac{Q_1}{4m_1^3} q^2 V_c(\mathbf{k}_2) + \frac{Q_2}{4m_2^3} q^2 V_c(\mathbf{k}_1), \quad (3.14)$$

$$\begin{aligned} \rho_{\text{ex}}^{\text{g}} &= \frac{Q_1}{4m_1^2} \left[ \frac{\mathbf{q} \cdot \mathbf{k}_2}{m_1} + \frac{2}{3} \frac{\mathbf{q} \cdot \mathbf{k}_2 \boldsymbol{\sigma}_1 \cdot \boldsymbol{\sigma}_2}{m_2} \right] V_g(\mathbf{k}_2) + \frac{Q_2}{4m_2^2} \left[ \frac{\mathbf{q} \cdot \mathbf{k}_1}{m_2} \right. \\ &\quad \left. + \frac{2}{3} \frac{\mathbf{q} \cdot \mathbf{k}_1 \boldsymbol{\sigma}_1 \cdot \boldsymbol{\sigma}_2}{m_1} \right] V_g(\mathbf{k}_1). \end{aligned} \quad (3.15)$$

In the above expressions,  $V_c$  and  $V_g$  denote the Fourier transforms of the confining and OGE interactions, respectively. Evaluation of eq. (3.13) thus yields the dipole operators

$$\mathbf{d}_{\text{ex}}^{\text{Conf}}(\mathbf{r}) = q_f^2 \left[ \frac{Q_1}{4m_1^3} \frac{m_2}{m_1 + m_2} - \frac{Q_2}{4m_2^3} \frac{m_1}{m_1 + m_2} \right] \mathbf{r} V_c(r) e^{i\vec{q}_f \cdot \vec{r}/2}, \quad (3.16)$$

$$\mathbf{d}_{\text{ex}}^{\text{Oge}}(\mathbf{r}) = \left[ \frac{Q_1}{4m_1^2} \left( \frac{1}{m_1} + \frac{2}{3} \frac{\boldsymbol{\sigma}_1 \cdot \boldsymbol{\sigma}_2}{m_2} \right) - \frac{Q_2}{4m_2^2} \left( \frac{1}{m_2} + \frac{2}{3} \frac{\boldsymbol{\sigma}_1 \cdot \boldsymbol{\sigma}_2}{m_1} \right) \right] \mathbf{r} e^{i\vec{q}_f \cdot \vec{r}/2} \frac{\partial V_g(r)}{r \partial r}.$$

Here  $V_c(r)$  is the linear confining interaction, while  $V_g(r)$  denotes the form of the OGE interaction in configuration space, which is taken to include the effects of the running coupling of QCD.

### 3.2 Current density and magnetic moment operators

In the impulse approximation, the spin-flip magnetic moment operator for M1 transitions between  $S$ -wave heavy quarkonium states have been derived from the amplitude

$$T_{fi} = -(2\pi)^3 \delta^3(P_f - P_i - q_f) \int d^3r \varphi_f^*(\mathbf{r}) \hat{\boldsymbol{\epsilon}} \cdot \left[ e^{i\vec{q}\cdot\vec{r}/2} \mathbf{J}_1(\mathbf{q}) + e^{-i\vec{q}\cdot\vec{r}/2} \mathbf{J}_2(\mathbf{q}) \right] \varphi_i(\mathbf{r}), \quad (3.17)$$

where  $\mathbf{r} = \mathbf{r}_1 - \mathbf{r}_2$ . Expansion of the exponential in eq. (3.2) according to  $\simeq 1 + i\mathbf{q} \cdot \mathbf{r}'$  then yields the M1 and E2 amplitudes for photon emission. Upon isolation of the M1 contribution, the matrix element for  $J/\psi \rightarrow \eta_c \gamma$  and  $\psi' \rightarrow \eta_c \gamma$  may be written in the form

$$\mathcal{M}_{fi} = i \int d^3r \varphi_f^*(\mathbf{r}) \mathbf{q} \times \hat{\boldsymbol{\epsilon}} \cdot \boldsymbol{\mu}_{\text{sf}} \varphi_i(\mathbf{r}), \quad (3.18)$$

where  $\boldsymbol{\mu}_{\text{sf}}$  denotes the spin-flip part of the magnetic moment operator

$$\boldsymbol{\mu} = \frac{1}{2} \int d^3r' \mathbf{r}' \times \mathbf{j}(\mathbf{r}'). \quad (3.19)$$

In eq. (3.19), the current operator consists of a single quark contribution  $\mathbf{j}_{\text{sq}}$  and a two-quark contribution  $\mathbf{j}_{\text{ex}}$ , which arises from the pair terms given in Fig. 3.1. The corresponding single quark magnetic moment operator may be expressed as

$$\boldsymbol{\mu}_{\text{sq}} = \frac{1}{2} \int \frac{d^3q}{(2\pi)^3} d^3r' \left[ \mathbf{r}' \times \mathbf{J}_1(\mathbf{q}) e^{i\vec{q}\cdot(\vec{r}'/2 - \vec{r}')} + \mathbf{r}' \times \mathbf{J}_2(\mathbf{q}) e^{-i\vec{q}\cdot(\vec{r}'/2 + \vec{r}')} \right], \quad (3.20)$$

which yields

$$\boldsymbol{\mu}_{\text{sq}} = \lim_{\vec{q} \rightarrow 0} \left[ -\frac{i}{2} \nabla_q \times \left( e^{i\vec{q}\cdot\vec{r}'/2} \mathbf{J}_1(\mathbf{q}) + e^{-i\vec{q}\cdot\vec{r}'/2} \mathbf{J}_2(\mathbf{q}) \right) \right]. \quad (3.21)$$

The magnetic moment operator is given by eq. (3.21) in the nonrelativistic impulse approximation. However, previous work has demonstrated that the static magnetic moment operators of the baryons receive large corrections from the canonical boosts of the constituent quark spinors [48]. Furthermore, it has been shown in paper I that the nonrelativistic impulse approximation does not provide a satisfactory description of the spin-flip magnetic moment operators for  $Q\bar{Q}$  systems, even though the masses of the charm and bottom constituent quarks are large. The matrix element that corresponds to eq. (3.18) in the relativistic impulse approximation is of the form

$$\mathcal{M}_{fi}^{\text{Rel}} = i \int \frac{d^3P}{(2\pi)^3} d^3r d^3r' e^{i\vec{P}\cdot(\vec{r}' - \vec{r})} \varphi_f^*(\mathbf{r}') \mathbf{q} \times \hat{\boldsymbol{\epsilon}} \cdot \boldsymbol{\mu}_{\text{sq}}^{\text{Rel}}(\mathbf{P}) \varphi_i(\mathbf{r}), \quad (3.22)$$

where the final and initial state coordinates  $\mathbf{r}'$  and  $\mathbf{r}$  are defined as  $\mathbf{r}'_1 - \mathbf{r}'_2$  and  $\mathbf{r}_1 - \mathbf{r}_2$  respectively. In eq. (3.22), the momentum variable  $\mathbf{P}$  is defined as  $\mathbf{P} = (\mathbf{p}' + \mathbf{p})/2$ , where  $\mathbf{p}'$  and  $\mathbf{p}$  are the relative momenta in the representation  $\mathbf{p}_1 = \mathbf{P}_i/2 + \mathbf{p}$ ,  $\mathbf{p}_2 = \mathbf{P}_i/2 - \mathbf{p}$  and  $\mathbf{p}'_1 = \mathbf{P}_f/2 + \mathbf{p}'$ ,  $\mathbf{p}'_2 = \mathbf{P}_f/2 - \mathbf{p}'$ . The relativistic single quark magnetic moment operator that appears in the matrix element (3.22) is of the form

$$\boldsymbol{\mu}_{\text{sq}}^{\text{Rel}} = \lim_{\vec{q} \rightarrow 0} \left[ -\frac{i}{2} \nabla_q \times \left[ e^{i\vec{q}\cdot(\vec{r}' + \vec{r})/4} (\mathbf{J}_1(\mathbf{q}, \mathbf{P}) + \mathbf{J}_2(\mathbf{q}, \mathbf{P})) \right] \right], \quad (3.23)$$

where the single quark current operators  $\mathbf{j}_i(\mathbf{q}, \mathbf{P})$  are now treated without approximation.

In the nonrelativistic approximation, the spin-dependent part of the single quark current operator is given by

$$\mathbf{J}_{\text{sq}}^{\text{spin}} = \frac{ie}{2} (\boldsymbol{\sigma}_1 + \boldsymbol{\sigma}_2) \times \mathbf{q} \left[ \frac{Q_1}{2m_1} + \frac{Q_2}{2m_2} \right] + \frac{ie}{2} (\boldsymbol{\sigma}_1 - \boldsymbol{\sigma}_2) \times \mathbf{q} \left[ \frac{Q_1}{2m_1} - \frac{Q_2}{2m_2} \right], \quad (3.24)$$

where the first term describes the magnetic moment of the two-quark system whereas the second term is the spin-flip operator for an M1 transition in the nonrelativistic impulse approximation (NRIA). In order to obtain the relativistic single quark current operator to be used with eq. (3.23), the nonrelativistic current operator for quark 1 should be replaced according to

$$\begin{aligned} \mathbf{J}_1 &= \frac{eQ_1}{2m_1} [\mathbf{p}_1 + \mathbf{p}'_1 + i\boldsymbol{\sigma}_1 \times (\mathbf{p}'_1 - \mathbf{p}_1)] \\ &\rightarrow eQ_1 \sqrt{\frac{(E'_1 + m_1)(E_1 + m_1)}{4E'_1 E_1}} \left[ \frac{\mathbf{p}_1}{E_1 + m_1} + \frac{\mathbf{p}'_1}{E'_1 + m_1} \right. \\ &\quad \left. + i\boldsymbol{\sigma}_1 \times \left( \frac{\mathbf{p}'_1}{E'_1 + m_1} - \frac{\mathbf{p}_1}{E_1 + m_1} \right) \right], \end{aligned} \quad (3.25)$$

and similarly for quark 2. In the above equation, the energy factors of the quarks are defined as  $E_1 = \sqrt{\mathbf{p}_1^2 + m_1^2}$  and  $E'_1 = \sqrt{\mathbf{p}'_1^2 + m_1^2}$ . The spin-flip magnetic moment operator in the non-relativistic impulse approximation (NRIA) may be obtained by insertion of eq. (3.24) into eq. (3.21), giving

$$\boldsymbol{\mu}_{\text{sq}} = \frac{e}{2} \left[ \frac{Q_1}{2m_1} - \frac{Q_2}{2m_2} \right] (\boldsymbol{\sigma}_1 - \boldsymbol{\sigma}_2). \quad (3.26)$$

The corresponding operator in the relativistic impulse approximation (RIA) has been considered in refs. [38, 48], and may for transitions between  $S$ -wave states be expressed as

$$\boldsymbol{\mu}_{\text{sq}}^{\text{Rel}} = \frac{e}{2} \left[ \frac{Q_1}{2m_1} f_1^\gamma - \frac{Q_2}{2m_2} f_2^\gamma \right] (\boldsymbol{\sigma}_1 - \boldsymbol{\sigma}_2), \quad (3.27)$$

where the relativistic factors  $f_i^\gamma$  are defined as

$$f_i^\gamma = \frac{m_i}{3E_i} \left[ 2 + \frac{m_i}{E_i} \right], \quad (3.28)$$

where  $E_i$  denotes the energy factor  $E_i = \sqrt{\mathbf{P}^2 + m_i^2}$ . This shows that a relativistic treatment will lead to an effective weakening of the NRIA spin-flip operator.

In addition to the above single quark current operators, the pair terms in Fig. 3.1 also give large contributions to the magnetic moment operators of mesons and baryons [49]. However, in the case of the magnetic moments of the baryons, additional complications are known to arise from flavor dependent meson exchange interactions which also contribute significant exchange current operators [48]. If the exchange current operators of Fig. 3.1 are decomposed as  $\mathbf{J}_{\text{ex}}(\mathbf{q}, \mathbf{k}_1, \mathbf{k}_2) = \mathbf{J}_{\text{ex1}}(\mathbf{q}, \mathbf{k}_2) + \mathbf{J}_{\text{ex2}}(\mathbf{q}, \mathbf{k}_1)$ , then the contribution to the two-quark magnetic moment operator may be written in the form

$$\boldsymbol{\mu}_{\text{ex}} = \frac{1}{2} \int \frac{d^3 q d^3 k_2}{(2\pi)^6} d^3 r' \left[ e^{i\bar{\mathbf{q}} \cdot (\bar{\mathbf{r}}/2 - \bar{\mathbf{r}}')} e^{i\bar{\mathbf{k}}_2 \cdot \bar{\mathbf{r}}} \mathbf{r}' \times \mathbf{J}_{\text{ex1}}(\mathbf{q}, \mathbf{k}_2) + (1 \rightarrow 2) \right], \quad (3.29)$$

where it is again understood that  $\mathbf{r} \rightarrow -\mathbf{r}$  in the contribution from quark 2. Evaluation of the above equation leads to an expression analogous to eq. (3.21),

$$\boldsymbol{\mu}_{\text{ex}} = \lim_{\vec{q} \rightarrow 0} \left[ -\frac{i}{2} \nabla_{\mathbf{q}} \times \left( e^{i\vec{q}\cdot\vec{r}/2} \int \frac{d^3 k_2}{(2\pi)^3} e^{-i\vec{k}_2\cdot\vec{r}} \mathbf{J}_{\text{ex1}}(\mathbf{q}, \mathbf{k}_2) + e^{-i\vec{q}\cdot\vec{r}/2} \int \frac{d^3 k_1}{(2\pi)^3} e^{i\vec{k}_1\cdot\vec{r}} \mathbf{J}_{\text{ex2}}(\mathbf{q}, \mathbf{k}_1) \right) \right]. \quad (3.30)$$

As the exchange current operators for most Lorentz invariants do not depend explicitly on the photon momentum  $\mathbf{q}$ , one notable exception being that for the scalar invariant [49], then the exchange magnetic moment operators turn out to be difficult to calculate directly from eq. (3.30). It has therefore been shown in paper **VI** that a convenient way to extract the two-quark magnetic moment operators results, if eq. (3.30) is cast in the form

$$\boldsymbol{\mu}_{\text{ex}} = \lim_{\vec{q} \rightarrow 0} \left[ -\frac{i}{2} \int \frac{d^3 k}{(2\pi)^3} e^{-i\vec{k}\cdot\vec{r}} \nabla_{\mathbf{q}} \times \left\{ \mathbf{J}_{\text{ex1}} \left( \frac{\mathbf{q}}{2} + \mathbf{k} \right) + \mathbf{J}_{\text{ex2}} \left( \frac{\mathbf{q}}{2} - \mathbf{k} \right) \right\} \right], \quad (3.31)$$

which is similar to that obtained in ref. [49]. By means of eq. (3.31), it is now possible to consider the two-quark current operators for the scalar confining and vector OGE interactions, as calculated from the diagrams in Fig. 3.1 in paper **V** and ref. [49]. The two-quark current operator associated with the scalar confining interaction is then of the form

$$\mathbf{J}_{\text{ex}}^{\text{c}}(\mathbf{q}, \mathbf{k}_1, \mathbf{k}_2) = -e \left( \frac{Q_1^* \mathbf{P}_1}{m_1^2} + \frac{Q_2^* \mathbf{P}_2}{m_2^2} + \frac{i}{2} (\boldsymbol{\sigma}_1 + \boldsymbol{\sigma}_2) \times \mathbf{q} \left[ \frac{Q_1^*}{2m_1^2} + \frac{Q_2^*}{2m_2^2} \right] + \frac{i}{2} (\boldsymbol{\sigma}_1 - \boldsymbol{\sigma}_2) \times \mathbf{q} \left[ \frac{Q_1^*}{2m_1^2} - \frac{Q_2^*}{2m_2^2} \right] \right), \quad (3.32)$$

where the variables  $Q_1^*$  and  $Q_2^*$  are defined as  $Q_1^* = V_c(\mathbf{k}_2)Q_1$  and  $Q_2^* = V_c(\mathbf{k}_1)Q_2$ , respectively. The corresponding current operator for the OGE interaction may be expressed as

$$\mathbf{J}_{\text{ex}}^{\text{g}}(\mathbf{q}, \mathbf{k}_1, \mathbf{k}_2) = -e \left( Q_1^* \left[ \frac{i\boldsymbol{\sigma}_1 \times \mathbf{k}_2}{2m_1^2} + \frac{2\mathbf{P}_2 + i\boldsymbol{\sigma}_2 \times \mathbf{k}_2}{2m_1 m_2} \right] + Q_2^* \left[ \frac{i\boldsymbol{\sigma}_2 \times \mathbf{k}_1}{2m_2^2} + \frac{2\mathbf{P}_1 + i\boldsymbol{\sigma}_1 \times \mathbf{k}_1}{2m_1 m_2} \right] \right), \quad (3.33)$$

with  $Q_1^* = V_g(\mathbf{k}_2)Q_1$  and  $Q_2^* = V_g(\mathbf{k}_1)Q_2$ . As the above equation depends only on  $\mathbf{k}_1$  and  $\mathbf{k}_2$ , the OGE magnetic moment operator is most conveniently calculated using eq. (3.31). The corresponding spin-flip operators for transitions between  $S$ -wave quarkonium states have been obtained in paper **V** as

$$\boldsymbol{\mu}_{\text{ex}}^{\text{Conf}} = -\frac{eV_c(r)}{4} \left\{ \left[ \frac{Q_1}{m_1^2} - \frac{Q_2}{m_2^2} \right] (\boldsymbol{\sigma}_1 - \boldsymbol{\sigma}_2) + \left[ \frac{Q_1}{m_1^2} + \frac{Q_2}{m_2^2} \right] (\boldsymbol{\sigma}_1 + \boldsymbol{\sigma}_2) \right\} \quad (3.34)$$

for the scalar confining interaction, and

$$\boldsymbol{\mu}_{\text{ex}}^{\text{Oge}} = -\frac{eV_g(r)}{8} \left\{ \left[ \frac{Q_1}{m_1^2} - \frac{Q_2}{m_2^2} - \frac{Q_1 - Q_2}{m_1 m_2} \right] (\boldsymbol{\sigma}_1 - \boldsymbol{\sigma}_2) + \left[ \frac{Q_1}{m_1^2} + \frac{Q_2}{m_2^2} + \frac{Q_1 + Q_2}{m_1 m_2} \right] (\boldsymbol{\sigma}_1 + \boldsymbol{\sigma}_2) \right\} \quad (3.35)$$

for the OGE interaction.

For equal constituent quark masses, eqs. (3.34) and (3.35) reduce to the expressions given in ref. [49]. Note that the presence of a spin-flip term in the OGE operator (3.35) is solely a consequence of the difference in mass between the constituent quarks, and will thus not contribute to the M1 widths of the charmonium and bottomonium states. Similarly, the terms that are symmetric in the quark spins vanish for equal mass quarkonia. However, in the case of the  $B_c^\pm$  system, these terms will contribute to the magnetic moment of the  $c\bar{b}$  system. Also the spin-flip M1 transitions in the  $B_c^\pm$  system will receive a contribution from the OGE operator.

### 3.3 Widths for radiative decay

The widths for E1 dominated transitions of the type  $\chi_{cJ} \rightarrow J/\psi \gamma$  or  $\psi' \rightarrow \chi_{cJ} \gamma$  have in paper **VI** been calculated according to

$$\Gamma = \mathcal{S}_{fi} \frac{2J_f+1}{3} q^3 \alpha \frac{M_f}{M_i} \left[ \frac{4}{9} |\mathcal{M}_0|^2 + \frac{8}{9} |\mathcal{M}_2|^2 \right], \quad (3.36)$$

where  $J_f$  is the total angular momentum of the final quarkonium state, and  $q$  is the momentum of the emitted photon. The widths for  $\psi' \rightarrow \chi_{cJ} \gamma$  with  $J = 0, 1, 2$  are then expected to scale as  $1 : 3 : 5$  respectively, but that result is highly modified by the large hyperfine splittings of the  $Q\bar{Q}$  with  $L = 1$ . The statistical factor  $\mathcal{S}_{fi}$  is defined as in ref. [50] and assumes the values  $\mathcal{S}_{fi} = 1$  for a triplet-triplet transition and  $\mathcal{S}_{fi} = 3$  for a singlet-singlet transition. On the other hand, in paper **VI** the widths for transitions between  $D$ - and  $P$ -wave states were obtained from

$$\Gamma = 4 \mathcal{S}_{fi} \frac{2J_f+1}{27} q^3 \alpha \frac{M_f}{M_i} |\mathcal{M}_0|^2, \quad \mathcal{S}_{fi} = 18 \left\{ \begin{matrix} 2 & 1 & J_d \\ J_p & 1 & 1 \end{matrix} \right\}^2, \quad (3.37)$$

where  $J_d$  and  $J_p$  are the total angular momenta of the  $D$ - and  $P$ -wave states, respectively. The values of  $\mathcal{S}_{fi}$  are then given by the above Wigner  $6j$  symbol. Note that the triangularity of the  $6j$  symbol requires that  $|J_d - J_p| = 1$  or  $0$ . Transitions that change the value of  $J$  by more than one unit are thus forbidden. In eqs. (3.36) and (3.37),  $\mathcal{M}_0$  and  $\mathcal{M}_2$  denote radial matrix elements for  $S$ - and  $D$ -wave photon emission, respectively. The radial matrix element for  $S$ -wave emission receives contributions not only from the impulse approximation, eq. (3.9), but also from the confinement and OGE operators in eq. (3.16). That matrix element may thus be expressed as

$$\mathcal{M}_0 = \int_0^\infty dr r u_f(r) u_i(r) j_0\left(\frac{qr}{2}\right) \left[ \langle Q \rangle_{\text{IA}} + q^2 V_c(r) \langle Q \rangle_c + \left( \frac{\partial V_g(r)}{r \partial r} \right) \langle Q \rangle_g \right], \quad (3.38)$$

where  $u_i$  and  $u_f$  are the reduced radial wave functions for the initial and final heavy quarkonium states. Similarly, the matrix element for  $D$ -wave emission, which vanishes in the E1 approximation, is of the form

$$\mathcal{M}_2 = \langle Q \rangle_{\text{ID}} \int_0^\infty dr r u_f(r) u_i(r) j_2\left(\frac{qr}{2}\right). \quad (3.39)$$

The contribution from this matrix element is usually very small as the product  $qr \ll 1$  for typical values of the photon momenta and quarkonium radii. Therefore, that matrix element has not been included in eq. (3.37).

The impulse approximation charge factor  $\langle Q \rangle_{\text{IA}}$ , and the exchange charge factors  $\langle Q \rangle_c$  for the scalar confining interaction and  $\langle Q \rangle_g$  for the OGE interaction that appear in eqs. (3.38) and (3.39) are of the form

$$\langle Q \rangle_{\text{IA}} = \left[ Q_1 \left( 1 - \frac{q^2}{8m_1^2} \right) \frac{m_2}{m_1 + m_2} - Q_2 \left( 1 - \frac{q^2}{8m_2^2} \right) \frac{m_1}{m_1 + m_2} \right] \quad (3.40)$$

for the impulse approximation, where the quark charge operators have been multiplied with the Darwin-Foldy terms from eq. (3.10), and

$$\begin{aligned} \langle Q \rangle_c &= \left[ \frac{Q_1}{4m_1^3} \frac{m_2}{m_1 + m_2} - \frac{Q_2}{4m_2^3} \frac{m_1}{m_1 + m_2} \right], \\ \langle Q \rangle_g &= \left[ \frac{Q_1}{4m_1^2} \left( \frac{1}{m_1} + \frac{2 \langle S_f | \boldsymbol{\sigma}_1 \cdot \boldsymbol{\sigma}_2 | S_i \rangle}{3 m_2} \right) - \frac{Q_2}{4m_2^2} \left( \frac{1}{m_2} + \frac{2 \langle S_f | \boldsymbol{\sigma}_1 \cdot \boldsymbol{\sigma}_2 | S_i \rangle}{3 m_1} \right) \right], \end{aligned} \quad (3.41)$$

for the charge factors that are associated with the scalar confining and OGE interactions, respectively. In the spin dependent terms of eqs. (3.41),  $S_i$  and  $S_f$  denote the total spins of the initial and final quarkonium states. For triplet-triplet and singlet-singlet transitions,  $\langle S_f | \boldsymbol{\sigma}_1 \cdot \boldsymbol{\sigma}_2 | S_i \rangle = +1$  and  $-3$ , respectively. The charge factor  $\langle Q \rangle_{\text{ID}}$  in eq. (3.39) is defined as  $\langle Q \rangle_{\text{ID}} = \lim_{q \rightarrow 0} \langle Q \rangle_{\text{IA}}$ . This is permissible since the Darwin-Foldy and exchange charge terms are very small compared to the dominant dipole contribution, which in itself is already insignificant because of the suppression by the  $j_2$  function in the matrix element.

The expression for the width of a spin-flip M1 transition between  $S$ -wave heavy quarkonium states can be written in the form

$$\Gamma_{\text{M1}} = \frac{16}{2S_i + 1} q^3 \alpha \frac{M_f}{M_i} |\mathcal{M}_\gamma|^2, \quad (3.42)$$

where  $\mathcal{M}_\gamma$  denotes the radial matrix element for an M1 transition and  $S_i$  is the total spin of the initial state. That matrix element consists of the relativistic impulse approximation, scalar confining and OGE components, according to

$$\mathcal{M}_\gamma = \mathcal{M}_\gamma^{\text{RIA}} + \mathcal{M}_\gamma^{\text{Conf}} + \mathcal{M}_\gamma^{\text{Oge}}, \quad (3.43)$$

where the matrix element in the relativistic impulse approximation is defined according to

$$\mathcal{M}_\gamma^{\text{RIA}} = \frac{2}{\pi} \int_0^\infty dr dr' r r' u_f(r') u_i(r) \int_0^\infty dP P^2 \frac{1}{4} \left[ \frac{Q_1}{m_1} f_1^\gamma - \frac{Q_2}{m_2} f_2^\gamma \right] j_0(r'P) j_0(rP), \quad (3.44)$$

where the factors  $f_i^\gamma$  are given by eq. (3.28). The matrix elements associated with the scalar confining and vector OGE interactions, which have been shown to be large in papers **I**, **V** and **VI** are, in the nonrelativistic approximation, of the form

$$\mathcal{M}_\gamma^{\text{Conf}} = - \int_0^\infty dr u_f(r) u_i(r) \frac{V_c(r)}{4} \left[ \frac{Q_1}{m_1^2} - \frac{Q_2}{m_2^2} \right], \quad (3.45)$$

$$\mathcal{M}_\gamma^{\text{Oge}} = - \int_0^\infty dr u_f(r) u_i(r) \frac{V_g(r)}{8} \left[ \frac{Q_1}{m_1^2} - \frac{Q_2}{m_2^2} - \frac{Q_1 - Q_2}{m_1 m_2} \right]. \quad (3.46)$$

In particular, eq. (3.45) is shown, in the next section, to provide an explanation for the experimental width of the M1 transition  $J/\psi \rightarrow \eta_c \gamma$ .

## 3.4 E1 and M1 transitions in heavy quarkonia

A detailed comparison of the numerical results obtained in papers **V** and **VI** with experimental results and other theoretical calculations is instructive, as there are issues with several of the E1 and M1 transitions that are not readily apparent by casual inspection of the large amount of numerical data presented in those papers. This is even more important as the branching fractions for various transitions are typically better known than the total width of the initial state. With this in mind, the most important ones of the M1 and E1 transitions given in Tables 3.1 and 3.2 are discussed below.

### 3.4.1 The M1 transition $J/\psi \rightarrow \eta_c \gamma$

The major importance of this M1 transition, from both experimental and theoretical points of view, has been stated e.g. in the review of ref. [18]. The experimental width of  $1.14 \pm 0.39$  keV has been difficult to explain theoretically, since nonrelativistic calculations overestimate this width by a factor  $\sim 3$ . A possible solution for this overprediction, which was already hinted at in ref. [47], is presented in Table 3.1, where the exchange current contribution from the scalar confining interaction brings the width down to the desired level. The importance of such negative energy components for the transition  $J/\psi \rightarrow \eta_c \gamma$  has also been demonstrated within the framework of the instantaneous approximation to the Bethe-Salpeter equation in ref. [17] and within the Schrödinger approach in paper **I**.

If the entire  $Q\bar{Q}$  potential had effective vector coupling structure, which has often been suggested in the literature [51], then no exchange current contributions would arise, as a vector interaction contributes a significant spin-flip operator only if the quark and antiquark masses are unequal, and agreement with experiment would thus be excluded. Furthermore, a large family of effective vector confining interactions have been shown to be inconsistent with QCD by ref. [52]. However, it has also been shown in paper **I** that an expansion of the RIA spin-flip operator to order  $v^2/c^2$  overestimates the relativistic correction to the static (NRIA) result, which originally led to an opposite conclusion [47] concerning the usefulness of a scalar two-quark spin-flip operator. It was also suggested that the charm quark might possess a large anomalous magnetic moment, but that possibility has apparently not been substantiated.

### 3.4.2 The M1 transition $\psi' \rightarrow \eta_c \gamma$

This nonrelativistically forbidden M1 transition has also proved challenging to explain theoretically, since the (near) orthogonality of the quarkonium wave functions renders the results hypersensitive to small effects. In the recent calculation by ref. [17], where good agreement with experiment was found for  $J/\psi \rightarrow \eta_c \gamma$ , the width for  $\psi' \rightarrow \eta_c \gamma$  was however overpredicted by almost an order of magnitude. It is shown in Table 3.1 that the M1 model employed in paper **VI** gives a width of  $\sim 1.1$  keV for that transition, which is close to the upper uncertainty limit of the current empirical result  $0.84 \pm 0.24$  keV [46]. That such a favorable result is obtained depends on several factors in the present work, such as the employment of  $\psi'$  and  $\eta_c$  wave functions that model the spin-spin interaction in the  $S$ -wave.

The choice of approximation for the M1 matrix element is also important in this respect. The amplitude (3.17) has the additional advantage of allowing the use of a realistic photon momentum in the expression (3.42) for the M1 width. Also, this treatment yields the same spin-flip operators as in the calculation of the exchange magnetic moment operators in ref. [49], where the rigorous M1 approximation was used. Furthermore, the M1 approximation has been taken to affect the entire factor in brackets in eq. (3.17), which leads to the elimination of the photon momentum  $\mathbf{q}$  from the RIA matrix element (3.44). If the exponentials were separated from the current operators in eq. (3.17), then the width for  $\psi' \rightarrow \eta_c \gamma$  would be overpredicted by a factor  $\sim 4$ . However, if spin-averaged wave functions were employed, as in paper **I**, then the conclusion would be exactly the opposite; In that case the present treatment would lead to unfavorable results. As seen from Table 3.1, the exchange current operator associated with the scalar confining interaction gives the main contribution to the width for  $\psi' \rightarrow \eta_c \gamma$  within this calculation.

The present treatment of the M1 approximation may be regarded as consistent since it leads to the correct spin-flip operators and simultaneously allows a realistic photon momentum to be used. However, the large photon momentum introduces an additional uncertainty, which involves boosts on the  $Q\bar{Q}$  wavefunction in the final state, an effect which is yet to be considered.

### 3.4.3 Other M1 transitions

In principle, the width for  $\Upsilon \rightarrow \eta_b \gamma$  could be predicted with much better accuracy than the corresponding one in the  $c\bar{c}$  system, because of the large mass of the bottom quark. In particular, the exchange current contribution from the scalar confining interaction is much smaller than for  $c\bar{c}$ . The largest uncertainty is introduced by the unknown photon momentum for the  $\Upsilon \rightarrow \eta_b \gamma$  transition, as the mass of the  $\eta_b$  state is not known empirically. As realistic models of the spin-spin splittings for  $S$ -wave quarkonia give an  $\eta_b$  mass around 9400 MeV, then the width for  $\Upsilon \rightarrow \eta_b \gamma$  is likely to be less than 10 eV, as given in Table 3.1.

In addition to the M1 transitions discussed above, predictions have also been given in paper **VI** for M1 transitions between  $Q\bar{Q}$  states below the thresholds for fragmentation. Among these is the transition  $\psi' \rightarrow \eta'_c \gamma$ , which is similar to  $J/\psi \rightarrow \eta_c \gamma$ . As recent experimental results indicate that the mass of the  $\eta'_c$  is much higher than previously thought [33], then the amount of phase space available for  $\psi' \rightarrow \eta'_c \gamma$  is also smaller. The predicted width for that transition is thus significantly smaller than the values suggested by previous work [17]. The width for  $\eta'_c \rightarrow J/\psi \gamma$  is also sensitive to particulars of the model because of cancellations in the matrix element and the large photon momentum involved. The results in Table 3.1 suggest that the width for this transition should be around 2 keV. As the experimental situation concerning the  $\eta'_c$  continues to improve, then the width for  $\eta'_c \rightarrow J/\psi \gamma$  may possibly be measured in the near future.

In the case of the  $b\bar{b}$  system, the number of measurable M1 transitions is larger since the  $3S$  states of bottomonium lie below the threshold for  $B\bar{B}$  fragmentation. These widths are difficult to predict and provide an important test for models of the M1 transitions. The results of paper **VI** suggest that the widths for transitions which do not change the principal quantum number of the quarkonium state should be highly suppressed, whereas the widths for transitions from excited  $\eta_b$  states to the  $\Upsilon$  ground state are predicted to have larger widths of about 100 eV.

Table 3.1: The M1 transitions between low-lying  $S$ -wave states in the charmonium ( $c\bar{c}$ ), bottomonium ( $b\bar{b}$ ) and  $B_c^\pm$  ( $c\bar{b}, \bar{c}b$ ) systems. Experimental data [46] is available only for  $J/\psi \rightarrow \eta_c\gamma$  and  $\psi' \rightarrow \eta_c\gamma$ . The quoted photon momenta  $q_\gamma$  have been obtained by combination of the empirical masses of the spin triplet states with splittings given by the Hamiltonian model of paper VI in Table 2.1. Note that the OGE interaction contributes only to M1 transitions between  $B_c$  states.

Transition	Matrix element [fm]			Width		
	NRIA	RIA	Exch	NRIA	RIA	RIA+Exch
$J/\psi \rightarrow \eta_c\gamma$ $q_\gamma : 116 \text{ MeV}$	$4.356 \cdot 10^{-2}$	$3.762 \cdot 10^{-2}$	$-8.724 \cdot 10^{-3}$	2.85	2.12	<b>1.25 keV</b> ex: $1.14 \pm 0.39$
$\psi' \rightarrow \eta_c\gamma$ $q_\gamma : 639 \text{ MeV}$	$3.985 \cdot 10^{-3}$	$-5.14 \cdot 10^{-4}$	$2.826 \cdot 10^{-3}$	3.35	0.06	<b>1.13 keV</b> ex: $0.84 \pm 0.24$
$\psi' \rightarrow \eta'_c\gamma$ $q_\gamma : 46 \text{ MeV}$	$4.344 \cdot 10^{-2}$	$3.735 \cdot 10^{-2}$	$-1.870 \cdot 10^{-2}$	0.18	0.13	<b>0.03 keV</b>
$\eta'_c \rightarrow J/\psi\gamma$ $q_\gamma : 502 \text{ MeV}$	$-4.271 \cdot 10^{-3}$	$-7.584 \cdot 10^{-3}$	$5.206 \cdot 10^{-3}$	5.89	18.6	<b>1.83 keV</b>
$\Upsilon \rightarrow \eta_b\gamma$ $q_\gamma : 59 \text{ MeV}$	$-6.71 \cdot 10^{-3}$	$-6.39 \cdot 10^{-3}$	$2.41 \cdot 10^{-4}$	9.2	8.3	<b>7.7 eV</b>
$\Upsilon' \rightarrow \eta_b\gamma$ $q_\gamma : 603 \text{ MeV}$	$-3.94 \cdot 10^{-4}$	$-1.44 \cdot 10^{-4}$	$-8.76 \cdot 10^{-5}$	31.8	4.3	<b>11.0 eV</b>
$\Upsilon' \rightarrow \eta'_b\gamma$ $q_\gamma : 25 \text{ MeV}$	$-6.70 \cdot 10^{-3}$	$-6.39 \cdot 10^{-3}$	$5.45 \cdot 10^{-4}$	0.70	0.64	<b>0.53 eV</b>
$\eta'_b \rightarrow \Upsilon\gamma$ $q_\gamma : 530 \text{ MeV}$	$4.18 \cdot 10^{-4}$	$6.30 \cdot 10^{-4}$	$-1.31 \cdot 10^{-4}$	71.5	162	<b>102 eV</b>
$\Upsilon'' \rightarrow \eta''_b\gamma$ $q_\gamma : 16 \text{ MeV}$	$-6.70 \cdot 10^{-3}$	$-6.35 \cdot 10^{-3}$	$8.02 \cdot 10^{-4}$	0.18	0.16	<b>0.13 eV</b>
$\Upsilon'' \rightarrow \eta'_b\gamma$ $q_\gamma : 350 \text{ MeV}$	$-3.59 \cdot 10^{-4}$	$-1.11 \cdot 10^{-4}$	$-1.55 \cdot 10^{-4}$	5.3	0.5	<b>2.9 eV</b>
$\Upsilon'' \rightarrow \eta_b\gamma$ $q_\gamma : 910 \text{ MeV}$	$-2.10 \cdot 10^{-4}$	$-6.59 \cdot 10^{-5}$	$-3.77 \cdot 10^{-5}$	30.2	3.0	<b>7.3 eV</b>
$\eta''_b \rightarrow \Upsilon'\gamma$ $q_\gamma : 311 \text{ MeV}$	$3.96 \cdot 10^{-4}$	$6.05 \cdot 10^{-4}$	$-2.25 \cdot 10^{-4}$	13.7	32.0	<b>12.6 eV</b>
$\eta''_b \rightarrow \Upsilon\gamma$ $q_\gamma : 842 \text{ MeV}$	$2.05 \cdot 10^{-4}$	$3.02 \cdot 10^{-4}$	$-4.68 \cdot 10^{-5}$	68.7	149	<b>106 eV</b>
$B_c^* \rightarrow B_c\gamma$ $q_\gamma : 53 \text{ MeV}$	$1.851 \cdot 10^{-2}$	$1.496 \cdot 10^{-2}$	$0.326 \cdot 10^{-3}$	50.0	32.6	<b>34.0 eV</b>
$B_c^{*'} \rightarrow B_c\gamma$ $q_\gamma : 576 \text{ MeV}$	$1.015 \cdot 10^{-3}$	$-1.437 \cdot 10^{-3}$	$2.524 \cdot 10^{-3}$	179	360	<b>206 eV</b>
$B_c^{*'} \rightarrow B'_c\gamma$ $q_\gamma : 22 \text{ MeV}$	$1.849 \cdot 10^{-2}$	$1.480 \cdot 10^{-2}$	$-5.186 \cdot 10^{-3}$	3.61	2.31	<b>0.98 eV</b>
$B'_c \rightarrow B_c^*\gamma$ $q_\gamma : 507 \text{ MeV}$	$-1.067 \cdot 10^{-3}$	$-3.089 \cdot 10^{-3}$	$1.028 \cdot 10^{-2}$	411	3440	<b>39.5 eV</b>

### 3.4.4 The E1 transitions $\chi_{cJ} \rightarrow J/\psi \gamma$ and $\psi' \rightarrow \chi_{cJ} \gamma$

The E1 transitions from the spin-triplet  $P$ -wave states are in principle the simplest to predict accurately, as the wave functions involved do not contain any nodes. Although the empirical data from ref. [32] has suggested that the E1 widths are generally over-predicted [44], that discrepancy is apparently resolved by the new data presented in the 2002 edition of the PDG [46]. However, the results in Table 3.2 indicate that the rigorous E1 approximation, with  $q = M_i - M_f$ , overpredicts the widths by a factor  $\sim 2$ . If the E1 approximation is removed, the recoil of the  $J/\psi$  can be accounted for, in which case that overprediction is eliminated.

Prediction of the widths for  $\gamma$  transitions from the  $\psi'$  state has proved to be difficult, as the E1 approximation typically overpredicts the widths by at least a factor  $\sim 2$ . The present empirical data [46] on the  $\psi'$  suggests that the widths for  $\psi' \rightarrow \chi_{cJ} \gamma$  should be around 25 keV. As demonstrated in paper **VI**, the E1 approximation yields widths in excess of 40 keV. This is puzzling, since recoil effects are small and cannot explain this overprediction. Also, it is seen by inspection of Table 3.2 that the predicted relative widths also do not agree well with experiment, although the experimental uncertainties are considerable. Not surprisingly, the matrix elements in Table 3.2 reveal that these transitions are very sensitive to small hyperfine effects in the  $Q\bar{Q}$  wave functions, which has also been demonstrated in ref. [47]. It is therefore conceivable that small modifications of the  $Q\bar{Q}$  wave functions may be sufficient to solve this overprediction. It should also be noted that significant reductions of the E1 widths were achieved in ref. [53] by consideration of closed  $c\bar{q} - q\bar{c}$  fragmentation channels.

### 3.4.5 The E1 transitions from the $\chi_{bJ}$ states

The calculated widths for the  $\chi_{bJ} \rightarrow \Upsilon \gamma$  transitions agree rather well with those of the other models presented in Table 3.3, although they appear to be slightly larger. If the calculated E1 widths are used to predict the total widths of the  $\chi_{bJ}$  states, then it is found that the width of the  $\chi_{b2}$  should be  $164 \pm 22$  keV and that of the  $\chi_{b1}$  about  $93 \pm 22$  keV. Similarly, the calculated E1 width of the  $\chi_{b0}$  suggests that the total width of that state is at least  $\sim 440$  keV. This situation is similar to that observed for  $c\bar{c}$  [32], where the  $\chi_{c2}$  is wider than the  $\chi_{c1}$  by about a factor  $\sim 2$ .

The E1 transitions from the  $\chi_{bJ}(2P)$  states in bottomonium provide a useful test for theoretical models since experimental data is available on all six branching fractions [32], even though the total widths of the  $\chi_{bJ}(2P)$  states are not known. These data indicate that the widths for transitions to the  $\Upsilon$  should be about one half of those for transitions to the  $\Upsilon(2S)$ , even though much more phase space is available for the former. Indeed, it can be seen from Table 3.3 that spin-averaged wave functions do not provide a good description of the experimental branching fractions even though the hyperfine splittings of the  $\chi_{bJ}(2P)$  states are small. On the other hand, much better agreement with experiment is obtained if the hyperfine effects are accounted for by the  $Q\bar{Q}$  wave functions. The calculated widths for  $\chi_{bJ}(2P) \rightarrow \Upsilon(2S) \gamma$  may be used to estimate the total widths of the  $\chi_{bJ}(2P)$  states from the known branching fractions. The predicted width of the  $\chi_{b2}(2P)$  state is then  $100 \pm 15$  keV, while that of the  $\chi_{b1}(2P)$  is  $72 \pm 14$  keV. The  $\chi_{b0}(2P)$  state appears to be significantly broader, but because of the large errors in the reported E1 branching fractions, only a rough estimate of  $267 \pm 140$  keV is possible.

Table 3.2: The E1 dominated transitions between low-lying states in the charmonium ( $c\bar{c}$ ) system, together with the empirical data given by ref. [32]. The column "IA" contains the matrix element (3.38) in the impulse approximation, while in the column labeled "DYN", the exchange charge contributions have been included. Note that a good experimental candidate [32] for the  $^3D_1$  state is the  $\psi(3770)$  resonance.

Transition	$\mathcal{M}_0$ [fm]			$\mathcal{M}_2$ [fm]	Width	
	IA	DYN	E1		E1	DYN
$\chi_{c2} \rightarrow J/\psi \gamma$ $q_\gamma : 429 \text{ MeV}$	0.2389	0.2442	0.2632	$7.145 \cdot 10^{-3}$	558 keV	<b>343 keV</b> ex: $389 \pm 60$
$\chi_{c1} \rightarrow J/\psi \gamma$ $q_\gamma : 390 \text{ MeV}$	0.2464	0.2519	0.2673	$5.729 \cdot 10^{-3}$	422 keV	<b>276 keV</b> ex: $290 \pm 60$
$\chi_{c0} \rightarrow J/\psi \gamma$ $q_\gamma : 303 \text{ MeV}$	0.2556	0.2612	0.2701	$3.345 \cdot 10^{-3}$	196 keV	<b>144 keV</b> exp: $165 \pm 40$
$\psi' \rightarrow \chi_{c0} \gamma$ $q_\gamma : 261 \text{ MeV}$	-0.2685	-0.2686	-0.2840	$-6.106 \cdot 10^{-3}$	44.6 keV	<b>33.1 keV</b> ex: $26.1 \pm 4.5$
$\psi' \rightarrow \chi_{c1} \gamma$ $q_\gamma : 171 \text{ MeV}$	-0.3126	-0.3126	-0.3202	$-3.028 \cdot 10^{-3}$	45.8 keV	<b>38.7 keV</b> ex: $25.2 \pm 4.5$
$\psi' \rightarrow \chi_{c2} \gamma$ $q_\gamma : 127 \text{ MeV}$	-0.3440	-0.3442	-0.3489	$-1.871 \cdot 10^{-3}$	37.1 keV	<b>33.1 keV</b> ex: $20.4 \pm 4.0$
$h_c \rightarrow \eta_c \gamma$ $q_\gamma : 493 \text{ MeV}$	0.2098	0.2091	0.2289	$7.377 \cdot 10^{-3}$	661 keV	<b>370 keV</b>
$\eta'_c \rightarrow h_c \gamma$ $q_\gamma : 125 \text{ MeV}$	-0.3420	-0.3424	-0.3465	$-1.618 \cdot 10^{-3}$	61.5 keV	<b>55.0 keV</b>
$\psi'' \rightarrow \chi_{c0} \gamma$ $q_\gamma : 577 \text{ MeV}$	-0.0456	-0.0450	-0.0199	$0.926 \cdot 10^{-2}$	2.69 keV	<b>9.86 keV</b>
$\psi'' \rightarrow \chi_{c1} \gamma$ $q_\gamma : 494 \text{ MeV}$	-0.0306	-0.0298	-0.0033	$1.016 \cdot 10^{-2}$	0.13 keV	<b>9.57 keV</b>
$\psi'' \rightarrow \chi_{c2} \gamma$ $q_\gamma : 455 \text{ MeV}$	-0.0168	-0.0161	0.0123	$1.099 \cdot 10^{-2}$	2.38 keV	<b>5.75 keV</b>
$\psi'' \rightarrow \chi'_{c0} \gamma$ $q_\gamma : 153 \text{ MeV}$	-0.4315	-0.4315	-0.4497	$-7.344 \cdot 10^{-3}$	21.3 keV	<b>17.8 keV</b>
$\psi'' \rightarrow \chi'_{c1} \gamma$ $q_\gamma : 125 \text{ MeV}$	-0.4860	-0.4861	-0.4995	$-5.399 \cdot 10^{-3}$	42.6 keV	<b>37.3 keV</b>
$\psi'' \rightarrow \chi'_{c2} \gamma$ $q_\gamma : 109 \text{ MeV}$	-0.5280	-0.5283	-0.5391	$-4.367 \cdot 10^{-3}$	53.7 keV	<b>48.2 keV</b>
$^3D_3 \rightarrow \chi_{c2} \gamma$ $q_\gamma : 227 \text{ MeV}$	0.4164	0.4194	0.4353	–	243 keV	<b>192 keV</b>
$^3D_2 \rightarrow \chi_{c2} \gamma$ $q_\gamma : 221 \text{ MeV}$	0.4188	0.4219	0.4367	–	56.5 keV	<b>45.2 keV</b>
$^3D_2 \rightarrow \chi_{c1} \gamma$ $q_\gamma : 263 \text{ MeV}$	0.3920	0.3953	0.4145	–	262 keV	<b>198 keV</b>
$^3D_1 \rightarrow \chi_{c2} \gamma$ $q_\gamma : 206 \text{ MeV}$	0.4216	0.4246	0.4372	–	5.06 keV	<b>4.13 keV</b>
$^3D_1 \rightarrow \chi_{c1} \gamma$ $q_\gamma : 248 \text{ MeV}$	0.3963	0.3997	0.4164	–	123 keV	<b>94.9 keV</b>
$^3D_1 \rightarrow \chi_{c0} \gamma$ $q_\gamma : 336 \text{ MeV}$	0.3578	0.3619	0.3889	–	370 keV	<b>251 keV</b>

### 3.4.6 The E1 transitions from the $\Upsilon$ states

The experimental situation concerning the  $\Upsilon(2S) \rightarrow \chi_{bJ} \gamma$  transitions has lately become more uncertain since the total width of the  $\Upsilon(2S)$  as reported by ref. [32], originally given as  $\sim 27$  keV, has increased over time and now stands at  $44 \pm 7$  keV. This situation is analogous to that for the  $\psi'$ , which has undergone a similar, albeit smaller, increase. This has made the model predictions in Table 3.3, which originally fitted the experimental data very well, much less satisfactory. It is therefore very difficult to judge the quality of any given prediction until the experimental situation is stabilized. Still, it is noteworthy that the calculation of paper **VI** gives slightly better agreement with experiment than the other models in Table 3.3.

As the reported total width of the  $\Upsilon(3S)$  state [32],  $26.3 \pm 3.5$  keV, is better known than that of the  $\Upsilon(2S)$  state, then it is expected that systematic uncertainties in the reported experimental results for  $\Upsilon(3S) \rightarrow \chi_{bJ}(2P) \gamma$  should be smaller than for the analogous  $\Upsilon(2S) \rightarrow \chi_{bJ} \gamma$  transitions. By inspection of Table 3.3, it can be seen that the  $\Upsilon(3S) \rightarrow \chi_{bJ}(2P) \gamma$  transitions are generally rather well described by a number of models, although the calculation of ref. [47], where spin-averaged wave functions were employed, apparently underpredicts the empirical widths. Also, the results of ref. [54] appear to compare slightly more favorably with experiment than those of the calculation in paper **VI**.

While the  $\Upsilon(3S) \rightarrow \chi_{bJ}(2P) \gamma$  transitions are relatively well described by different models, the situation concerning the  $\Upsilon(3S) \rightarrow \chi_{bJ} \gamma$  transitions remains unsettled because of a strong cancellation in the E1 matrix element. However, experimental detection of these transitions may be a formidable task since the widths are an order of magnitude smaller than those of any previously measured E1 transition in the  $b\bar{b}$  system. Inspection of the results in paper **VI** reveals that within the dynamical model, the width for  $\Upsilon(3S) \rightarrow \chi_{b0} \gamma$  should be the largest and that for  $\Upsilon(3S) \rightarrow \chi_{b2} \gamma$  the smallest. It is encouraging that the same pattern is also predicted in Table 3.2 for the analogous transitions in the  $c\bar{c}$  system, where the widths are much larger relative to the other E1 transitions.

### 3.4.7 Other E1 transitions

The widths for E1 transitions from the  $\psi(3S)$  state have also been given in Table 3.2. Those results suggest that the transitions to the  $(2P)$  states should have widths that are comparable to those for the  $\psi' \rightarrow \chi_{cJ} \gamma$  transitions. On the other hand, the widths for the  $\psi(3S) \rightarrow \chi_{cJ} \gamma$  transitions are predicted to be smaller by factors 3–4. The empirical detection of any of these transitions will probably be difficult since the  $\psi(3S)$  state lies above the  $D\bar{D}$  threshold. However, since the spin singlet  $h_c$  state is well below threshold, then the photon produced in the  $h_c \rightarrow \eta_c \gamma$  transition may be detected in the near future. The dynamical model yields a width of 370 keV for this transition, which is then the largest E1 width in the  $c\bar{c}$  system, although the difference between the E1 approximation and the dynamical model is large for that transition.

The E1 transitions from the  ${}^3D_1$  state are also of particular interest, as that state probably corresponds to the empirical  $\psi(3770)$  resonance. The predictions of paper **VI** suggest that the transitions to the  $\chi_{c1}$  and  $\chi_{c0}$  states should be detectable by experiment, whereas that to the  $\chi_{c2}$  state is highly suppressed by the statistical factor  $\mathcal{S}_{fi}$ .

Table 3.3: Comparison of the predicted E1 widths in the bottomonium ( $b\bar{b}$ ) system with those of other models that use a scalar confining interaction. All widths are given in keV. The experimental widths have been extracted from the branching fractions and total widths reported by ref. [32].

	GS (ref. [47])	GZ (ref. [54])	paper VI	Exp (ref. [32])
$\chi_{b2} \rightarrow \Upsilon \gamma$	33.0	33.8	<b>36.0</b>	$22 \pm 3\%$
$\chi_{b1} \rightarrow \Upsilon \gamma$	29.8	30.4	<b>32.5</b>	$35 \pm 8\%$
$\chi_{b0} \rightarrow \Upsilon \gamma$	25.7	25.3	<b>26.6</b>	$< 6\%$
$\Upsilon' \rightarrow \chi_{b0} \gamma$	0.73	0.76	<b>1.01</b>	$1.7 \pm 0.5$ keV
$\Upsilon' \rightarrow \chi_{b1} \gamma$	1.62	1.37	<b>1.80</b>	$3.0 \pm 0.7$ keV
$\Upsilon' \rightarrow \chi_{b2} \gamma$	1.84	1.45	<b>2.03</b>	$3.1 \pm 0.7$ keV
$\chi'_{b2} \rightarrow \Upsilon' \gamma$	12.9	16.2	<b>16.4</b>	$16.4 \pm 2.4\%$
$\chi'_{b1} \rightarrow \Upsilon' \gamma$	11.9	14.7	<b>15.1</b>	$21 \pm 4\%$
$\chi'_{b0} \rightarrow \Upsilon' \gamma$	10.6	12.3	<b>12.3</b>	$4.6 \pm 2.1\%$
$\chi'_{b2} \rightarrow \Upsilon \gamma$	18.2	10.4	<b>11.4</b>	$7.1 \pm 1.0\%$
$\chi'_{b1} \rightarrow \Upsilon \gamma$	11.8	7.51	<b>8.40</b>	$8.5 \pm 1.3\%$
$\chi'_{b0} \rightarrow \Upsilon \gamma$	6.50	3.57	<b>4.93</b>	$0.9 \pm 0.6\%$
$\Upsilon'' \rightarrow \chi_{b0} \gamma$	0.114	0.029	<b>0.15</b>	–
$\Upsilon'' \rightarrow \chi_{b1} \gamma$	0.003	0.095	<b>0.11</b>	–
$\Upsilon'' \rightarrow \chi_{b2} \gamma$	0.194	0.248	<b>0.04</b>	–
$\Upsilon'' \rightarrow \chi'_{b0} \gamma$	1.09	1.30	<b>1.14</b>	$1.4 \pm 0.3$ keV
$\Upsilon'' \rightarrow \chi'_{b1} \gamma$	2.15	2.34	<b>2.12</b>	$3.0 \pm 0.5$ keV
$\Upsilon'' \rightarrow \chi'_{b2} \gamma$	2.29	2.71	<b>2.50</b>	$3.0 \pm 0.6$ keV

The determination of the photon momenta for transitions in the bottom-charm  $B_c^\pm$  system has to rely on model predictions for the masses of the  $c\bar{b}$  states. The uncertainty introduced by this is, however, rather small for the E1 transitions, as the model predictions for the major level splittings agree with each other to a large extent [50]. Inspection of the results in paper VI reveals that the predicted widths are similar to those obtained by ref. [50], although differences exist for transitions like  $B_c^*(2S) \rightarrow B_{c0}^* \gamma$  and  $B_{c2}^*(2P) \rightarrow B_c^*(2S) \gamma$ , where the widths are sensitive to the effects of the hyperfine components of the  $Q\bar{Q}$  interaction. It is noteworthy that while the predicted widths for the  $B_{cJ}^* \rightarrow B_c^* \gamma$  transitions agree rather well with those from ref. [50], there is a significant disagreement for  $B_{c1} \rightarrow B_c \gamma$ . When the somewhat different photon momenta are accounted for, this disagreement amounts to about a factor  $\sim 3$ .

An issue not considered in paper VI is the spin mixing of the  $L = 1$  states with  $J = 1$ , that is due to the antisymmetric spin-orbit interaction which was not included in the  $Q\bar{Q}$  interaction Hamiltonian. This mixing, which was considered in ref. [50], has the effect of allowing "spin-flip" E1 transitions of the type  $B_{c1}^* \rightarrow B_c \gamma$ . However, the widths for such "forbidden" transitions were found in ref. [50] to be typically suppressed by a factor  $\sim 100$  relative to the "allowed" ones considered in paper VI.

### 3.5 M1 transitions in heavy-light mesons

The M1 widths of the spin-flip M1 transition between the vector and pseudoscalar states in the charm mesons have been calculated in paper **V**, where the  $Q\bar{q}$  interaction was modeled as a scalar confining + OGE potential. A comparison of the results presented in Table 3.4 is instructive since the total width of the  $D^{\pm*}$  state has recently been measured by the CLEO collaboration [55]. The width is reported as  $\Gamma(D^{\pm*}) = 96 \pm 4 \pm 22$  keV, where the latter error represents the systematic uncertainty. The reported [32] branching ratio of  $1.6 \pm 0.4\%$  for radiative decay then gives a width of  $1.5 \pm 0.6$  keV for the M1 transition  $D^{\pm*} \rightarrow D^{\pm}\gamma$ . Here most of the uncertainty can be traced to the systematic errors of the experimental result. Such a comparison shows that the results of Table 3.4 reproduce the empirical width fairly well for a range of values of the light constituent quark mass  $m_q$ . The value  $m_q = 450$  MeV corresponds to the potential model of ref. [38], while the value  $m_q = 420$  MeV has been suggested in ref. [30]. Indeed, for a light constituent quark mass of 420 MeV, a width for radiative M1 decay which is close to 1.5 keV is reproduced. Values close to that are also favored by the analysis within the framework of the Gross equation by ref. [56].

$D^{0*} \rightarrow D^0\gamma$	NRIA	RIA	RIA + Exch
450 MeV	21.1 keV	8.86 keV	<b>8.95 keV</b>
420 MeV	23.5 keV	9.18 keV	<b>9.89 keV</b>
390 MeV	26.4 keV	9.52 keV	<b>11.1 keV</b>

$D^{\pm*} \rightarrow D^{\pm}\gamma$	NRIA	RIA	RIA + Exch
450 MeV	0.58 keV	$9.4 \cdot 10^{-3}$ keV	<b>1.09 keV</b>
420 MeV	0.79 keV	$1.5 \cdot 10^{-2}$ keV	<b>1.43 keV</b>
390 MeV	1.07 keV	$2.2 \cdot 10^{-2}$ keV	<b>1.90 keV</b>

$D_s^{\pm*} \rightarrow D_s^{\pm}\gamma$	NRIA	RIA	RIA + Exch
560 MeV	0.18 keV	$2.6 \cdot 10^{-4}$ keV	<b>0.38 keV</b>
530 MeV	0.26 keV	$3.9 \cdot 10^{-5}$ keV	<b>0.49 keV</b>
500 MeV	0.36 keV	$8.6 \cdot 10^{-4}$ keV	<b>0.64 keV</b>

Table 3.4: Numerical results from paper **V** for the M1 transitions between ground state vector and pseudoscalar mesons in the  $D$  and  $D_s$  systems, for different values of the light and strange constituent quark masses. The charm quark mass of 1580 MeV corresponds to the potential model of ref. [38]. In the right-hand column, the two-quark exchange current contributions from the scalar confining and OGE interactions have been added to the RIA result.

Even though the total width of the neutral  $D^{0*}$  meson has not yet been determined [32], considerable information about the expected width for  $D^{0*} \rightarrow D^0\gamma$  may be extracted from the reported branching fraction of  $38.1 \pm 2.9\%$  [32], since the corresponding width for pion emission can be constrained by means of the empirically determined width of the  $D^{\pm*}$  and model calculations of the pionic transitions in  $D$  mesons [56, 57]. If one notes that the branching fraction of  $D^{\pm*} \rightarrow D^0\pi^{\pm}$  is reported as  $67.7 \pm 0.5\%$  [32] which implies a width for this transition of  $\sim 65 \pm 14$  keV, then it is found from the model calculation of paper **III** that this corresponds to a width of  $\sim 40 \pm 10$  keV for  $D^{0*} \rightarrow D^0\pi^0$ . As the relative branching fractions for  $\pi^0$  and  $\gamma$  emission by the  $D^{0*}$  are well known [32], the

best estimate for the width of  $D^{0*} \rightarrow D^0\gamma$  is  $\sim 25$  keV, which is close to that preferred by ref. [56]. There remains, however, a considerable uncertainty of  $\sim \pm 10$  keV from the systematic errors in the empirical measurement of  $\Gamma(D^{\pm*})$ .

The results of paper **V** in Table 3.4 underpredict this expectation by about a factor  $\sim 2$ , which underlines a basic weakness of the present approach to the M1 transitions in the  $D$  mesons. Firstly, as the two-quark spin-flip operators of eqs. (3.34) and (3.35) are given for the nonrelativistic approximation, a relativistic treatment of those operators will, in general, lead to a weakening of the two-quark contributions to the matrix element for an M1 transition. It is thus entirely possible that a fully relativistic treatment will render the two-quark contributions too weak to account for the experimental data on M1 decay of the  $D^{\pm}$  meson as well. This conclusion is in line with that reached in ref. [56], where the discrepancy between the model and experiment was parameterized in terms of a large anomalous magnetic moment for the light quark.

Another interesting possibility discussed in paper **V** suggests itself, in view of the problems of fitting the spectra of the  $Q\bar{q}$  mesons within the framework of the BSLT equation using a OGE interaction alone, namely that the instanton induced interaction for  $Q\bar{q}$  systems given in ref. [30] may also contribute a significant two-quark current. The interaction of ref. [30], which was found to be short-ranged, attractive and with negative sign, has scalar coupling to the light constituent quark. It has been noted in paper **V** that such an interaction adds up constructively with the OGE contribution, and counteracts that from the scalar confining interaction. An overall favorable effect on the widths for M1 transitions may thus be obtained, which may be inferred from the matrix elements given in paper **V**.

## Chapter 4

# Pionic Transitions

The pionic transitions in the heavy-light  $D$  mesons are instructive, as they can provide direct information on the strength of the coupling between pions and light constituent quarks. Furthermore, as the charm quark in the  $D$  mesons does not couple to pions, the decay mechanism is governed by the pion coupling to the light constituent quark alone. As a first approximation, the pion-light constituent quark coupling can be taken as being independent of the quark-antiquark interaction in the  $D$  meson. It has been shown in paper **II**, where the pion emission was modeled in terms of the chiral pseudovector Lagrangian, that while this assumption is reasonable for the axial current term, it leads to a large overestimate of the axial charge contribution. In this case two-quark pair terms analogous to those that are required for a realistic description of the M1 transition  $J/\psi \rightarrow \eta_c \gamma$  may reduce the axial charge amplitude to a realistic level. An analogous suppression of the  $S$ -wave pion transitions was achieved in ref. [56] within the framework of the Gross quasipotential reduction.

The empirical information on the widths and branching fractions of excited charm mesons is still very limited. Absolute values, albeit with large uncertainties, are known for the  $D_1(2420)$  and  $D_2^*(2460)$  mesons, and recently the width of the  $D^*(2010)^\pm$ , for which only an upper bound of 0.131 MeV [32] was available earlier, has now been reported as  $96 \pm 4 \pm 22$  keV by the CLEO collaboration [55]. This result is shown to be consistent with values of the pion-quark axial coupling  $g_A^q$  that are slightly smaller than 1. The observed widths of the  $L = 1$   $D_1(2420)$  and  $D_2^*(2460)$  mesons are also shown to be fairly well described, although a slight underprediction is expected as it has been demonstrated in paper **III** that two-pion  $\pi\pi$  decay may also contribute significantly to the total widths of those mesons. In particular, the analogy with the  $K_2^*(1430)$  strange meson suggests that  $\pi\pi$  transitions may account for a significant fraction of the observed total widths.

The flavor symmetry breaking decay mode  $D_s^* \rightarrow D_s \pi^0$ , which has been considered in paper **V** is mainly due to a small isoscalar  $\eta$  meson component in the physical  $\pi^0$  meson, as only the  $\eta$  meson can couple to the strange quark in the  $D_s$  meson. The known ratio of the branching fractions for  $D_s^* \rightarrow D_s \pi^0$  and  $D_s^* \rightarrow D_s \gamma$  may be used to extract the coupling of  $\eta$  mesons to strange quarks, once the value of the  $\pi^0$ - $\eta$  mixing angle is known. Applied to the quark model for the baryons, an  $\eta NN$  pseudovector coupling constant, small enough to be consistent with the phenomenological analysis of photoproduction of the  $\eta$  on the nucleon and the reaction  $pp \rightarrow pp\eta$ , has been obtained in paper **V**.

## 4.1 The amplitude for pion emission

In paper **II**, the emission of pions from a  $D$  meson was described by the pseudovector Lagrangian, which constitutes the lowest order chiral coupling for pions to light constituent quarks:

$$\mathcal{L}_{qq\pi} = i \frac{g_A^q}{2f_\pi} \bar{\psi}_q \gamma_5 \gamma_\mu \partial_\mu \pi_a \tau_a \psi_q. \quad (4.1)$$

Here  $g_A^q$  denotes the axial coupling constant of pions to light constituent quarks, and  $f_\pi$  is the pion decay constant, the empirical value of which is 93 MeV. The axial coupling constant is conventionally taken to be equal to, or somewhat less than, unity [58]. The Lagrangian (4.1) yields the following transition amplitude for pion emission:

$$T_\pi = \xi \frac{g_A^q}{2f_\pi} \bar{u}_q(\mathbf{p}') \gamma_5 \gamma_\mu q_\mu u_q(\mathbf{p}), \quad (4.2)$$

where  $\xi$  is an isospin factor, the value of which is  $\sqrt{2}$  for  $\pi^\pm$  and 1 for  $\pi^0$  emission. Decomposition of the above amplitude into axial current and axial charge components yields the pion emission amplitude in the impulse approximation,

$$\begin{aligned} T_\pi = & -i \xi \frac{g_A^q}{2f_\pi} \sqrt{\frac{(E'_q + m_q)(E_q + m_q)}{4E'_q E_q}} \left[ 1 - \frac{\mathbf{P}^2 - \mathbf{q}^2/4}{3(E'_q + m_q)(E_q + m_q)} \right] \boldsymbol{\sigma}_q \cdot \mathbf{q} \\ & + i \xi \frac{g_A^q}{2f_\pi} \frac{2m_q + E_q + E'_q}{\sqrt{4E_q E'_q (E_q + m_q)(E'_q + m_q)}} \omega_\pi \boldsymbol{\sigma}_q \cdot \mathbf{P}, \end{aligned} \quad (4.3)$$

where the first (axial current) term gives rise to the  $P$ -wave transitions  $D^* \rightarrow D\pi$  and the  $D$ -wave transitions from the  $L = 1$  charm mesons. On the other hand, the axial charge term leads to  $S$ -wave transitions from states with  $L = 1$ .

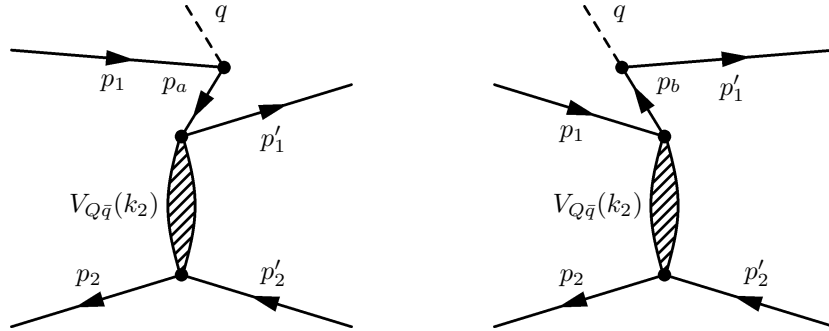


Figure 4.1: Irreducible two-quark contributions associated with the  $Q\bar{q}$  interaction to the axial current and axial charge operators, with four-momentum variables defined as for Fig. 3.1. The pion always interacts with the light constituent quark, as the charm quark does not couple to pions.

As demonstrated in paper **II**, two-quark axial exchange current operators illustrated by Fig. 4.1 give large contributions to several  $\pi$  transitions, in particular to those which involve the axial charge amplitude. In that case the axial exchange charge operator is of equal magnitude as the single quark operator, while the axial exchange current operators typically represent  $\sim 10\%$  corrections to the impulse approximation result. If, in the static approximation, the axial current  $A_{\mu a} = (\mathbf{A}_a, iA_{0a})$  of the light constituent quark is expressed as

$$\mathbf{A}_a = -g_A^q \boldsymbol{\sigma}_q \tau_a, \quad (4.4)$$

then the contribution to the axial current from a scalar confining interaction is, to lowest order in  $v/c$ , of the form [59]

$$\mathbf{A}_a^{\text{Conf}} = -\frac{g_A^q}{4m_q^3} V_c(\mathbf{k}_2) \left[ 3 \boldsymbol{\sigma}_q \mathbf{P}^2 - \frac{1}{4} \boldsymbol{\sigma}_q \mathbf{k}_2^2 - 4 \mathbf{P} \boldsymbol{\sigma}_q \cdot \mathbf{P} + 2i \mathbf{P} \times \mathbf{k}_2 \right] \tau_a, \quad (4.5)$$

where  $V_c(\mathbf{k}_2)$  is the Fourier transform of the scalar confining interaction. The above expression does not include the corrections from the canonical boost factors on the single quark spinors that are included in the single quark operator, eq. (4.3). Moreover, a factor  $m_q^{-2}$  in the axial exchange current operator (4.5) arises as the static approximation to the propagator of the intermediate negative energy quark.

Hence a more realistic evaluation requires that those factors are taken into account. For simplicity, the same spinor factors as for the single quark operator were used in paper **II**. The so obtained results indicate that the static approximation implies a very large overestimate of the axial exchange current contribution. Nevertheless, as shown in Tables 4.1 and 4.2, it serves to increase the calculated widths for pion emission. A complete calculation would also require consideration of the axial exchange currents associated with the short-range OGE or instanton induced interactions, which was not attempted in paper **II**.

Both the scalar confining and OGE interactions contribute a two-quark operator to the axial charge amplitude in eq. (4.3). These operators have been calculated in ref. [60] and are of the form

$$A_{0a}^{\text{Conf}} = \frac{g_A^q}{m_q} V_c(\mathbf{k}_2) \boldsymbol{\sigma}_q \cdot \mathbf{P} \tau_a, \quad (4.6)$$

for the scalar confining interaction, and

$$A_{0a}^{\text{Oge}} = \frac{g_A^q}{m_q M_{\bar{Q}}} V_g(\mathbf{k}_2) \left[ \boldsymbol{\sigma}_q \cdot \mathbf{P}_{\bar{Q}} + \frac{1}{2} \boldsymbol{\sigma}_q \times \boldsymbol{\sigma}_{\bar{Q}} \cdot \mathbf{k}_2 \right] \tau_a, \quad (4.7)$$

for the OGE interaction, which, when compared with the single quark axial charge

$$A_{0a} = -\frac{g_A^q}{m_q} \boldsymbol{\sigma}_q \cdot \mathbf{P} \tau_a \quad (4.8)$$

reveals that the scalar confining interaction will tend to cancel out the axial charge component of the amplitude for pion emission. However, the calculations in paper **II** show that the OGE contribution is also large, although formally suppressed by a factor  $m_q/M_{\bar{Q}}$ . It has also been shown in paper **II** that a relativistic treatment of the axial exchange charge operators will weaken them significantly. Although qualitative, these conclusions are in line with the experimentally small width of the  $L = 1, J = 1 D_1$  resonance.

## 4.2 The pionic widths of the $D$ mesons

The pionic decays of the  $D^*$  mesons presented in Table 4.1 are intriguing since the emitted pions are extremely soft. Due to the very small phase space, the transition  $D^{*0} \rightarrow D^\pm \pi^\mp$  is kinematically forbidden. The results appear to favor the value of  $g_A^q = 0.87$ , although that is accidental since only an upper limit on the width of the  $D^{\pm*}$  was known [32] when paper **II** was published. For this value of  $g_A^q$ , the total widths of the  $L = 1$   $D$  mesons in Table 4.2 appear to be underpredicted, although  $\pi\pi$  transitions may contribute significantly to these, as proposed in paper **III**. However, the empirical widths are still rather uncertain [46], and have decreased over time.

The results for the pionic widths of the excited  $D$  mesons are rather similar to those of ref. [56], especially for the transitions  $D^* \rightarrow D\pi$ , even though the Gross framework was employed in that paper. That calculation was restricted to the transitions allowed by the lowest order selection rules suggested by Heavy Quark Symmetry (HQS) [61], whereas the present work uses the  $LS$ -coupling scheme, which is more appropriate for equal mass quarkonia. The connection between the present calculation and the heavy quark limit remains as yet unexplored.

Table 4.1: The calculated and experimental [46, 55] pionic widths in MeV for the  $D^*$  mesons, corresponding to  $g_A^q = 0.87$ . The single quark approximation, with relativistic corrections is denoted RIA, and the result obtained upon addition of the axial exchange current contribution is denoted RIA + EXCH. The net results are also shown for  $g_A^q = 1$ .

Transition	$\pi$ mom.	RIA	RIA + EXCH	$g_A^q = 1$	Experiment
$D^{*\pm} \rightarrow D^\pm \pi^0$	38.3 keV	0.026	<b>0.029</b>	0.038	$0.029 \pm 0.008$ MeV
$D^{*\pm} \rightarrow D^0 \pi^\pm$	39.6 keV	0.056	<b>0.064</b>	0.084	$0.065 \pm 0.017$ MeV
$D^{*0} \rightarrow D^0 \pi^0$	43.1 keV	0.036	<b>0.041</b>	0.054	< 1.3 MeV

Table 4.2: Calculated and empirical pion decay widths of the  $D_1$  and  $D_2^*$  mesons driven by the axial current and charge operators respectively, for  $g_A^q = 0.87$ . The empirical values are total widths [46], which should mainly be due to pionic transitions to the ground state. The numbers in parentheses are the widths obtained without the axial exchange current contribution. The calculated values are also shown for  $g_A^q = 1$ .

Transition	Current (RIA)	Charge	Total	$g_A^q = 1$	Experiment
$D_1 \rightarrow D^* \pi$	4.2 (3.4)	6.1	<b>10.3 MeV</b>	13.6	$18.9_{-3.5}^{+4.6}$ MeV
$D_2^* \rightarrow D \pi$	8.1 (6.7)	–	<b>8.1 MeV</b>	10.6	–
$D_2^* \rightarrow D^* \pi$	3.9 (3.1)	–	<b>3.9 MeV</b>	5.1	–
$D_2^* \rightarrow D \pi + D^* \pi$	11.9 (9.9)	–	<b>11.9 MeV</b>	15.7	$25_{-7}^{+8}$ MeV

### 4.3 $\pi^0$ and $\gamma$ transitions from the $D_s^*$ meson

Consideration of the coupling of the octet of light pseudoscalar mesons to the light ( $u, d, s$ ) quarks yields, analogously to eq. (4.1) the couplings

$$\mathcal{L}_{qq\varphi} = i \frac{g_A^q}{2f_\varphi} \bar{\psi}_q \gamma_5 \gamma_\mu \partial_\mu \varphi_a \lambda_a \psi_q. \quad (4.9)$$

For the pions and the  $\eta$  meson, the empirical decay constants are  $f_\pi = 93$  MeV and  $f_\eta = 112$  MeV, respectively, so at least for the decay constants  $SU(3)$  flavor symmetry is broken only at the 10% level. Combination of the chiral coupling (4.9) with the representation

$$\varphi_a \lambda_a = \sqrt{2} \begin{bmatrix} \frac{\pi^0}{\sqrt{2}} + \frac{\eta^0}{\sqrt{6}} & \pi^+ & K^+ \\ \pi^- & -\frac{\pi^0}{\sqrt{2}} + \frac{\eta^0}{\sqrt{6}} & K^0 \\ \bar{K}^- & \bar{K}^0 & -\sqrt{\frac{2}{3}}\eta^0 \end{bmatrix}, \quad \psi_q = \begin{pmatrix} u \\ d \\ s \end{pmatrix} \quad (4.10)$$

gives the following definitions for the quark-level pseudovector coupling constants  $f_{\varphi qq}$ ,

$$f_{\pi qq} = \frac{m_\pi}{2f_\pi} g_A^q, \quad f_{\eta qq} = \frac{m_\eta}{2\sqrt{3}f_\eta} g_A^q, \quad f_{\eta ss} = -\frac{m_\eta}{\sqrt{3}f_\eta} g_A^q. \quad (4.11)$$

The above relations then suggest that the magnitude of the coupling of  $\eta$  mesons to  $u, d$  quarks should be one-half that of the  $\eta$  coupling to strange quarks, independently of the  $\eta$  meson mass. In the static quark model the meson-quark coupling constants of eq. (4.11) are related to the meson-nucleon coupling constants as

$$f_{\pi NN} = \frac{5}{3} f_{\pi qq}, \quad f_{\eta NN} = f_{\eta qq}. \quad (4.12)$$

Application of the relations (4.11) together with eq. (4.9) yields a coupling of  $\eta$  mesons to strange quarks in terms of  $f_{\eta ss}$ . The coupling of the  $\pi^0$  meson to the strange quark may thus be expressed in terms of the "effective" mixing angle  $\theta_m$ , which corresponds to the sum of the  $\pi^0-\eta$  and  $\pi^0-\eta'$  contributions. The width for the process  $D_s^* \rightarrow D_s \pi^0$  can then be conveniently obtained from the expression for  $D^{\pm*} \rightarrow D^\pm \pi^0$  given in paper **II** by the replacement  $g_A^q/2f_\pi \rightarrow f_{\eta ss} \theta_m/m_\eta$ , giving

$$\Gamma(D_s^* \rightarrow D_s \pi^0) = \frac{1}{6\pi} \frac{M_{D_s}}{M_{D_s^*}} \frac{f_{\eta ss}^2}{m_\eta^2} \theta_m^2 q_\pi^3 |\mathcal{M}_\pi|^2, \quad (4.13)$$

if the  $\pi^0$  emission takes place at the strange quark. Here  $\mathcal{M}_\pi$  is a radial matrix element for pion emission. On the other hand, the width for the radiative M1 transition  $D_s^* \rightarrow D_s \gamma$  was obtained, in paper **V**, as

$$\Gamma(D_s^* \rightarrow D_s \gamma) = \frac{16}{3} \frac{M_{D_s}}{M_{D_s^*}} \alpha q_\gamma^3 |\mathcal{M}_\gamma|^2, \quad (4.14)$$

where  $\mathcal{M}_\gamma$  is a radial matrix element for M1 decay. By means of eqs. (4.13) and (4.14), the ratio of the  $\pi^0$  and  $\gamma$  widths of the  $D_s^*$  meson is then obtained as

$$\frac{\Gamma_\pi}{\Gamma_\gamma} = \frac{8}{9\pi} \frac{f_{\eta ss}^2 \theta_m^2}{m_\eta^2 \alpha} \left( \frac{q_\pi}{q_\gamma} \right)^3 \left( \frac{|\mathcal{M}_\pi|}{|\mathcal{M}_\gamma|} \right)^2, \quad (4.15)$$

where the dimension of  $|\mathcal{M}_\gamma|$  is  $[\text{MeV}]^{-1}$ .

## 4.4 Estimation of $f_{\eta NN}$

Through use of the empirical ratio of pion and photon momenta [32] known to be approximately 139/48 and the  $\eta$  meson mass of 547 MeV one may solve for the coupling constant  $f_{\eta ss}$  to get

$$f_{\eta ss}^2 = \theta_m^{-2} \frac{\Gamma_\pi}{\Gamma_\gamma} \left( \frac{|\mathcal{M}_\gamma|}{|\mathcal{M}_\pi|} \right)^2 \cdot 4.814 \text{ fm}^{-2}. \quad (4.16)$$

As the ratio of the  $\pi^0$  and  $\gamma$  decay rates is experimentally known, albeit with quite large errors, to be  $0.062 \pm 0.028$  [32], it is, given the rather well known value of  $\theta_m$ , possible to obtain an estimate for the coupling constant  $f_{\eta ss}$ . However, if the charm quark also couples to  $\pi^0$ , which is suggested by the empirically detected transitions  $\psi' \rightarrow J/\psi \eta$  and  $\psi' \rightarrow J/\psi \pi^0$ , then eq. (4.16) should be modified. The appropriate modifications are given in paper **V**, where it was found that a significant coupling of the  $\pi^0$  to the charm quark will increase the value of  $f_{\eta NN}$ . For that calculation, a matrix element for  $\pi^0$  emission by the charm quark is also required.

The matrix elements required for eq. (4.16) were in paper **V** found to be

$$\mathcal{M}_\gamma = -1.22 \cdot 10^{-2} \text{ fm}$$

for the M1 transition  $D_s^* \rightarrow D_s \gamma$ , and

$$\mathcal{M}_\pi^s = 0.794, \quad \mathcal{M}_\pi^c = 0.949,$$

for  $\pi^0$  emission by the strange and charm quarks. Assuming that in the  $\pi^0$  emission by the  $D_s^*$ , the pion couples mostly to the strange constituent quark, eq. (4.16) may be used directly together with the above matrix elements for the  $\pi^0$  and  $\gamma$  transitions. Insertion of those matrix elements for a value of the  $\pi^0 - \eta$  mixing angle of  $\theta_m \sim 0.012$  yields  $|f_{\eta ss}| \sim 0.70$ . If the uncertainties in the mixing angle and the empirical widths for the  $\pi^0$  and  $\gamma$  transitions are taken into account, then the best estimate of paper **V** for the coupling of the  $\eta$  meson to strange constituent quarks is

$$f_{\eta ss} = -0.7^{+0.5}_{-0.3}.$$

In the above result, the negative sign is suggested by the relations in eq. (4.11). The static quark model then implies, through eq. (4.12), that the magnitude of the corresponding pseudovector  $\eta$ -nucleon coupling constant  $f_{\eta NN}$  should be one half of this value. Thus one obtains the following final result for the  $\eta$ -nucleon coupling:

$$f_{\eta NN} = 0.35^{+0.15}_{-0.25}$$

This result should be compared with the value for  $f_{\eta NN}$  or the equivalent pseudoscalar coupling constant  $g_{\eta NN} = (2m_N/m_\eta)f_{\eta NN}$ , which has been determined by phenomenological model fits to photoproduction of  $\eta$  mesons on the nucleon [62]. The latter value for  $f_{\eta NN}$  is  $\sim 0.64$ . That value has also been found to be realistic in calculations of the cross section for  $pp \rightarrow pp\eta$  near threshold [63]. Although the result obtained above for  $f_{\eta NN}$  has quite large uncertainties which are mostly of empirical origin, it still appears to be significantly smaller. A larger value for  $f_{\eta NN}$  could, of course, be obtained by decreasing the mixing angle  $\theta_m$ .

## Chapter 5

# Two-pion Transitions

As the orbitally excited  $L = 1$   $D_1(2420)$  and  $D_2^*(2460)$  charm meson states lie well above the threshold, not only for single pion but also for two pion decay, then it is likely that a significant fraction of their total widths are made up by  $\pi\pi$  transitions to the ground state  $D$  and  $D^*$  mesons. It is thus particularly instructive to obtain theoretical predictions and empirical information on the branching ratios for the latter decay modes. At present, however, the total widths of the  $D_1(2420)$  and  $D_2^*(2460)$  states are known only within a very wide uncertainty range, and the remaining two members of the  $L = 1$  multiplet have not yet been discovered. Paper **III** reports a calculation of the  $\pi\pi$  decay widths of the excited  $L = 1$  charm meson states, by extending a similar calculation of the widths of their single pion transitions in paper **II**.

Two pion emission from radially excited heavy quarkonium ( $Q\bar{Q}$ ) states empirically constitutes a significant fraction of their total decay widths [32]. Indeed, in the case of the  $\psi'$  (or  $\psi(2S)$ ), the branching ratio is empirically as large as  $\sim 50\%$ . As the charm quarks themselves do not couple to pions, the  $\pi\pi$  coupling to heavy flavor mesons (or quarks) involves at least two gluons if not a glueball. A number of different theoretical approaches for the coupling of two-pions to heavy mesons have been proposed, from effective field theory descriptions [67] and directly QCD-motivated models [68] to phenomenological models [69]. In ref. [70], a Lagrangian motivated by chiral perturbation theory has been fitted to experiment. In paper **IV**, the  $\pi\pi$  transitions from excited  $Q\bar{Q}$  states has been described by a derivative  $Q\pi\pi$  coupling, mediated by a heavy scalar resonance.

### 5.1 The width for a $\pi\pi$ transition

The  $\pi\pi$  width of an excited heavy flavor meson is of the form

$$\Gamma_{\pi\pi} = (2\pi)^4 \int \frac{d^3k_a}{(2\pi)^3} \frac{d^3k_b}{(2\pi)^3} \frac{d^3P_f}{(2\pi)^3} \frac{M_f M_i}{E_f E_i} \frac{|T_{fi}|^2}{4\omega_a \omega_b} \delta^{(4)}(P_f + k_a + k_b - P_i), \quad (5.1)$$

where  $k_a$  and  $k_b$  are the four-momenta of the emitted pions,  $P_i$  and  $P_f$  are those of the initial and final state quarkonia, while  $\omega_a$  and  $\omega_b$  denote the energies of the emitted pions, respectively. The factors  $M/E$  are normalization factors for the heavy meson states similar to those employed in ref. [56].

Evaluation of the above expression leads to the following form for the differential width of a  $\pi\pi$  transition,

$$\frac{d\Gamma_{\pi\pi}}{d\Omega_q} = \frac{1}{4} \frac{1}{(2\pi)^4} \int_0^{q_f} dq q^2 \int_{-1}^1 dz \frac{Q_f^2(q, z)}{\omega_a(q, z) (Q_f + \frac{qz}{2}) + \omega_b(q, z) (Q_f - \frac{qz}{2})} \frac{M_f}{E_f(q)} |T_{fi}|^2, \quad (5.2)$$

where the variable  $z$  is defined by  $\mathbf{Q} \cdot \mathbf{q} = Qqz$ , and the energies of the pions and the final state quarkonium are given by

$$\omega_a = \sqrt{m_\pi^2 + Q_f^2 + \mathbf{q}^2/4 - Q_f qz}, \quad (5.3)$$

$$\omega_b = \sqrt{m_\pi^2 + Q_f^2 + \mathbf{q}^2/4 + Q_f qz}, \quad (5.4)$$

$$E_f = \sqrt{\mathbf{q}^2 + M_f^2}. \quad (5.5)$$

In the above expressions, the relative momentum of the emitted pions has been fixed by the delta functions in eq. (5.1), and can be expressed as

$$Q_f^2 = \frac{(E_f - M_i)^4 - (4m_\pi^2 + \mathbf{q}^2)(E_f - M_i)^2}{4(E_f - M_i)^2 - 4\mathbf{q}^2 z^2}. \quad (5.6)$$

The integration limit  $q_f$  corresponds to the maximal momentum of any one of the final state particles, e.g. the final state quarkonium. Thus  $q_f$  can be calculated as the  $q$ -value of a transition  $A' \rightarrow AX$ , where  $X$  is a particle with mass  $M_X = 2m_\pi$ .

The above formalism is adapted for computation of a  $\pi\pi$  width using a hadronic matrix element  $T_{fi}$ . However, since experiments generally measure the invariant mass  $\sqrt{s_{\pi\pi}}$ , then it is useful to define a dimensionless variable  $x$ ,

$$x = \frac{m_{\pi\pi} - 2m_\pi}{\Delta M}, \quad (5.7)$$

where  $m_{\pi\pi}$  denotes the invariant mass  $\sqrt{s_{\pi\pi}}$  of the two-pion system and  $\Delta M = M_i - M_f - 2m_\pi$ . The relation between  $q$  ( $= |\mathbf{q}|$ ) and  $m_{\pi\pi}$  may then be obtained as [32]

$$|\mathbf{q}| = \frac{[M_i^2 - (M_f + m_{\pi\pi})^2] [M_i^2 - (M_f - m_{\pi\pi})^2]}{4M_i^2}. \quad (5.8)$$

From this relation, the transformation Jacobian may be obtained as

$$\frac{dq}{dx} = \frac{\Delta M}{|\mathbf{q}|} \left\{ \left[ \frac{M_i^2 - (M_f + m_{\pi\pi})^2}{4M_i^2} \right] (M_f - m_{\pi\pi}) - \left[ \frac{M_i^2 - (M_f - m_{\pi\pi})^2}{4M_i^2} \right] (M_f + m_{\pi\pi}) \right\}, \quad (5.9)$$

where  $|\mathbf{q}|$  is given in terms of  $m_{\pi\pi}$  by eq. (5.8). The width for a  $\pi\pi$  transition may thus be calculated as

$$\Gamma_{\pi\pi} = \int_0^{q_f} dq \frac{d\Gamma_{\pi\pi}}{dq} = - \int_0^1 dx \frac{d\Gamma_{\pi\pi}}{dq} \frac{dq}{dx}. \quad (5.10)$$

In the above equation, the latter form turns out to be the most useful, since the experimental  $\pi\pi$  spectra are presented either in terms of  $\Gamma^{-1} d\Gamma/dx$  or  $d\Gamma/dx$  versus  $x$ .

## 5.2 $\pi\pi$ transitions in heavy-light mesons

The emission of two pions from the light constituent quarks is modeled in paper **III** in terms of the conventional chiral pion-quark pseudovector coupling model, augmented by a pointlike Weinberg-Tomozawa term. The only free parameter in this model is the axial coupling  $g_A^q$  of the light constituent quarks, as the quark masses and other parameters of the Hamiltonian model were fitted to the  $D$  meson spectrum. In addition to the single quark amplitude for two-pion emission, the exchange current contribution to the Weinberg-Tomozawa interaction was also considered, and found to interfere destructively with the single quark amplitude.

The pion-quark pseudovector coupling (4.1) gives rise to Born and crossed Born amplitudes of conventional form for the emission of two pions from an interacting constituent quark. The chiral model for the  $\pi\pi$  emission amplitude is completed by the Weinberg-Tomozawa (WT) interaction, which is described by the Lagrangian

$$\mathcal{L}_{\text{WT}} = -\frac{i}{4f_\pi^2} \bar{\psi}_q \gamma_\mu \tau_a \pi_a \times \partial_\mu \pi_a \psi_q. \quad (5.11)$$

The general isospin decomposition of the  $\pi\pi$  emission amplitude for constituent quarks is, in analogy with that for nucleons,

$$T = \delta_{ab} T^+ + \frac{1}{2} [\tau_b, \tau_a] T^-, \quad (5.12)$$

while the general expression for the amplitudes  $T^+$  and  $T^-$  is

$$T^\pm = \bar{u}(\mathbf{p}') (A^\pm - i\gamma_\mu Q_\mu B^\pm) u(\mathbf{p}). \quad (5.13)$$

In these expressions,  $Q$  denotes the relative four-momentum  $Q = (k_b - k_a)/2$  of the emitted pions. In this notation the Born, crossed Born and Weinberg-Tomozawa amplitudes are, respectively

$$T_{\text{B}} = i \left( \frac{g_A^q}{2f_\pi} \right)^2 \left[ \gamma_\mu Q_\mu - 2im_q - 4m_q^2 \frac{\gamma_\mu Q_\mu}{p_a^2 + m_q^2} \right] \left( \delta_{ba} + \frac{1}{2} [\tau_b, \tau_a] \right), \quad (5.14)$$

$$T_{\text{CB}} = -i \left( \frac{g_A^q}{2f_\pi} \right)^2 \left[ \gamma_\mu Q_\mu + 2im_q - 4m_q^2 \frac{\gamma_\mu Q_\mu}{p_b^2 + m_q^2} \right] \left( \delta_{ba} - \frac{1}{2} [\tau_b, \tau_a] \right), \quad (5.15)$$

$$T_{\text{WT}} = -i \frac{\gamma_\mu Q_\mu}{4f_\pi^2} [\tau_b, \tau_a]. \quad (5.16)$$

Comparison of these amplitudes with eq. (5.13) yields the desired expressions for the sub-amplitudes  $A^\pm$  and  $B^\pm$ , which are of the form

$$A^+ = \left( \frac{g_A^q}{2f_\pi} \right)^2 4m_q, \quad (5.17)$$

$$A^- = 0, \quad (5.18)$$

$$B^+ = - \left( \frac{g_A^q}{2f_\pi} \right)^2 4m_q^2 \left[ \frac{1}{s - m_q^2} - \frac{1}{u - m_q^2} \right], \quad (5.19)$$

$$B^- = - \left( \frac{g_A^q}{2f_\pi} \right)^2 \left( 2 + 4m_q^2 \left[ \frac{1}{s - m_q^2} + \frac{1}{u - m_q^2} \right] \right) + \frac{1}{2f_\pi^2}. \quad (5.20)$$

Here the identities  $p_a^2 = -s$  and  $p_b^2 = -u$ , where  $s$  and  $u$  are the invariant Mandelstam variables, have been used. These results for the  $A$  and  $B$  amplitudes are formally equivalent to the corresponding results for the two-pion emission amplitude for nucleons [64]. Note that in eq. (5.20), the contribution from the Weinberg-Tomozawa interaction tends to cancel the constant term in the  $B^-$  amplitude that arises from the Born terms. If the axial coupling constant  $g_A^q$  is taken to equal 1, then this cancellation is exact.

For calculational purposes, eq. (5.13) was split in paper **III** into spin-independent and spin-dependent parts according to

$$T^\pm = \alpha^\pm + i\sigma_q \cdot \beta^\pm. \quad (5.21)$$

The spin and isospin summed squared amplitude for a given  $\pi\pi$  transition is then expressed in the form

$$|T|^2 = |T|_{\alpha^+}^2 + |T|_{\alpha^-}^2 + |T|_{\beta^+}^2 + |T|_{\beta^-}^2, \quad (5.22)$$

from which the  $\pi\pi$  width is obtained by insertion into eq. (5.2). The explicit expressions for the above squared amplitudes, given in paper **III**, are different for each transition because of the summation over spin and isospin. The numerical results for the above squared amplitudes are presented in Table 5.1.

It is instructive for the determination of the two-quark contribution to the Weinberg-Tomozawa interaction to write the Lagrangian (5.11) in the form of a current-current coupling,

$$\mathcal{L}_{\text{WT}} = -\frac{1}{4f_\pi^2} V_{\mu a} \pi_a \times \partial_\mu \pi_a, \quad (5.23)$$

where  $V_{\mu a} = i\bar{\psi}_q \gamma_\mu \psi_q \tau_a$  is the isovector current of the light constituent quark and  $\pi_a \times \partial_\mu \pi_a$  is the current of the  $\pi\pi$  system. Given this expression, it becomes natural to describe the irreducible two-quark contribution to the  $\pi\pi$  production operator by means of two-quark interaction current contributions to the isovector current  $V_{\mu a}$ .

In the non-relativistic limit, the spatial term in the isovector current  $V_{\mu a} = (\mathbf{V}_a, iV_{0a})$  of the light constituent quark takes the form

$$\mathbf{V}_a = \left[ \frac{\mathbf{p}'_q + \mathbf{p}_q - i\sigma_q \times \mathbf{q}}{2m_q} \right] \tau_a, \quad (5.24)$$

where  $m_q$  is the light constituent quark mass and  $\mathbf{p}_q$  and  $\mathbf{p}'_q$  the initial and final quark momenta, respectively. The expressions for the exchange current contributions for the scalar confining and OGE interactions have been calculated in ref. [49], and may be expressed as

$$\mathbf{V}_a^{\text{Conf}} = -\frac{V_c(\mathbf{k}_2)}{m_q} \mathbf{V}_a, \quad (5.25)$$

$$\mathbf{V}_a^{\text{Oge}} = -\frac{V_g(\mathbf{k}_2)}{2m_q^2} \left[ \frac{m_q}{M_Q} (\mathbf{p}'_Q + \mathbf{p}_Q + i\sigma_Q \times \mathbf{k}_2) + i\sigma_q \times \mathbf{k}_2 \right] \tau_a. \quad (5.26)$$

In paper **III**, the above operators contribute only to  $|T|_{\alpha^-}^2$ , and were found to reduce the widths for  $\pi\pi$  transitions. However, it was also found that the nonrelativistic treatment of the two-quark operators is somewhat unrealistic because of the small mass of the light constituent quark. An approximate relativistic treatment akin to that employed for the single pion transitions in paper **II** was therefore used in paper **III**. The results obtained upon addition of the two-quark operators (5.25) and (5.26) are shown in Table 5.2.

Table 5.1: Numerical results from paper **III** with single-quark amplitudes and relativistic matrix elements for the  $\pi\pi$  widths of the spin triplet  $D_2^*$ ,  $D_1$ ,  $D_0^*$  and the spin singlet  $D_1^*$  mesons. The individual results from the spin independent ( $\alpha^\pm$ ) and spin dependent amplitudes ( $\beta^\pm$ ) are shown for  $g_A^q = 1$ .

Transition	$ T _{\alpha^+}^2$	$ T _{\alpha^-}^2$	$ T _{\beta^-}^2$	$ T _{\beta^+}^2$	$g_A^q = 1$	$g_A^q = 0.87$
$D_2^* \rightarrow D^* \pi\pi$	0.896	2.864	$5.06 \cdot 10^{-3}$	$1.17 \cdot 10^{-3}$	<b>3.77 MeV</b>	2.39 MeV
$D_2^* \rightarrow D\pi\pi$	–	–	$6.45 \cdot 10^{-2}$	$7.51 \cdot 10^{-3}$	<b>0.07 MeV</b>	0.05 MeV
$D_1 \rightarrow D^* \pi\pi$	0.367	1.291	$2.33 \cdot 10^{-3}$	$7.85 \cdot 10^{-4}$	<b>1.66 MeV</b>	1.05 MeV
$D_1^* \rightarrow D^* \pi\pi$	–	–	$6.54 \cdot 10^{-4}$	$3.30 \cdot 10^{-4}$	$\simeq 0$ MeV	$\simeq 0$ MeV
$D_1^* \rightarrow D\pi\pi$	2.749	7.915	–	–	<b>10.7 MeV</b>	6.80 MeV
$D_0^* \rightarrow D^* \pi\pi$	0.020	0.098	–	–	<b>0.12 MeV</b>	0.07 MeV
$D_0^* \rightarrow D\pi\pi$	–	–	$1.43 \cdot 10^{-2}$	$2.86 \cdot 10^{-3}$	<b>0.02 MeV</b>	0.01 MeV

Table 5.2: Numerical results from paper **III** for the most important  $\pi\pi$  transitions, upon addition of the two-quark contributions associated with the scalar confining and OGE interactions to the Weinberg-Tomozawa Lagrangian, for  $g_A^q = 1$ .

Transition	Rel	$ T _{\alpha^-}^2$		Total	
		+Conf	+OGE	$g_A^q = 1$	$g_A^q = 0.87$
$D_2^* \rightarrow D^* \pi\pi$	2.864	2.377	2.144	<b>3.05 MeV</b>	1.82 MeV
$D_1 \rightarrow D^* \pi\pi$	1.291	1.076	0.974	<b>1.34 MeV</b>	0.80 MeV
$D_1^* \rightarrow D\pi\pi$	7.915	6.535	5.872	<b>8.62 MeV</b>	5.17 MeV

The results for the  $\pi\pi$  widths of the positive parity charm mesons with  $L = 1$  in Table 5.1 reveal a strong sensitivity to the value of  $g_A^q$  as well as the large hyperfine splittings in the empirical  $D$  meson spectrum. Consequently, some transitions are kinematically favored, while others, in particular  $D_0^* \rightarrow D^* \pi\pi$ , are strongly inhibited by the small phase space available. The  $\pi\pi$  widths of the  $L = 1$   $D$  mesons are, therefore, also very sensitive to the spin-orbit structure of the  $Q\bar{q}$  interaction, which was also found to be the case for the analogous single pion transitions in paper **II**. In the absence of empirical information and definite QCD lattice calculations [65], the energies of the as yet undiscovered  $D_0^*$  and  $D_1^*$  mesons were in paper **III** taken to equal those predicted by the calculation of ref. [38].

The predicted total widths of the  $L = 1$   $D$  mesons may be obtained by adding the calculated  $\pi\pi$  widths in Table 5.1 to those for the  $\pi$  transitions obtained in paper **II**. With  $g_A^q = 1$  the total calculated  $\pi\pi$  width in the single quark approximation of the  $D_2^*(2460)$  is 3.8 MeV and that of the  $D_1(2420)$  is 1.7 MeV. Such an addition brings the total calculated width of the  $D_2^*(2460)$  to 19.5 MeV, which is well within the uncertainty margin of the empirical value  $25_{-7}^{+8}$  MeV [32]. In the case of the  $D_1(2420)$  meson, the total calculated width for  $\pi$  and  $\pi\pi$  emission comes to 15.3 MeV, which is close to the empirical uncertainty margin of the total width  $18.9_{-3.5}^{+4.6}$  MeV [32]. However, reduction of the value for  $g_A^q$  to 0.87 brings the calculated widths for  $\pi$  and  $\pi\pi$  emission somewhat below the empirical values for the total widths. Likewise, employment of the two-quark contributions associated with the  $Q\bar{q}$  interaction has the effect of reducing the calculated  $\pi\pi$  widths, as shown in Table 5.2.

### 5.3 $\pi\pi$ transitions in heavy quarkonia

Theoretical work on the  $\pi\pi$  decays of excited heavy quarkonia has demonstrated that the empirical energy spectra of the emitted  $\pi\pi$  system demands that the pions be derivatively coupled to the heavy quarkonium states. This is consistent with the role of the pions as Goldstone bosons of the spontaneously broken approximate chiral symmetry of QCD. Most models [67, 68, 69, 70] have dealt with the coupling of two-pions to the heavy meson as a whole rather than to its constituent quarks. The satisfactory description obtained suggests that the decay amplitude  $T_{fi}$  at the quark level should be a smooth function of the  $\pi\pi$  momentum  $\mathbf{q}$ , which is dominated by single-quark mechanisms for  $\pi\pi$  emission. However, the pion rescattering or pion exchange term that appears naturally as a consequence of the coupling of two-pions to constituent quarks has been found, in paper **IV**, to be dominant since it is not suppressed by the orthogonality of the quarkonium wave functions.

It was shown in paper **IV** that an unrealistically large pion rescattering contribution may be avoided if the  $Q\pi\pi$  vertex involves an intermediate, fairly light and broad  $\sigma$  meson, in line with the phenomenological resonance model of ref. [69]. An intermediate  $\sigma$  meson suppresses the contributions from pion rescattering mechanisms, while single quark amplitudes are but slightly affected. Together with a relativistic treatment of the single quark amplitude, this suppression of the pion rescattering contribution has been shown in paper **IV** to reproduce the expected smooth behavior of the transition amplitude.

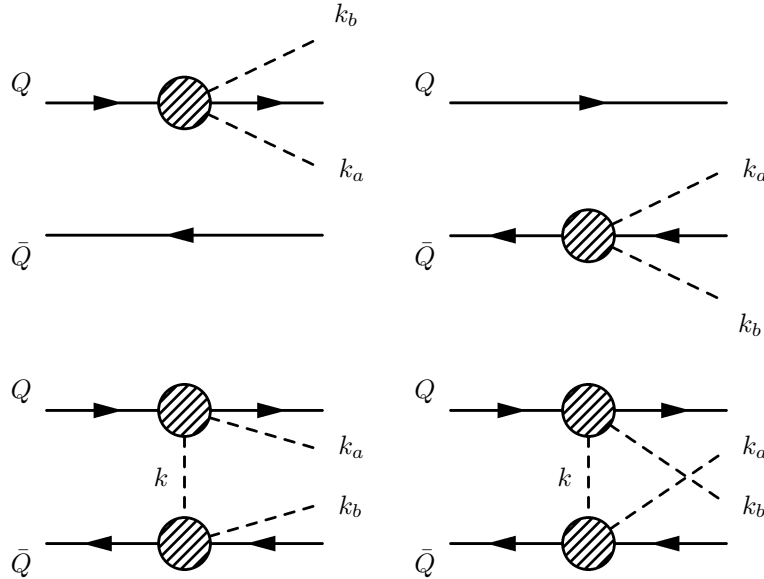


Figure 5.1: Tree-level Feynman diagrams for the emission of two-pions by heavy constituent quarks. The two upper diagrams correspond to the single-quark amplitudes  $T_Q$  and  $T_{\bar{Q}}$  respectively, while the two lower diagrams describe the pion rescattering amplitudes  $T_{\text{ex}}$  and  $T_{\text{exc}}$  which involve a pion exchange between the heavy constituent quarks.

If the coupling of the pions to the constituent quark does not involve derivatives of the pion field, then agreement with experiment is excluded for the pion invariant mass distributions in the decays  $\Upsilon' \rightarrow \Upsilon \pi\pi$  and  $\psi' \rightarrow J/\psi \pi\pi$  [66, 69]. Derivative couplings for the pions are also consistent with the role of pions as Goldstone bosons of the spontaneously broken approximate chiral symmetry of QCD. The effective  $Q\pi\pi$  interaction Lagrangian is therefore expected to have the form

$$\mathcal{L}_{Q\pi\pi} = 4\pi\lambda \bar{\psi}_Q \partial_\mu \pi_a \partial_\mu \pi_a \psi_Q, \quad (5.27)$$

where  $\lambda$  is a coupling constant of dimension  $[\text{MeV}]^{-3}$  and  $\psi_Q, \bar{\psi}_Q$  denote the heavy quark spinors. The total tree-level amplitude for  $\pi\pi$  emission can then be expressed in terms of single quark and pion rescattering terms, as illustrated in Fig. 5.1. The isospin dependence of the dipion-quark coupling then implies that

$$|T|_{\pi\pi}^2 = 2|T|_{\pi^+\pi^-}^2 + |T|_{\pi^0\pi^0}^2. \quad (5.28)$$

As a consequence the width for emission of charged pions should be twice that for emission of neutral pions, which is in fair agreement with what is found experimentally [32, 66].

The effect of the strong interaction in the  $\pi\pi$  system may be approximately accounted for by inclusion of an intermediate scalar meson ( $\sigma$  or glueball) resonance in the vertex. This is brought about by modification of the coupling constant  $\lambda$  with a relativistic scalar meson propagator of the Breit-Wigner type:

$$\lambda \rightarrow \lambda \left( \frac{M_\sigma^2 + \Gamma_\sigma^2/4}{M_\sigma^2 + q^2 + \Gamma_\sigma^2/4} \right). \quad (5.29)$$

Here  $M_\sigma$  denotes the pole position  $m_\sigma - i\Gamma_\sigma/2$ , and  $q$  the four-momentum, of the effective scalar ( $\sigma$ ) meson resonance. The  $\sigma$  resonance appears by infinite iteration of the four-pion vertex in the isospin 0 spin 0 channel. Therefore, as pointed out in ref. [69], it is natural to describe the strongly interacting  $\pi\pi$  state by a broad  $\sigma$  pole rather than by the driving term (4-pion vertex) alone. When the modification (5.29) is taken into account, the expression for the single-quark amplitude becomes

$$T_{1q} = -16\pi\lambda \left( \frac{M_\sigma^2 + \Gamma_\sigma^2/4}{M_\sigma^2 + q^2 + \Gamma_\sigma^2/4} \right) \left[ m_\pi^2 - \frac{1}{2} ((\omega_a + \omega_b)^2 - \mathbf{q}^2) \right] \mathcal{M}_{1q}. \quad (5.30)$$

The nonrelativistic approximation for the matrix element  $\mathcal{M}_{1q}$  is unreliable, as the radial  $S$ -wave quarkonium wave functions are orthogonal. A relativistic form for the matrix element  $\mathcal{M}_{1q}$ , where  $P = |\mathbf{P}|$ ,  $q = |\mathbf{q}|$  and  $\mathbf{P} \cdot \mathbf{q} = Pqv$ , may be obtained as

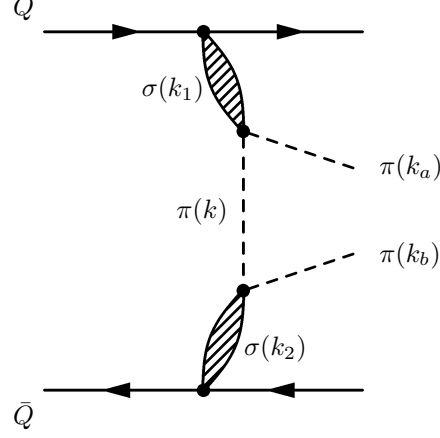
$$\begin{aligned} \mathcal{M}_{1q}^{\text{rel}} &= \frac{1}{\pi} \int_0^\infty dr' r' u_f(r') \int_0^\infty dr r u_i(r) \int_0^\infty dP P^2 \int_{-1}^1 dv \alpha(P, v, q) \\ &\quad j_0 \left( r' \sqrt{\mathbf{P}^2 + \frac{\mathbf{q}^2}{16} - \frac{Pqv}{2}} \right) j_0 \left( r \sqrt{\mathbf{P}^2 + \frac{\mathbf{q}^2}{16} + \frac{Pqv}{2}} \right), \end{aligned} \quad (5.31)$$

where  $\alpha(P, v, q)$  is a factor which includes the quark spinors in the coupling (5.27),

$$\alpha(P, v, q) = \sqrt{\frac{(E + M_Q)(E' + M_Q)}{4EE'}} \left( 1 - \frac{\mathbf{P}^2 - \mathbf{q}^2/4}{(E' + M_Q)(E + M_Q)} \right). \quad (5.32)$$

In principle the quark spinors in the coupling (5.27) also contain a spin dependent part that is proportional to  $\mathbf{q} \times \mathbf{P}$ . For the present purposes that contribution turns out to be very tiny and may be safely neglected. It has been shown in paper **IV** that the relativistic modifications to the single-quark matrix element increase the magnitude of the single quark amplitudes for  $\pi\pi$  decay.

Figure 5.2: Modeling of the pion rescattering term in Fig. 5.1 in terms of intermediate  $\sigma$  mesons. The four-momenta of the  $\sigma$  mesons are defined as  $k_1 = -k - k_a$  and  $k_2 = k - k_b$ . The crossed rescattering diagram in Fig. 5.1 can be obtained by interchanging  $k_a$  and  $k_b$ . The physically reasonable approximations  $\mathbf{k}_1 \approx -\mathbf{k}$ ,  $\mathbf{k}_2 \approx \mathbf{k}$ ,  $|k_1^0| \approx |k_2^0| \approx (\omega_a + \omega_b)/2$  and  $k_0 \approx (\omega_b - \omega_a)/2$  were made in paper **IV**, to allow for a simpler treatment of the triple propagators in the pion rescattering amplitudes.



The pion rescattering amplitude that corresponds to Fig. 5.2 may be expressed as

$$T_{\text{ex}} = -64 \pi^2 \lambda^2 (M_\sigma^2 + \Gamma_\sigma^2/4)^2 \frac{k_{a\mu} k_\mu k_{b\nu} k_\nu}{(k_1^2 + M_\sigma^2 + \Gamma_\sigma^2/4)(k^2 + m_\pi^2)(k_2^2 + M_\sigma^2 + \Gamma_\sigma^2/4)}, \quad (5.33)$$

where the momenta are defined as in Fig. 5.2. Upon simplification of the triple propagator according to the recipe of Fig. 5.2, the crossed pion rescattering diagram gives an extra factor of 2, yielding the expression

$$T_{2q} = -128 \pi^2 \lambda^2 \left\{ \frac{1}{3} \left( \frac{\mathbf{q}^2}{4} - Q_f^2 \right) [\mathcal{M}_{e1} - A^2(\mathcal{M}_{e2} - \mathcal{M}_{e3})] \right. \\ \left. + \left( \frac{\mathbf{q}^2 z^2}{4} - \frac{2}{3} Q_f^2 - \frac{\mathbf{q}^2}{12} \right) \mathcal{M}_{e4} + \frac{\omega_a \omega_b}{4} (\omega_a - \omega_b)^2 (\mathcal{M}_{e2} - \mathcal{M}_{e3}) \right\}, \quad (5.34)$$

where the term which is proportional to the matrix element  $\mathcal{M}_{e4}$  represents an amplitude for  $D$ -wave  $\pi\pi$  emission. The matrix elements in eq. (5.34) may, in the non-relativistic approximation, be expressed as

$$\mathcal{M}_{e1} = \int_0^\infty dr u_f(r) u_i(r) j_0(Q_f r) \frac{(M_\sigma^2 + \Gamma_\sigma^2/4)^2}{4\pi} \left( \frac{e^{-Xr}}{2X} \right), \quad (5.35)$$

$$\mathcal{M}_{e2} = \int_0^\infty dr u_f(r) u_i(r) j_0(Q_f r) \frac{(M_\sigma^2 + \Gamma_\sigma^2/4)^2}{4\pi(X^2 - A^2)^2} A Y_0(Ar), \quad (5.36)$$

$$\mathcal{M}_{e3} = \int_0^\infty dr u_f(r) u_i(r) j_0(Q_f r) \frac{(M_\sigma^2 + \Gamma_\sigma^2/4)^2}{4\pi(X^2 - A^2)^2} \left[ X Y_0(Xr) + \frac{(X^2 - A^2)}{2X} e^{-Xr} \right], \quad (5.37)$$

$$\mathcal{M}_{e4} = \int_0^\infty dr u_f(r) u_i(r) j_2(Q_f r) \frac{(M_\sigma^2 + \Gamma_\sigma^2/4)^2}{4\pi(X^2 - A^2)^2} F_2(r). \quad (5.38)$$

In the above matrix elements,  $X$  is defined as  $X = \sqrt{M_\sigma^2 + \Gamma_\sigma^2/4 - (\omega_a + \omega_b)^2/4}$ , while  $Y_0(r)$  denotes the Yukawa function  $e^{-r}/r$ . Note that when the value of  $k_0^2$  exceeds  $m_\pi^2$ , the

analytic continuation  $A \rightarrow -i\sqrt{k_0^2 - m_\pi^2}$  [71] is employed for the matrix element (5.36). Further,  $u_f(r)$  and  $u_i(r)$  denote the reduced radial wave functions for the final and initial state heavy quarkonia, respectively. The function  $F_2(r)$ , which is defined in paper **IV**, is closely related to, and in the limit  $m_\sigma \rightarrow \infty$  actually reduces to, a Yukawa  $Y_2$  function [71]. It turns out that the matrix element (5.38) is numerically quite insignificant, because of the strong suppression caused by the  $j_2$  function for small values of  $Qr$ . Also, the smallness of  $k_0$  as compared with  $\mathbf{k}$  precludes any terms proportional to  $k_0$  or  $k_0^2$  from playing any major role.

In view of the many approximations involved in the above treatment of the pion rescattering terms, a check against an unapproximated calculation is desirable. This is possible since the triple propagator in eq. (5.33) may also be considered without any approximation in  $k_1$  and  $k_2$ , at the price of numerically much more cumbersome expressions. By means of the Feynman parameterization

$$\frac{1}{ABC} = 2 \int_0^1 dx x \int_0^1 dy \frac{1}{[A(1-x) + Bxy + Cx(1-y)]^3}, \quad (5.39)$$

the two-quark amplitudes of Fig. 5.2 may be cast in the form

$$\begin{aligned} T_{2q} = & -(8\pi\lambda)^2 \left\{ \frac{1}{3} \left( \frac{\mathbf{q}^2}{4} - Q_f^2 \right) \left[ \int_0^1 dx x \int_0^1 dy \{ \mathcal{M}_I - A^2 \mathcal{M}_{II} \} \right] \right. \\ & + \int_0^1 dx x \int_0^1 dy \left( -\frac{\mathbf{q}^2}{4}(1-2x+xy) - Q_f^2(1-xy) + qQ_f z(1-x) \right) \\ & \quad \mathcal{M}_{II} \left( -\frac{\mathbf{q}^2}{4}(1-2x+xy) + Q_f^2(1-xy) + qQ_f z x(1-y) \right) \\ & \left. + \omega_a \omega_b k_0^2 \int_0^1 dx x \int_0^1 dy \mathcal{M}_{II} \right\} + T_{\text{exc}}, \quad (5.40) \end{aligned}$$

where the matrix elements are given by

$$\begin{aligned} \mathcal{M}_I = & 2 \int_0^\infty dr u_f(r) u_i(r) \frac{(M_\sigma^2 + \Gamma_\sigma^2/4)^2}{8\pi A} e^{-Ar} \\ & j_0 \left( r \sqrt{\frac{\mathbf{q}^2}{4}(1-2x+xy)^2 + Q_f^2 x^2 y^2 + qQ_f z(1-2x+xy)xy} \right), \quad (5.41) \end{aligned}$$

$$\begin{aligned} \mathcal{M}_{II} = & 2 \int_0^\infty dr u_f(r) u_i(r) \frac{(M_\sigma^2 + \Gamma_\sigma^2/4)^2}{32\pi A^3} e^{-Ar} (rA + 1) \\ & j_0 \left( r \sqrt{\frac{\mathbf{q}^2}{4}(1-2x+xy)^2 + Q_f^2 x^2 y^2 + qQ_f z(1-2x+xy)xy} \right). \quad (5.42) \end{aligned}$$

Here the term proportional to  $k_0^2$  is again only of minor importance. Note that in order to obtain the contribution  $T_{\text{exc}}$  to eq. (5.40), it is necessary to make the substitution  $k_a \leftrightarrow k_b$ , which implies  $\omega_a \leftrightarrow \omega_b$  and  $Q_f \rightarrow -Q_f$ . In the above matrix elements, the quantity  $A$  is now defined as  $A = \sqrt{m_*^2 - K_0^2}$  and involves an effective mass  $m_*$  and an energy transfer variable  $K_0$ . These are abbreviations of the following expressions:

$$m_*^2 = \left( M_\sigma^2 + \frac{\Gamma_\sigma^2}{4} \right) (1 - xy) - m_\pi^2 x (2(1-x)(1-y) - xy^2) \quad (5.43)$$

$$+ 2 \left( \frac{q^2}{4} - Q_f^2 \right) x(1-x)(1-y),$$

$$K_0 = \omega_a(1-x) - \omega_b x(1-y) + k_0, \quad (5.44)$$

where  $M_\sigma$  and  $k_0$  are defined as  $m_\sigma - i\Gamma_\sigma/2$  and  $(\omega_b - \omega_a)/2$ , respectively. Numerical comparison of the above formalism with the approximate model of paper **IV** indicates that eq. (5.34) is accurate to within  $\sim 3\%$ .

All pion rescattering matrix elements have, in paper **IV**, been considered in the non-relativistic limit, even though it was noted that that limit is not realistic in the case of the single quark amplitudes. This treatment is expected to be permissible in the case of two-quark amplitudes, since the Yukawa functions from the propagators of the exchanged pions and  $\sigma$  mesons cancel the orthogonality of the radial  $S$ -wave quarkonium wave functions. Relativistic effects thus constitute only a correction to the pion rescattering matrix elements, which is expected to be rather small because of the large constituent masses of the charm and bottom quarks.

## 5.4 The transitions $\Upsilon' \rightarrow \Upsilon \pi\pi$ and $\psi' \rightarrow J/\psi \pi\pi$

If a  $\sigma$  meson lighter than about 1 GeV is employed, together with a relativistic treatment of the single quark amplitudes, then the effects of pion rescattering diagrams may be reduced, and they may become subdominant as compared to the single quark amplitudes, which allows for agreement with experiment. The results of paper **IV** indicate that a  $\sigma$  mass of  $\sim 500$  MeV gives a favorable description of the present experimental data on the  $\pi\pi$  transitions from the  $2S$  states of heavy quarkonia.

The calculated widths and  $\pi\pi$  energy distributions were obtained by simultaneously optimizing the results for  $\Upsilon' \rightarrow \Upsilon \pi^+\pi^-$  and  $\psi' \rightarrow J/\psi \pi^+\pi^-$ . The best results from paper **IV**, which yielded the  $\sigma$  meson parameters  $m_\sigma = 450$  MeV and  $\Gamma_\sigma = 550$  MeV, are shown in Table 5.3 and Fig. 5.3. A coupling constant close to  $\lambda = -0.02 \text{ fm}^3$  was found to provide an optimal description of the  $\pi\pi$  widths and energy spectra, where the sensitivity to the sign of  $\lambda$  is due to the consideration of pion rescattering amplitudes. The heavy quark masses correspond to those of the  $Q\bar{Q}$  Hamiltonian model in paper **IV**.

Table 5.3: Experimental data [32] and calculated widths for  $\pi\pi$  transitions from the  $\Upsilon'$  and  $\psi'$  states, for  $\lambda = -0.02 \text{ fm}^3$ ,  $m_\sigma = 450$  MeV and  $\Gamma_\sigma = 550$  MeV, together with experimental widths, branching fractions, and maximal momenta for each transition.

Transition	$\Gamma_{\text{tot}}$	% of $\Gamma_{\text{tot}}$	$\Gamma_{\text{exp}}$	$\Gamma_{\text{calc}}$	$q_{\text{max}}$
$\Upsilon' \rightarrow \Upsilon \pi^+\pi^-$	$44 \pm 7$ keV	$18.8 \pm 0.6$ %	$8.3 \pm 1.3$ keV	<b>5.89 keV</b>	475 MeV
$\Upsilon' \rightarrow \Upsilon \pi^0\pi^0$		$9.0 \pm 0.8$ %	$4.0 \pm 0.8$ keV	<b>3.07 keV</b>	480 MeV
$\psi' \rightarrow J/\psi \pi^+\pi^-$	$277 \pm 31$ keV	$31.0 \pm 2.8$ %	$86 \pm 12$ keV	<b>53.5 keV</b>	477 MeV
$\psi' \rightarrow J/\psi \pi^0\pi^0$		$18.2 \pm 2.3$ %	$50 \pm 10$ keV	<b>27.8 keV</b>	481 MeV

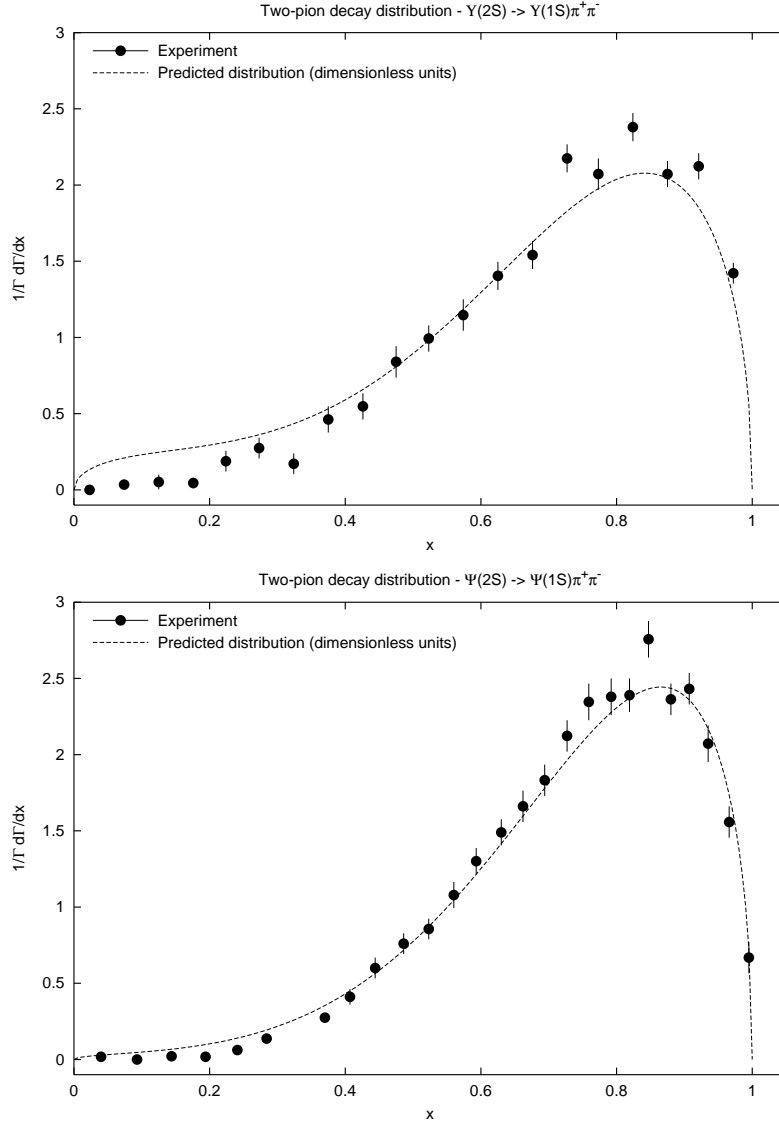


Figure 5.3: Comparison of calculated and experimental [66]  $\pi\pi$  energy distributions for  $\Upsilon' \rightarrow \Upsilon\pi^+\pi^-$  and  $\psi' \rightarrow J/\psi\pi^+\pi^-$ , for  $m_\sigma = 450$  MeV,  $\Gamma_\sigma = 550$  MeV and  $\lambda = -0.02 \text{ fm}^3$ . The calculated width for  $\pi^+\pi^-$  decay is 5.89 keV for  $b\bar{b}$  and 53.5 keV for  $c\bar{c}$ . The scaled  $\pi\pi$  invariant mass  $x$  is defined in eq. (5.7).

The results presented in Fig. 5.3 indicate that the shapes of the experimental  $\pi\pi$  spectra for  $b\bar{b}$  and  $c\bar{c}$  are slightly different. In particular, the peak at high  $x$  appears somewhat lower for  $b\bar{b}$ , while the tail at low  $x$  is more pronounced for  $b\bar{b}$ . It was therefore noted in ref. [66] that the resonance model of ref. [69] cannot be simultaneously fitted to both the  $b\bar{b}$  and  $c\bar{c}$  data. This is because the shape of the  $\pi\pi$  energy distribution is rather insensitive to the properties of the  $\sigma$  meson when only amplitudes of the single quark type are considered. Thus widely different masses and widths of the  $\sigma$  meson have to be employed to fit the empirical  $\pi\pi$  energy spectra in the  $c\bar{c}$  and  $b\bar{b}$  systems.

However, if pion rescattering amplitudes are considered as well, then a  $\sigma$  mass higher than about 450 MeV was shown in paper **IV** to lead to unrealistically large pion rescattering contributions, as the  $\pi\pi$  energy spectrum then begins to develop a second peak at low  $x$ . As the pion rescattering effects are of a short-ranged character, then it turns out that they are significant only for the  $\pi\pi$  spectrum in the bottomonium system. While the pion rescattering contribution is seen from Fig. 5.3 to account for the qualitative differences between the  $\pi\pi$  spectra for  $b\bar{b}$  and  $c\bar{c}$ , it nevertheless appears to be somewhat overpredicted. This problem can be traced to the nonrelativistic treatment of the pion rescattering contribution, and may be alleviated if relativistic matrix elements are employed, as discussed in paper **IV**.

It may be seen from Table 5.3 that the  $\pi\pi$  widths of the  $b\bar{b}$  system are somewhat underpredicted. This is because the presence of the pion rescattering terms precludes an independent fit of the width and the  $\pi\pi$  spectrum. A larger value of  $\lambda$ , which would improve the  $\pi\pi$  widths, would then worsen the description of the  $\pi\pi$  spectrum presented in Fig. 5.3. However, in the case of the transition  $\psi' \rightarrow J/\psi \pi^+\pi^-$ , it may actually be desirable to employ a 20 – 30 % larger value of  $\lambda$ , as was also suggested in ref. [70].

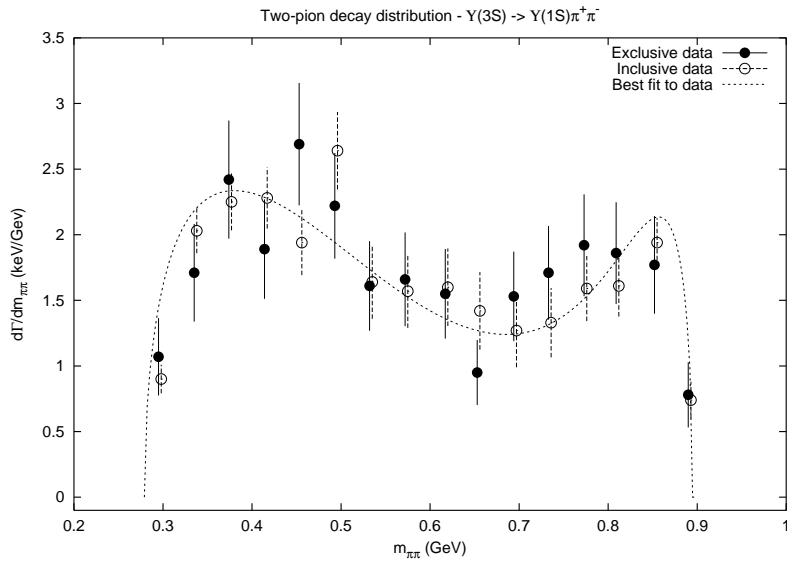


Figure 5.4: The empirical double-peaked  $\Upsilon(3S) \rightarrow \Upsilon \pi\pi$  spectrum, fitted in paper **IV** by the parameters  $m_\sigma = 1400$  MeV,  $\Gamma_\sigma = 100$  MeV,  $\lambda = 2.7 \cdot 10^{-3}$ , yielding a width of  $\Gamma_{\pi^+\pi^-} = 1.07$  keV.

An outstanding problem, lately verified by experimental reanalysis [72], is the double-peaked structure of the empirical  $\Upsilon(3S) \rightarrow \Upsilon \pi\pi$  spectrum, which cannot be explained by models dominated by single-quark amplitudes, such as the one employed in paper **IV**. However, it was also shown that single-quark + pion rescattering models do in fact have sufficient freedom to accommodate a double-peaked  $\pi\pi$  spectrum, as may be seen from Fig. 5.4. As a much heavier scalar meson is employed, the contributions from the pion rescattering and single quark amplitudes are of equal magnitude. Incidentally, the best fit parameters fall within the range of the empirical scalar resonances  $f_0(1370)$  and  $f_0(1500)$  [32], both of which possess a strong coupling to  $\pi\pi$ .

# Chapter 6

## Conclusions

The electromagnetic and pionic transitions in the heavy  $Q\bar{Q}$  and heavy-light  $Q\bar{q}$  mesons have been calculated within the framework of the covariant BSLT equation, with the assumption that the quark-antiquark interaction can be modeled in terms of a long-range confining interaction and a short-ranged OGE or instanton induced interaction. It has been demonstrated that a reasonable description of the empirical heavy meson spectra can be achieved within such an approach, which also yields reasonable values for the confining string tension, constituent quark masses and the parameters  $\Lambda_{\text{QCD}}$  and  $m_g$  which control the strong coupling  $\alpha_s$ . However, the question of the effective Lorentz structure of the quark-antiquark interaction cannot be answered by the quarkonium spectra alone, since there are many models which produce equally satisfactory spectra using different assumptions for the Lorentz structure of the effective confining interaction. Numerical lattice QCD is unrevealing in this case, as the different components of the  $Q\bar{q}$  interaction that can be measured on the lattice may also be well fitted by different assumptions for the effective confining interaction.

In this situation, a study of electromagnetic and pionic transitions is instructive, as two-quark or negative energy contributions have been shown, within the framework of e.g. the Schrödinger and Gross equations, or the instantaneous approximation to the Bethe-Salpeter equation, to be significant for several of these transitions. As the computation of these effects requires an explicit assumption of the Lorentz structure of the confining interaction, then it is possible that the question may be settled in the future when adequate experimental data on electromagnetic and pionic transitions is available. For the time being, the M1 transitions in the charmonium system are the most instructive, as the two-quark effects for those transitions have been shown to be large. Furthermore, as the OGE interaction does not contribute any two-quark operator for M1 transitions in equal-mass quarkonia, then the transition  $J/\psi \rightarrow \eta_c \gamma$  may provide direct insight into the Lorentz structure of the confining interaction. Such a calculation has been described in this thesis, where it is found that the two-quark operator associated with a scalar confining interaction can explain the observed width of about 1 keV.

The theoretical importance of the M1 transition  $J/\psi \rightarrow \eta_c \gamma$  suggests that a new and more accurate measurement of the width for that transition should be performed as soon as possible. The experimental situation is similar to that for the E1 transitions  $\chi_{cJ} \rightarrow J/\psi \gamma$ , which were thought to be overpredicted by most model calculations for a

long time, until the issue was resolved by the new data on these E1 transitions reported in the latest edition of the PDG [46]. Thus, in order to avoid prolonged speculation, a new and independent measurement of  $J/\psi \rightarrow \eta_c \gamma$  is desirable. More empirical information is also needed on the total widths of the  $b\bar{b}$  states and their E1 branching fractions, as the E1 widths are very sensitive to the  $Q\bar{Q}$  wave functions, if not to the Lorentz structure of the quark-antiquark interaction. Progress has recently been made for the E1 transitions in the  $b\bar{b}$  and  $c\bar{c}$  systems as well, since models that employ nonperturbative hyperfine interactions have become available. It was found in the calculation reported in this thesis that many of the E1 transitions in the bottomonium system cannot be accurately modeled with spin-averaged wave functions.

A realistic description of the heavy-light  $Q\bar{q}$  mesons, most notably the charmed  $D$  meson, presents much more serious theoretical challenges for a number of reasons, most notably the uncertain composition of the  $Q\bar{q}$  interaction, the relativistic nature of the light constituent quark and the limited empirical knowledge of the excitation spectra. It has nevertheless been demonstrated in this thesis that the M1 transitions provide an instructive test for the Lorentz structure of the  $Q\bar{q}$  interaction Hamiltonian. Promising results have been obtained for a Hamiltonian with scalar confining and vector OGE components, possibly augmented by an instanton induced interaction. The single pion transitions of the  $D$  meson are likewise instructive in this sense since the two-quark contributions to the axial charge component of the transition amplitude are large. Consequently, transitions that involve  $S$ -wave pion emission are predicted to be suppressed, an effect which has also been observed within the framework of the Gross equation.

The recently measured total width of the  $D^*$  vector meson has been shown to provide useful and constraining information on the pion-quark axial coupling constant  $g_A^q$ . Also, the flavor symmetry violating  $D_s^* \rightarrow D_s \pi^0$  transition can not only provide constraining information on the magnitude of  $\pi^0 - \eta$  mixing, but can also be used to estimate the magnitude of the  $\eta$ -quark, and in particular, the  $\eta$ -nucleon coupling  $f_{\eta NN}$ . In addition to single pion emission,  $\pi\pi$  transitions have also been found to contribute significantly to the predicted total widths of the  $L = 1$   $D$  mesons, a situation which is similar to that in the well explored  $K$  meson spectrum. These  $\pi\pi$  transitions were found to be very sensitive, both to the value of  $g_A^q$ , as well as to the hyperfine splittings in the  $D$  meson spectrum. In all likelihood, the  $\pi\pi$  transitions will be found to contribute several MeV to the total widths for strong decay. The empirically strong  $\pi\pi$  transitions in the charmonium and bottomonium systems have been investigated by means of a phenomenological model, where the  $Q\pi\pi$  interaction is mediated by a broad scalar  $\sigma$  meson. It has been shown that such a model can explain several features of the empirically observed  $\pi\pi$  transitions in heavy quarkonia, although a completely satisfactory description was not achieved.

An important conclusion reached in this thesis is that the most instructive test for a given  $Q\bar{Q}$  or  $Q\bar{q}$  interaction Hamiltonian is not the excitation spectrum but rather the radiative M1 transitions between the ground state vector and pseudoscalar mesons. Once the question of hyperfine splittings and total widths has been settled by experiment, then the pionic transitions from the  $L = 1$   $D$  mesons will provide a similar testing ground. So far, a pure scalar confining interaction has passed the above tests, although other conceivable forms have not been systematically ruled out.

# Svenskspråkigt sammandrag

Denna avhandling presenterar en uträkning av elektromagnetiska och starka övergångar i mesoner med en ( $Q\bar{q}$ ) eller två ( $Q\bar{Q}$ ) tunga kvarkar. Dessa mesoner har beskrivits med hjälp av den kovarianta Blankenbecler-Sugar (BSLT) ekvationen, under antagandet att växelverknigen mellan kvarkarna kan beskrivas som summan av en effektiv fjättrande växelverknig med lång räckvidd och en kort-räckviddskomponent, vilken ger upphov till hyperfinstruktur i mesonernas excitationsspektrum. En dylik växelverknig ger en acceptabel beskrivning av det empiriska mass-spektrat, ifall kort-räckviddskomponenten beskrivs med hjälp av störningsteoretiskt gluon-utbyte (OGE) eller en instanton-inducerad växelverknig. Emellertid kan mass-spektrat inte ensamt avgöra den relativistiska Lorentz-strukturen hos den fjättrande växelverknigen, eftersom flera olika ansatser ger ekvivalenta beskrivningar av det empiriska spektrat.

I denna situation är de elektromagnetiska och starka övergångarna av stor betydelse, eftersom dessa har visats vara känsliga för negativ-energi bidrag till övergångsamplituden, vilka i sin tur beror uttryckligen på växelverknigens Lorentz-struktur. Dessa effekter har, till dags dato, påvisats inom ett antal teoretiska beskrivningar, däribland Schrödinger- och Gross-ekvationerna. Eftersom uträkningen av dessa bidrag till sönderfallsvidderna kräver en ansats för kvark-antikvark växelverknigens Lorentz-struktur, kan de starka och elektromagnetiska sönderfallen utgöra ett test för olika modeller för den fjättrande växelverknigen. För ögonblicket är den magnetiska (M1) dipolövergången  $J/\psi \rightarrow \eta_c \gamma$  av största betydelse, eftersom den experimentellt uppmätta vidden på  $\sim 1$  keV beskrivs dåligt av den icke-relativistiska kvarkmodellen, vilken leder till en tredubbel överuppskattning av detta resultat. Ett av nyckelresultaten i denna avhandling är, att en skalärt kopplad effektiv fjättrande växelverknig kan förklara den uppmätta vidden på  $\sim 1$  keV. Emellertid bör en ny experimentell mätning utföras innan en definitiv slutsats kan dras av det ovanstående resultatet.

En annan slutsats, presenterad i denna avhandling, angår de elektriska (E1) dipolsönderfallen i charmonium ( $c\bar{c}$ ) och bottomonium ( $b\bar{b}$ ). I detta fall visar det sig att Lorentz-strukturen hos kvark-antikvark växelverknigen i de flesta fall endast har en försvinnande liten effekt på övergångsamplituden. Däremot är E1 övergångarna känsliga för små effekter i mesonernas vågfunktioner. Därmed kan en realistisk beskrivning av ett flertal sönderfall endast uppnås, ifall kvark-antikvark växelverknigens hyperfinstruktur behandlas fullständigt, vilket är möjligt ifall mesonerna beskrivs med hjälp av BSLT-ekvationen.

Jämfört med  $Q\bar{Q}$  mesonerna ställer en realistisk beskrivning av  $Q\bar{q}$  systemet mycket stora krav på de teoretiska modellerna, eftersom växelverknigens form mellan tunga och lätta kvarker är osäker, och den lätta kvarken i hög grad relativistisk. Dessutom

komplikerar situationen ytterligare av den knapphändiga empiriska kunskapen om  $Q\bar{q}$  mesonernas mass-spektrum. Inte desto mindre har det visats i denna avhandling, att M1 övergångarna i  $D$  mesonerna utgör ett viktigt test för  $Q\bar{q}$  växelverkningens Lorentz-struktur. Lovande resultat har erhållits för en skalär fjättrande + OGE växelverkning, möjligen med tillsats av en instanton-inducerad komponent. De starka pion-sönderfallen inom  $D$  mesonerna är också av stort intresse eftersom negativ-energi bidragen till den axiala laddningsamplituden är stora. En förutsägelse presenterad i denna avhandling är att pion-övergångar drivna av den axiala laddningsamplituden är starkt förhindrade, vilket nyligen också har observerats med hjälp av Gross-ekvationen.

Den nyligen uppmätta totala vidden för den exciterade  $D^*$  mesonen är av stor betydelse, eftersom den kan fixera värdet på den axiala kopplingskonstanten  $g_A^q$  för lätta kvarkar. Dessutom kan det smak-symmetri brytande sönderfallet  $D_s^* \rightarrow D_s \pi^0$  ge information om styrkan hos  $\eta$  mesonens koppling till kvarkar och baryoner, förutsatt av storleken hos  $\eta - \pi^0$  blandningsvinkeln är känd. Utöver sönderfall, i vilka endast en pion emitteras, kan även två-pion ( $\pi\pi$ ) sönderfall vara av betydelse i  $D$  mesonerna. Denna slutsats överensstämmer med den experimentella situationen i de sära  $K$  mesonerna, där  $\pi\pi$  sönderfallen är väl uppmätta. I denna avhandling befanns  $\pi\pi$  sönderfallen vara mycket känsliga både för värdet på  $g_A^q$  och det tillgängliga fasrummet. Det är därigenom sannolikt, att  $\pi\pi$  sönderfallen utgör flera MeV av de totala vidderna för starkt sönderfall i  $D$  mesonerna.

De empiriskt betydande  $\pi\pi$  övergångarna i charmonium ( $c\bar{c}$ ) och bottomonium ( $b\bar{b}$ ) har i denna avhandling undersökts med hjälp av en fenomenologisk modell, vilken beskriver kvark-pion växelverkningen med hjälp av en skalär  $\sigma$  resonans. En dylik modell befanns ge en god beskrivning av flera egenskaper hos  $\pi\pi$  övergångarna, även om en fullständigt tillfredställande beskrivning inte uppnåddes.

Den viktigaste slutsatsen i denna avhandling är att det mest betydelsefulla testet för en given kvark-antikvark växelverkningsmodell är inte mass-spektrat, utan snarare de elektromagnetiska M1 övergångarna där mesonernas grundtillstånd byter spinn. I framtiden, när hyperfin-nivåerna och de totala vidderna hos de exciterade  $D$  mesonerna är experimentellt kartlagda, kommer dessa att utgöra ett ytterligare test för de ovannämnda växelverkningsmodellerna. Hittills har en skalär fjättrande växelverkning klarat dessa test, även om andra tänkbara former inte har uteslutits systematiskt.

Helsingfors, Oktober 2002

*Timo Lähde*

# Suomenkielinen tiivistelmä

Tämä väitöskirja käsittelee sähkömagneettisia ja vahvoja siirtymiä mesoneissa, jotka koostuvat joko kahdesta raskaasta ( $Q\bar{Q}$ ) tai yhdestä raskaasta ja yhdestä kevyestä ( $Q\bar{q}$ ) kvarkista. Näitä mesoneja on kuvattu kovariantin Blankenbecler-Sugar (BSLT) yhtälön ratkaisuina, olettaen että kvarkkien välinen vuorovaikutus voidaan esittää efektiivisen, pitkän kantaman kvarkkeja kahlitsevan vuorovaikutuksen ja lyhyen kantaman ylihieno-vuorovaikutuksen summana. Mikäli lyhyen kantaman vuorovaikutus oletetaan joko häiriöteoreettiseksi gluonivaihdoiksi taikka instantoni-indusoiduksi, on tuloksena laadultaan hyväksyttävä malli mesonien kokeellisille vitysspektreille. Valitettavasti vitysspektrit eivät yksinään riitä antamaan ratkaisevaa tietoa kahlitsevan vuorovaikutuksen suhteellisuusteoreettisesta Lorentz-rakenteesta, sillä useampien eri oletusten on todettu johtavan samanlaatuisiin spektreihin.

Sähkömagneettisten ja vahvojen vuorovaikutusten merkitys on tässä tilanteessa erittäin suuri, sillä on osoitettu näiden riippuvan herkästi siirtymäamplitudin negatiivisen energian komponenteista. Nämä puolestaan riippuvat eksplisiittisesti kvarkkien välisen vuorovaikutuksen Lorentz-rakenteesta. Tähän johtopäätökseen on päädytty aikaisemmin m.m. Schrödingerin ja Grossin yhtälöiden kautta. Koska siirtymäamplitudien laskeminen vaatii oletuksen kvarkkien välisen vuorovaikutuksen Lorentz-rakenteesta, voivat nämä siis toimia testinä, millä voidaan vertailla eri mallien todenmukaisuutta myös silloin, kun vitysspektrien ennustukset ovat degeneroituneet. Tällä hetkellä magneettisen (M1) dipolisiirtymän  $J/\psi \rightarrow \eta_c \gamma$  merkitys on hyvin suuri, sillä sen kokeellinen viivavevyys  $\sim 1$  keV ei ole sopusoinnussa epärelativistisen ennustuksen kanssa, joka on kolme kertaa suurempi. Eräs tämän teoksen tärkeimmistä tuloksista on, että skalaarinen kahlitseva vuorovaikutus tarjoaa mahdollisen selityksen yllämainitulle kokeelliselle viivavevydelle. Lopullinen johtopäätös vaatii kuitenkin kokeellisen tuloksen varmistamisen uudella mitauksella.

Tässä väitöskirjassa on myös käsitelty raskaiden mesonien sähköisiä (E1) dipolisiirtymiä, jolloin on todettu että kvarkkien välisen vuorovaikutuksen Lorentz-rakenteella on useimmiten vain häviävän pieni vaikutus teoreettisiin viivavevyksiin. Toisaalta E1 siirtymät ovat herkkiä pienille muutoksille mesonien aaltofunktioissa. Näin ollen onkin tässä teoksessa osoitettu, että useita E1 siirtymiä voidaan kuvata onnistuneesti vain, mikäli kvarkkien välinen ylihieno-vuorovaikutus otetaan huomioon käyttämättä ensimmäisen kertaluvun häiriöteoriaa.

Mikäli mesoniin sisältyy kevyt kvarkki, on realistisen mallin rakentaminen heti huomattavasti vaikeampaa, koska raskaiden ja kevyiden kvarkkien välisen vuorovaikutuksen muoto on erittäin kyseenalainen. Lisäksi kevyt kvarkki on hyvin relativistinen, ja

viritysspektrin kokeellinen tuntemus vähäinen. Tästä huolimatta on tässä teoksessa osoitettu, että  $D$  mesonien M1 siirtymät tarjoavat mahdollisuuden tutkia  $Q\bar{q}$ -vuorovaikutuksen Lorentz-rakennetta, jolloin lupaavia tuloksia on saatu edellämainituilla vuorovaikutusmalleilla.  $D$  mesonien vahvat pionisiirtymät ovat myös tässä mielessä kiinnostavia, sillä pionin ja kevyen kvarkin välisen vuorovaikutuksen aksiaalinen varauskomponentti riippuu vahvasti kvarkkien välisen vuorovaikutuksen Lorentz-rakenteesta. Tässä väitöskirjassa on havaittu, että aksiaalisesta varauskomponentista riippuvat siirtymät lienevät voimakkaasti estyneitä. Samankaltaiseen johtopäätökseen ollaan päästy hiljattain myös Grossin yhtälön kautta.

Eksitoituneen  $D^*$  mesonin viivaveveys, josta hiljattain saatiin ensimmäinen kokeellinen mittausta, on teoreettisesti hyvin tärkeä suure, sillä sen avulla voidaan määrätä kevyiden kvarkkien aksiaalinen kytkinvakio  $g_A^q$ . Lisäksi voidaan makusymmetriaa rikkovan  $D_s^* \rightarrow D_s \pi^0$  siirtymän avulla tutkia  $\eta$  mesonin ja kvarkkien (tai baryonien) välistä vuorovaikutusta. Tämä edellyttää, että neutraalin pionin ja  $\eta$  mesonin välinen sekoi-tuskulma on tunnettu. Lisäksi on tässä väitöskirjassa tutkittu kahden pionin ( $\pi\pi$ ) siirtymiä, jotka hyvin todennäköisesti ovat merkityksellisiä  $D$  mesoneissa, mikä johtopäätös on yhtäpitävä oudosta  $K$  mesonista saadun kokeellisen tiedon kanssa. Tässä teoksessa on osoitettu  $D$  mesonien  $\pi\pi$  siirtymien olevan herkkiä  $g_A^q$ :n numeeriselle arvolle sekä käytettävissä olevalle faasiavaruudelle. Täten  $\pi\pi$  siirtymien viivavevydet ovat todennäköisesti muutaman MeV:n suuruisia.

Charmonium ( $c\bar{c}$ ) ja bottomonium ( $b\bar{b}$ ) mesonien kokeellisesti merkittäviä  $\pi\pi$  siirtymiä on tässä väitöskirjassa tutkittu fenomenologisella mallilla, jossa raskaiden kvarkkien ja pionien välistä vuorovaikutusta kuvataan skalaarin  $\sigma$  resonanssin avulla. Tällä mallilla saavutettiin tyydyttävä, joskaan ei täydellinen, kuvaus raskaiden mesonien  $\pi\pi$  siirtymistä.

Tämän väitöskirjan tärkein johtopäätös on, että sähkömagneettiset M1 siirtymät, joissa kvarkkien spin muuttuu, muodostavat viritysspektristä riippumattoman testin kvarkkeja kahlitsevan vuorovaikutuksen Lorentz-rakenteelle. Tulevaisuudessa, ylihienorakenteen ja viivavevyksien ollessa tunnettuja, tulevat  $D$  mesonien M1 ja pionisiirtymät tarjoamaan vastaavan testin. Tähän mennessä on skalaarinen yrite kvarkkeja kahlitsevalle vuorovaikutukselle osoittautunut menestyksekkääksi, vaikka muita mahdollisia muotoja ei ole järjestelmällisesti eliminoitu.

Helsingissä, Lokakuussa 2002

*Timo Lähde*

# Bibliography

- [1] M. Gell-Mann, *The Eightfold Way*, Caltech Report **CTSL-20** (1961).
- [2] Y. Ne'eman, Nucl. Phys. **26:222** (1961).
- [3] V.E. Barnes *et al.*, Phys. Rev. Lett. **12:204** (1964).
- [4] F.W. Busser *et al.*, Phys. Lett. **46B:471** (1973).
- [5] M.Y. Han and Y. Nambu, Phys. Rev. **139B:1006** (1965).
- [6] W. Marciano and H. Pagels, Phys. Rept. **36:137** (1978),  
A.J. Buras, Rev. Mod. Phys. **52:199** (1980),  
E. Reya, Phys. Rept. **69C:195** (1981).
- [7] J.E. Augustin *et al.*, Phys. Rev. Lett. **33:1406** (1974),  
G.S. Abrams *et al.*, Phys. Rev. Lett. **33:1453** (1974).
- [8] F. Abe *et al.*, Phys. Rev. Lett. **74:2626** (1995),  
S. Abachi *et al.*, Phys. Rev. Lett. **74:2632** (1995).
- [9] L.Ya. Glozman and D.O. Riska,  
Phys. Rep. **268:263** (1996), eprint hep-ph/9505422,  
L.Ya. Glozman and D.O. Riska,  
Nucl. Phys. **A603:326-344** (1996), erratum *ibid.* **A620:510** (1997),  
eprint hep-ph/9509269,  
F. Coester, K. Dannbom and D.O. Riska,  
Nucl. Phys. **A634:335** (1998), eprint hep-ph/9711458.
- [10] A.M. Green, J. Koponen, P. Pennanen and C. Michael (UKQCD Coll.),  
Phys. Rev. **D65:014512** (2002), eprint hep-lat/0105027.
- [11] T.A. Lähde, C.J. Nyfält and D.O. Riska,  
Nucl. Phys. **A645:587** (1999), eprint hep-ph/9808438,  
W. Buchmüller and S.H.H. Tye, Phys. Rev. **D24:132** (1981),  
E. Eichten *et al.*, Phys. Rev. **D21:203** (1980),  
*ibid.* Phys. Rev. **D17:3090** (1978).
- [12] R. Blankenbecler and R. Sugar, Phys. Rev. **142:1051** (1966).  
A.A. Logunov and A.N. Tavkhelidze, Nuovo Cim. **29:380** (1963).

- [13] F. Gross, Phys. Rev. **186:1448** (1969), *ibid.* Phys. Rev. **C26:2203** (1982),  
J. Zeng, J.W. Van Orden and W. Roberts,  
Phys.Rev. **D52:5229** (1995), eprint hep-ph/9412269.
- [14] J. Zeng, J.W. Van Orden and W. Roberts,  
Phys. Rev. **D52:5229** (1995), eprint hep-ph/9412269,  
T.A. Lähde, C.J. Nyfält and D.O. Riska,  
Nucl. Phys. **A674:141** (2000), eprint hep-ph/9908485.
- [15] C. Davies, in: *The Heavy Hadron Spectrum*, eprint hep-ph/9710394,  
G.S. Bali, K. Schilling and A. Wachter,  
Phys. Rev. **D56:2566** (1997), eprint hep-lat/9703019,  
S. Godfrey and N. Isgur, Phys. Rev. **D32:189** (1985),  
J. Zeng, J.W. Van Orden and W. Roberts,  
Phys. Rev. **D52:5229** (1995), eprint hep-ph/9412269,  
D. Ebert, V.O. Galkin and R.N. Faustov,  
Phys. Rev. **D57:5663** (1998), eprint hep-ph/9712318,  
T.A. Lähde, C.J. Nyfält and D.O. Riska,  
Nucl. Phys. **A645:587** (1999), eprint hep-ph/9808438,  
T.A. Lähde, to be published in Nucl. Phys. **A**, eprint hep-ph/0208110.
- [16] F. Coester and D.O. Riska, Ann. Phys. **234:141** (1994).
- [17] J. Linde and H. Snellman, Nucl. Phys. **A619:346** (1997), eprint hep-ph/9703383.
- [18] A.V. Smilga and M.A. Shifman (ed.), *Vacuum Structure and QCD Sum Rules*,  
p. 490, North Holland (1992).
- [19] C. Helminen, Phys. Rev. **C59:2829** (1999), eprint hep-ph/9711252.
- [20] T.A. Lähde, to be published in Nucl. Phys. **A**, eprint hep-ph/0208110.
- [21] M.H. Partovi and E.L. Lomon, Phys. Rev. **D2:1999** (1970).
- [22] D.O. Riska, Phys. Lett. **B40:177** (1972).
- [23] T.A. Lähde, C.J. Nyfält and D.O. Riska,  
Nucl. Phys. **A645:587** (1999), eprint hep-ph/9808438,  
T.A. Lähde, to be published in Nucl.Phys. **A**, eprint hep-ph/0208110.
- [24] R.H. Thompson, Phys. Rev. **D1:110** (1970).
- [25] J. Fleischer and J.A. Tjon, Phys. Rev. **D21:87** (1980),  
M.J. Zuilhof and J.A. Tjon, Phys. Rev. **C24:736** (1981).
- [26] E. Hummel and J.A. Tjon, Phys. Rev. **C42:423** (1990),  
V.B. Mandelzweig and S.J. Wallace, Phys. Lett. **B197:469** (1987).
- [27] F. Gross, Phys. Rev. **C26:2203** (1982).
- [28] G.E. Brown, A.D. Jackson and T.T.S. Kuo, Nucl. Phys. **A133:481** (1969).
- [29] A. De Rújula, H. Georgi and S.L. Glashow, Phys. Rev. **D12:147** (1975).

- [30] S. Chernyshev, M.A. Nowak and I. Zahed,  
Phys. Lett. **B350:238** (1995), eprint hep-ph/9409207,  
*ibid.* Phys. Rev. **D53:5176** (1996), eprint hep-ph/9510326.
- [31] A.C. Mattingly and P.M. Stevenson,  
Phys. Rev. **D49:437** (1994), eprint hep-ph/9307266,  
S.J. Brodsky *et al.*,  
Phys. Rev. **D57:245** (1998), eprint hep-ph/9705221,  
P.A. Movilla-Fernández, S. Bethke, O. Biebel and S. Kluth,  
Eur. Phys. J. **C22:1** (2001), eprint hep-ex/0105059.
- [32] D.E. Groom *et al.*, Eur. Phys. J. **C15:1** (2000) (Particle Data Group, ed. 2000).
- [33] S.K. Choi *et al.* (BELLE Coll.), Phys. Rev. Lett. **89:102001** (2002),  
eprint hep-ex/0206002.
- [34] F. Abe *et al.* (CDF Coll.), Phys. Rev. Lett. **81:2432** (1998), eprint hep-ex/9805034.
- [35] E.J. Eichten and C. Quigg, Phys. Rev. **D49:5845** (1994),  
E.J. Eichten and F. Feinberg, Phys. Rev. **D23:2724** (1981),  
S.S. Gershtein *et al.*, Yad. Fiz. **48:515** (1988).
- [36] Y.-Q. Chen and Y.-P. Kuang, Phys. Rev. **D46:1165** (1992).
- [37] G.S. Bali, K. Schilling and A. Wachter,  
Phys. Rev. **D56:2566** (1997), eprint hep-lat/9703019.
- [38] T.A. Lähde, C.J. Nyfält and D.O. Riska,  
Nucl. Phys. **A674:141** (2000), eprint hep-ph/9908485.
- [39] R. Lewis and R.M. Woloshyn,  
Phys. Rev. **D62:114507** (2000), eprint hep-lat/0003011,  
*ibid.* Nucl. Phys. Proc. Suppl. **93:192** (2001), eprint hep-ph/0010013.
- [40] N. Isgur, Phys. Rev. **D57:4041** (1998).
- [41] C. Bourdarios for DELPHI Coll., talk given at ICHEP 98, Vancouver, Canada (1998)  
eprint hep-ex/9811014,  
D. Abreu *et al.* (DELPHI Coll.), Phys. Lett. **B426:231** (1998).
- [42] V. Ciulli, eprint hep-ex/9911044,  
J.L. Rodriguez (CLEO Coll.), eprint hep-ex/9901008.
- [43] E. Shuryak and D.O. Riska, *private communication*.
- [44] R. McClary and N. Byers, Phys. Rev. **D28:1692** (1983),  
P. Moxhay and J.L. Rosner, Phys. Rev. **D28:1132** (1983),  
H. Grotch, D.A. Owen and K.J. Sebastian, Phys. Rev. **D30:1924** (1984),  
X. Zhang, K.J. Sebastian and H. Grotch, Phys. Rev. **D44:1606** (1991),  
E.J. Eichten and C. Quigg, Phys. Rev. **D49:5845** (1994).
- [45] P. Colangelo, G. Nardulli and N. Paver, Z. Phys. **C75:43** (1993),  
V.V. Kiselev, A.E. Kovalsky and A.K. Likhoded,  
Nucl. Phys. **B585:353** (2000), eprint hep-ph/0002127,  
R. Casalbuoni *et al.*, Phys. Lett. **B302:95** (1993),

- N. Brambilla, A. Pineda, J. Soto and A. Vairo,  
Nucl. Phys. **B566:275** (2000), eprint hep-ph/9907240.
- [46] K. Hagiwara *et al.*, Phys. Rev. **D66:010001** (2002) (Particle Data Group, ed. 2002).
- [47] H. Grotch, D.A. Owen and K.J. Sebastian, Phys. Rev. **D30:1924** (1984).
- [48] K. Dannbom, L.Ya. Glozman, C. Helminen and D.O. Riska,  
Nucl. Phys. **A616:555** (1997), eprint hep-ph/9610384,  
C. Helminen, Univ. of Helsinki Rep. Series in Phys. **HU-P-D81** (2000),  
<http://ethesis.helsinki.fi/julkaisut/mat/fysii/vk/helminen/>
- [49] K. Tsushima, D.O. Riska and P.G. Blunden, Nucl. Phys. **A559:543** (1993).
- [50] E.J. Eichten and C. Quigg, Phys. Rev. **D49:5845** (1994).
- [51] B. Metsch, Nucl. Phys. **A578:418** (1994),  
D. Ebert, V.O. Galkin and R.N. Faustov,  
Phys. Rev. **D57:5663** (1998), eprint hep-ph/9712318,  
Yu. S. Kalashnikova, A.V. Nefediev and Yu. A. Simonov,  
Phys. Rev. **D64:014037** (1998).
- [52] D. Gromes, Phys. Lett. **B202:262** (1988).
- [53] E. Eichten *et al.*, Phys. Rev. **D21:203** (1980), *ibid.* Phys. Rev. **D17:3090** (1978).
- [54] H. Grotch, X. Zhang and K.J. Sebastian, Phys. Rev. **D45:4337** (1992).
- [55] A. Anastassov *et al.* (CLEO Coll.)  
Phys. Rev. **D65:032003** (2002), eprint hep-ex/0108043.
- [56] J.L. Goity and W. Roberts,  
Phys. Rev. **D45:4337** (1992), eprint hep-ph/9809312.
- [57] M. Di Pierro and E. Eichten,  
Phys. Rev. **D64:114004** (2001), eprint hep-ex/0104208.
- [58] S. Weinberg, Phys. Rev. Lett. **65:1181** (1990),  
*ibid.*, Phys. Rev. Lett. **67:3473** (1991).
- [59] K. Tsushima and D.O. Riska, Nucl. Phys. **A549:313** (1992).
- [60] M. Kirchbach, D.O. Riska and K. Tsushima, Nucl. Phys. **A542:616** (1992).
- [61] N. Isgur and M. Wise, Phys. Rev. Lett. **66:1130** (1991).
- [62] L. Tiator, C. Bennhold and S.S. Kamalov,  
Nucl. Phys. **A580:455** (1994), eprint nucl-th/9404013.
- [63] M.T. Peña, H. Garcilazo and D.O. Riska,  
Nucl. Phys. **A683:322** (2001), eprint hep-ph/0006011.
- [64] J. Hamilton and E. Burhop (ed.), *High Energy Physics*,  
Vol. I, p. 193, Academic Press, New York (1967).

- 
- [65] R. Lewis and R.M. Woloshyn,  
Phys. Rev. **D62:114507** (2000), eprint hep-lat/0003011,  
A. Ali Khan *et al.*,  
Phys. Rev. **D62:054505** (2000), eprint hep-lat/9912034,  
P. Boyle for UKQCD Coll., Nucl. Phys. Proc. Suppl. **63:314** (1998).
- [66] ARGUS Coll. (H. Albrecht *et al.*), Z. Phys. **C35:283** (1987),  
F. Butler *et al.* (CLEO Coll.), Phys. Rev. **D49:40** (1994).
- [67] J.-W. Chen and M.J. Savage,  
Phys. Rev. **D57:2837** (1998), eprint hep-ph/9710338.
- [68] V.A. Novikov and M.A. Shifman, Z. Phys. **C8:43** (1981).
- [69] J. Schwinger *et al.*, Phys. Rev. **D12:2617** (1975).
- [70] T. Mannel and R. Urech,  
Z. Phys. **C73:541** (1997), eprint hep-ph/9510406.
- [71] J. Chai and D.O. Riska, Nucl. Phys. **A338:349** (1980).
- [72] T. Pedlar (CLEO Coll.), *private communication*.